People's Democratic Republic of Algeria
Ministry Of Higher Education and Scientific Research

University of El Oued
Faculty of Natural and Life Sciences
Department of Cellular and Molecular Biology

A thesis submitted in partial fulfillment of the requirements for the degree of Master of Science in Natural

Nanoparticle-based nutritional supplement aided by moringa leaf extract: a therapeutic approach for deltamethrin-induced liver disease

Submitted by:

- **Bedida Nadjah**
- **Berkan Lamia**
- **Choughrem Azzeddine**

Board of Examiners

Chairperson: DEROICH S	**Professor**	**University of El Oued**
Examiner: HOUMRI N	**M.C.A**	**University of El Oued**
Supervisor: GHANIA A	**M.A.A**	**University of El Oued**

2023/2024

ACKNOWLEDGEMENT

First of all, we thank "Allah" Almighty for giving us health, patience, strength and will to complete this work.

We would particularly like to thank our promoter, Mr. Ghania Ahmed, professor at the University of ELOUED, for accepting the mission so planned for this subject. for his judicious scientific advice and his follow-up during the period of carrying out this work. We can express our affection, gratitude and respect here.

We would like to thank the discussing professors; we will never know thank you enough for helping us to correct this dissertation and for helping us to correct our errors and agreeing to evaluate this work despite the many obligations they have.

We would also like to express our gratitude to all our ELOUED University teachers, all the members of the Educational Laboratories, a big thank you to them finally and above all, we express our deepest gratitude and all our love to our parents and our brothers who knew us trust and support us in circumstances as well as for all our close friends who have always supported and encouraged us even in the hardest times, we thank them from the bottom of our hearts.

DEDICATION

In The Name Of Allah, Most Gracius. Most Merciful.I dedicate this work to:

My parents for their love, encouragement, endless sacrifices, and for being special parents, and making me a special person.

My brothers & sisters.
All my teachers and all my family
Last but not least, I wanna thank me
I wanna thank me for believing in me
I wanna thank me for doing all this hard work
I wanna thank me for having no days off
I wanna thank me for, for never quitting
I wanna thank me for always being a giver
And tryna give more than I recieve
I wanna thank me for tryna do more right than wrong
I wanna thank me for just being me at all times.

*By : **Choughrem Azzeddine***

DEDICATION

Glory be to You, O our Lord. Praise and thanks be to You. Many good and blessed praises for Your constant success and generous grace.

Sincere thanks, appreciation and gratitude to my support, to the one with a good heart, to the one with a proud soul, to the one with a unique smile, to the one who fought and contributed so much for me.

Words of gratitude will not do you justice for everything you provided throughout the period, because you were the best loyal, supportive and supportive people. Thank you from the bottom of my heart for always giving.

You are credited with turning failure into success, and raising my resolve and morale. You are people of excellence and progress, may God protect and protect you.

To my dear husband, Derki Mohammed Nadjib

*By : **Berkan Lamia***

DEDICATION

God Almighty said: (And say, "Work, for God will see your work, and His Messenger and the believers.")

Praise be to God for completion and perfection. Praise be to God for every difficult thing that has passed. Praise be to God, thanks, love, and gratitude for the beginning and the end.

I dedicate this success to myself who knew no path to despair, to myself who broke the barriers of failure to reach her goal, to myself who deserves the highest expressions of appreciation and success.

To the man of struggle and the first reasons for my success, to the light that illuminated my path, to the great that no word or expression can describe, to my beloved father, Professor ***"Youcef Bedida."***

To the princess of women in my heart, to the one who placed paradise under her feet, to my steadfast side, to the great human being who made adversity easy for me, to my dear mother, ***"Nabila Bekakra."***

To the honorable professor, ***"Ghania Ahmed"****, who opened the path to many mysteries for us and made every detail of this work easy for us.*

To my companions who joined me on this journey, to those who helped me in times of difficulty, to those who encouraged me to persevere and complete the journey, I am very grateful to you, my colleague ***"Choughrem Azzeddine"*** *and my colleague* ***"Berkan Lamia."***

I also do not forget my brothers and sisters who have always been one of the reasons for my success and completion of this stage, my brothers and sisters.

To everyone who helped and supported me on this journey, to my grandmothers, to my uncles and aunts, to my maternal uncles and aunts, to everyone who expressed their feelings and sincere advice to me, I dedicate to you this achievement and the fruit of my success that I have always wished for on this day.

By ***: Bedida Nadjah***

ABSTRACT

This thesis investigates the development of a nutritional supplement aimed at treating liver diseases, using nanoparticles synthesized from Moringa oleifera leaf extract. Focusing on green synthesis, the study produces zinc oxide (ZnO), selenium (Se), and ZnO-doped Se nanoparticles, minimizing the use of toxic chemicals to align with sustainable practices.

The nanoparticles were characterized using various techniques: UV-Vis spectroscopy for optical properties, FT-IR spectroscopy for chemical bonds, XRD for crystal structure, and SEM for morphology. The study evaluates the antioxidant, anti-inflammatory, and antimicrobial properties of the nanoparticles, which are essential in combating oxidative stress and inflammation related to liver diseases.

In vitro and in vivo experiments were conducted to assess the therapeutic effects of the nanoparticles. Biochemical and hematological analyses, along with histological studies of liver tissues, were performed to determine the safety and efficacy of the nanoparticles. Results showed that Moringa oleifera-derived nanoparticles exhibit significant antioxidant and anti-inflammatory activities, indicating their potential to reduce liver damage and promote healing.

Despite the promising results, further research is necessary to understand the underlying mechanisms and optimize the dosage and administration for clinical applications. This research contributes to the growing body of knowledge on Moringa oleifera's therapeutic potential, paving the way for new, natural-based treatments for liver diseases.

Key Words: *Moringa oleifera*, nanoparticles, liver disease, dietary supplement.

RÉSUMÉ

Cette thèse étudie le développement d'un complément nutritionnel destiné au traitement des maladies du foie, utilisant des nanoparticules synthétisées à partir d'extrait de feuille de Moringa oleifera. En se concentrant sur la synthèse verte, l'étude produit des nanoparticules d'oxyde de zinc (ZnO), de sélénium (Se) et de Se dopées au ZnO, minimisant ainsi l'utilisation de produits chimiques toxiques pour s'aligner sur des pratiques durables.

Les nanoparticules ont été caractérisées à l'aide de diverses techniques : spectroscopie UV-Vis pour les propriétés optiques, spectroscopie FT-IR pour les liaisons chimiques, XRD pour la structure cristalline et SEM pour la morphologie. L'étude évalue les propriétés antioxydantes, anti-inflammatoires et antimicrobiennes des nanoparticules, essentielles dans la lutte contre le stress oxydatif et l'inflammation liées aux maladies du foie.

Des expériences in vitro et in vivo ont été menées pour évaluer les effets thérapeutiques des nanoparticules. Des analyses biochimiques et hématologiques, ainsi que des études histologiques des tissus hépatiques, ont été réalisées pour déterminer l'innocuité et l'efficacité des nanoparticules. Les résultats ont montré que les nanoparticules dérivées de Moringa oleifera présentent des activités antioxydantes et anti-inflammatoires significatives, indiquant leur potentiel à réduire les dommages au foie et à favoriser la guérison.

Malgré les résultats prometteurs, des recherches supplémentaires sont nécessaires pour comprendre les mécanismes sous-jacents et optimiser le dosage et l'administration pour les applications cliniques. Cette recherche contribue au corpus croissant de connaissances sur le potentiel thérapeutique du Moringa oleifera, ouvrant la voie à de nouveaux traitements naturels pour les maladies du foie.

Mots clés : *Moringa oleifera*, nanoparticules, maladie du foie, complément alimentaire,

ملخص

تركز هذه الأطروحة على تطوير مكمل غذائي يهدف إلى علاج أمراض الكبد، وذلك باستخدام الجسيمات النانوية المصنعة من مستخلص أوراق المورينغا أوليفيرا. بالتركيز على التخليق الأخضر، تنتج الدراسة أكسيد الزنك (ZnO)، والسيلينيوم (Se)، والجسيمات النانوية ZnO–doped Se، مما يقلل من استخدام المواد الكيميائية السامة للتوافق مع الممارسات المستدامة.

تم توصيف الجسيمات النانوية باستخدام تقنيات مختلفة: التحليل الطيفي للأشعة فوق البنفسجية والبصرية للخصائص البصرية، والتحليل الطيفي FT–IR للروابط الكيميائية، وXRD للبنية البلورية، وSEM للتشكل. تقوم الدراسة بتقييم خصائص الجسيمات النانوية المضادة للأكسدة والمضادة للالتهابات والمضادة للميكروبات، والتي تعتبر ضرورية في مكافحة الإجهاد التأكسدي والالتهابات المرتبطة بأمراض الكبد.

أجريت تجارب في المختبر وفي الجسم الحي لتقييم التأثيرات العلاجية للجسيمات النانوية. تم إجراء التحاليل البيوكيميائية والدموية، إلى جانب الدراسات النسيجية لأنسجة الكبد، لتحديد مدى سلامة وفعالية الجسيمات النانوية. وأظهرت النتائج أن الجسيمات النانوية المشتقة من المورينجا أوليفيرا تظهر أنشطة كبيرة مضادة للأكسدة ومضادة للالتهابات، مما يشير إلى قدرتها على تقليل تلف الكبد وتعزيز الشفاء.

على الرغم من النتائج الواعدة، من الضروري إجراء المزيد من الأبحاث لفهم الآليات الأساسية وتحسين الجرعة والإدارة للتطبيقات السريرية. يساهم هذا البحث في تنامي المعرفة حول الإمكانات العلاجية لمورينجا أوليفيرا، مما يمهد الطريق لعلاجات طبيعية جديدة لأمراض الكبد.

الكلمات الدالة: مورينجا اوليفيرا، جسيمات نانوية، امراض الكبد، مكمل غذائي.

LIST OF ABBREVIATION

DB: Data Basis

Abc: absorbance

Ac: Absorbance control

At: Absorbance tested

BHT: butyl hydroxytoluene

Cm: Centimeter

DDPH: 2,2 diphenyl 1-1 picryihydrazyl

XRD: X-ray diffractometer

DO: Long order

EDTA: Ethylene diamine teraacetic acid

Fe: Iron

Fe +2: Ferrous ion

Fe+3: Ferric ion

FRAP: Ferric Reducing Antioxidant power

I%: inhibition percentage

%: percentage

h: hour

nm: Nanometer

MB: methylene blue

mg/ml: Milligram per milliliter

min: minute

A: yield

TCK: Cephalin time – Kaolin

TP: Trombin time

PBS: Phosphate buffer

Ug/ml: Microgram per milliliter

Ul: Microliter

UV: Ultra Violent

SePNs: selenium nanoparticle

XP: Pure Extract

ZN-SeNPs: zinc nanoparticles doped with selenium.

ZN: zone of inhibition.

LIST OF TABLES

LIST OF FIGURES

LIST OF FIGURES

CONTENTS

Introduction

Moringa oleifera, commonly known as drumstick tree, horseradish tree, or ben oil tree, is a fast-growing, drought-resistant plant native to South Asia but now widely cultivated across tropical and subtropical regions around the world. It belongs to the family Moringaceae and is valued for its high nutritional content and medicinal properties. (Anwar et al., 2007)

Moringa oleifera has been recognized for its potential health benefits due to its rich nutrient profile. The plant contains significant amounts of vitamins (A, C, E), minerals (calcium, potassium, iron), antioxidants, and bioactive compounds such as phenolic acids and flavonoids. These components contribute to its therapeutic applications. (Fahey, J. W. 2005)

Despite the promising preliminary findings, more comprehensive and rigorous clinical trials are needed to validate the efficacy and safety of Moringa oleifera in treating these conditions. Additionally, understanding the optimal dosage and form (e.g., leaf powder, capsule) for consumption is crucial for maximizing its health benefits. (Rockwood et al., 2013. Leone et al., 2015)

From this standpoint, we pose the following problem: What are the biological activities and potential health benefits of consuming Moringa oleifera nanoparticles as part of dietary supplements, especially with regard to antioxidant activity, hypoglycemic effects, anti-inflammatory properties, and most importantly its effect on liver disease?

Part 1

BIBLIOGRAPHIC

Chapter 1

General on Moringa Oliveira

1.1. Definition of *Moringa Oliveira*

This study focused on the *Moringa oleifera* species that belongs to the *Moringa oleifera* Moringaceae family and is the most famous species of moringa oleifera plants, a traditionally known medical plant whose uses are known because it contains a very wide range of medicinal plants. A range of bioactive and nutritional compounds such as proteins, vitamins, carbohydrates, minerals, fats and fibres, these properties allow them to obtain medical, nutritional and pharmaceutical uses, including: Parasitic properties such as bacteria and fungi, antioxidant properties because they contain polyphenols of very high value, they are also known for their protective anti-liver and cardiac properties, have also been used to treat malnutrition in African children, and are also widely used for ornamental purposes in cities along Mexico's Pacific coast. (Anwar et al., 2007)

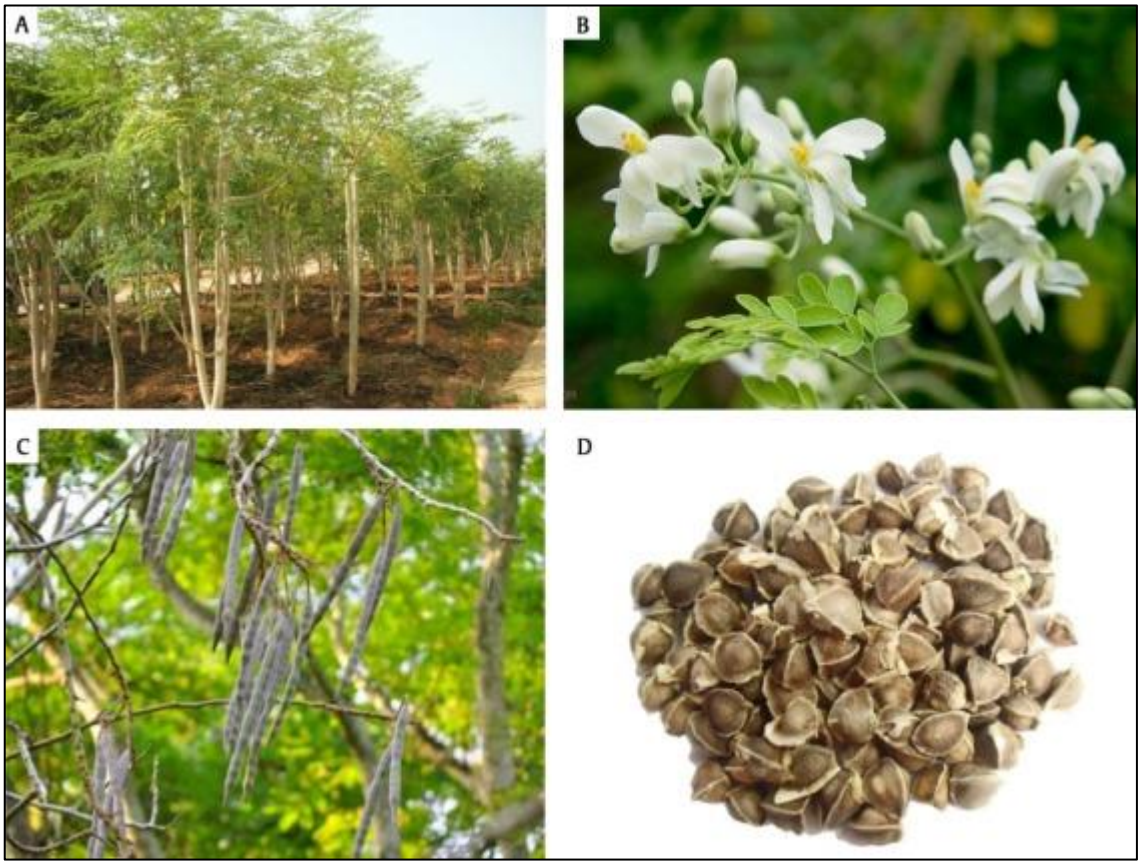

Figure 1:Different parts of Moringa oleifera (Yang Liu, et al. (2018))

1.2. Taxonomy of Moringa Olifeira

Moringa oleifera, commonly known as the drumstick tree, horseradish tree, or malunggay, belongs to the botanical family Moringaceae. Its scientific classification places it within the following hierarchical structure:

Tableau 1 Taxonomy of Moringa Olifeira (Animal and Plant Health Inspection Services., U.S. DEPARTMENT OF AGRICULTURE. 2024)

Kingdom	**Plantae**
Phylum	Tracheophyta
Class	Magnoliopsida
Order	Capparales
Family	Moringaceae
Genus	Moringa
Species	Moringa oleifera

1.3. Botanical description

Moringa oleifera is considered a small, fast-growing, oily tree. It is evergreen in the first year of its life (Godinoa et al.,2017). It reaches 4 or 5 years of age before being replanted. It is grown in tropical regions, even areas with a slightly high temperature, due to its ability to live in temperatures ranging between 12.6 And 40 degrees Celsius sometimes reaches 48 degrees (Roloff 2009), but some changes have been observed in the *Moringa oleifera* tree from one region to another in terms of its composition and nutritional properties, with the difference in temperature from one region to another affecting its composition and changing the nature of the proteins and enzymes present in the tree. This tree is grown in sandy or clay soil with a slightly acidic to slightly basic pH (M.D. Thurber, J.W. Fahey., 2010), ranging between 4.5 and 8. A slightly acidic pH is most likely more appropriate (Padilla et al., 2017). The length of the moringa tree may exceed 4 meters (Prabhakar 2008), and it can be grown easily from New, from a morphological standpoint, this tree is characterized by a spreading and open crown that is usually in the shape of an umbrella. It has drooping and fragile branches. The foliage is three-pointed, compound and thick, with a length of up to 45 cm. It has a single stem, but it is forked and usually has a rough texture. Its bark is It is made of cork and is gray in color, and sometimes you find it white. It has young branches and buds covered with short, dense purple or greenish-white hairs. The flowers of the Moringa plant are pentagonal in shape, white in color and fragrant in smell. They are multi-sided, ranging in length from 0.7 to 1.6 cm. The *Moringa oleifera* fruit is a capsule with 3 The valves, nicknamed “pods,” look like a drumstick. Their length ranges from 10 to 60 cm. They appear in summer. They are usually green in color, pale yellow when young, and turn brown and split lengthwise when mature (Monika Singh et

al.,2020). The diameter of Moringa seeds was measured and it was found that it ranges between 1 to 1.5 cm surrounded by three leafy wings up to 2.5 cm long (Foidl et al., 2001).

1.4. Moringa distribution in the world

A country-specific M. oleifera research database was taken from Scopus, and utilizing the GIS environment's "connect field" tool, the data were immediately linked to the nation shapefile for geographic mapping. Based on the investigations, it was found that between 2000 and 2022, researchers from around 15 different nations produced over 100 research papers. The most prolific nation was India (n = 1083), followed by Nigeria (n = 441), Brazil (n = 383), Egypt (n = 361), China (n = 331), Indonesia (n = 327), Pakistan (n = 281), South Africa (n = 272), Malaysia (n = 260), the United States (n = 214), Saudi Arabia (n = 205), Mexico (n = 163), Thailand (n = 127), and Italy (n = 105). (Pareek et al,. 2023)

Figure 2: ArcGIS 10.1-based spatial distribution map highlights research papers

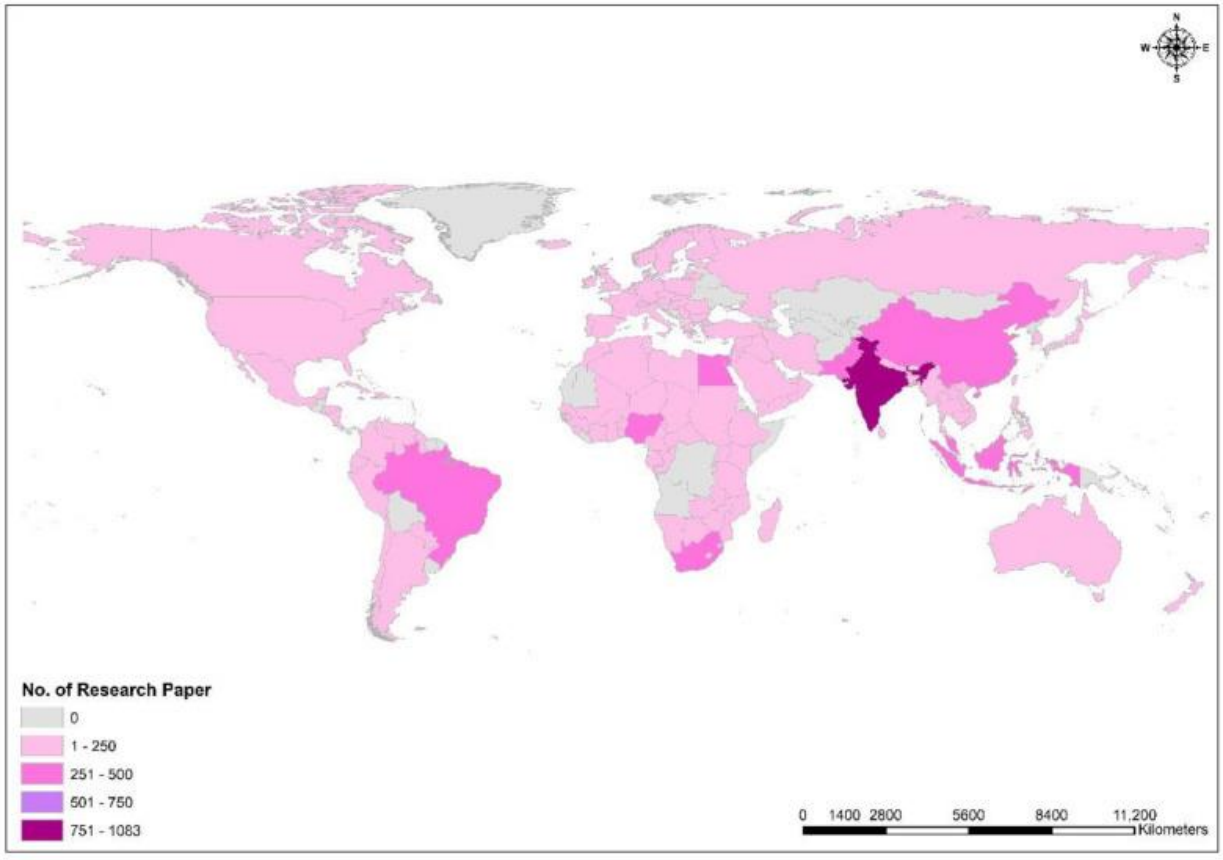

published on M. oleifera worldwide. A spatial technique was used to generate a map, and GIS layers were obtained from DIVA-GIS, an open-source web platform. (Pareek et al, 2023).

1.5. Chemical composition and nutritional value

1.5.1. Chemical composition

The green leaves of moringa contain carbohydrates (9.1 g), dietary fiber, fat, and protein. The same study showed that they are also rich invitamins such as vitamin A, thiamine (B1), riboflavin (B2), niacin (B3), pantothenic acids (B5), vitamin B6, folic acid (B9), vitamin C as well as minerals such as calcium, iron, magnesium, manganese, phosphorus, potassium, sodium and zinc. They are also rich in essential amino acids: Threonine, Valine, Methionine, Leucine, Isoleucine Phenylalanine, Histidine, Lysine and Arginine (Mukunzi et al., 2011; Mune, 2016; Abass et al., 2018; Kumar, 2018; González-Burgos, 2021; Sarret al., 2015).

Tableau 2 .The nutrient compositions of leaves, leaf powder, seeds and pods. (Rajbhar et al,. (2018))

Nutrients	Fresh leaves	Dry leaves	Leaf powder	Seed	Pods
Calories (cal)	92	329	205	–	26
Protein (g)	6.7	29.4	27.1	35.97 ± 0.19	2.5
Fat (g)	1.7	5.2	2.3	38.67 ± 0.03	0.1
Carbohydrate (g)	12.5	41.2	38.2	8.67 ± 0.12	3.7
Fibre (g)	0.9	12.5	19.2	2.87 ± 0.03	4.8
Vitamin B1 (mg)	0.06	2.02	2.64	0.05	0.05
Vitamin B2 (mg)	0.05	21.3	20.5	0.06	0.07
Vitamin B3 (mg)	0.8	7.6	8.2	0.2	0.2
Vitamin C (mg)	220	15.8	17.3	4.5 ± 0.17	120
Vitamin E (mg)	448	10.8	113	751.67 ± 4.41	–
Calcium (mg)	440	2185	2003	45	30
Magnesium (mg)	42	448	368	635 ± 8.66	24
Phosphorus (mg)	70	252	204	75	110
Potassium (mg)	259	1236	1324	–	259
Copper (mg)	0.07	0.49	0.57	5.20 ± 0.15	3.1
Iron (mg)	0.85	25.6	28.2	–	5.3
Sulphur (mg)	–	–	870	0.05	137

0g per plant material.[9–11]

Moringa oleifera seed has a high proportion of monounsaturated/saturated fatty acids (MUFA/SFA), sterols and tocopherols, as well as proteins rich in sulfur amino acids (Leone et al.,2016), In some studies, fatty acids and their percentage in *moringa oleifera* oil were discovered, namely behenic, linoleic, fatty, palmitic, oleic, arachidic, linolenic, eicosanoid, and heptadecanoic acids (Amaglo et al.,2010).

Tableau 3. Fatty acid compositions of Moringa oleifera see. (Ahaotu, et al. (2018))

Fatty acids	Mole Fraction (%)
Behenic acid (C22:0)	4.1
Myristic acid (C14:0) Erucic	0.5
Erucic acid (C22:1)	1.7
Oleic acid (C18)	67.3
Arachidic acid (C20)	5.5
Linolenic acid (C18:3)	1.1
Stearic acid (C:18)	4.5
Palmitoleic acid (C16:1)	2.5
Palmitic acid (C16)	7.9

The 163 chemical components, included flavonoids, carbamates, glucosinolates, phenols, saponins and so on with various bioactivities, such as anti-tumor, antioxidant, anti-inflammatory, and so on. Additionally, M. oleifera is toxic at certain doses; and overuse can cause genotoxicity, Table 04 shows the phytochemical compounds and their proportions.

Tableau 4.phytochemical composition of M. Oleifera leaf powder based on Dry weight (DW) (Nathaniel Ebenezar Udofia, Onyancha Jared Misonge, Mugambi Mworia, Ncene William, Moriasi Gervason Apiri, (2020)).

Phytoconstituents	**Mean values of percentage composition (g/100g of DW) for the current study**	**Range of Mean values of percentage composition (g/100g of DW) available in literature values**
Carbohydrate (%)	41.97 ± 0.72	0.1 to 50
Flavonoids (%)	1.12 ± 0.20	4.4 to 12.2
Alkaloids (%)	0.06 ± 0.00	0.1 to 8.0
Phenols (%)	46.81 ± 3.29	0.05
Saponins (%)	14.00 ± 0.51	0.23 to 4.2
Ash (%)	14.82 ± 0.63	3.8 to 10.2
Crude fibre (%)	1.58 ± 0.45	0.1 to 28.5
Crude Lipid (%)	6.06 ± 1.63	0.1 to 10.6
Crude Protein (%)	23.05 ± 0.62	24.2 to 30.3
Moisture (%)	12.92 ± 0.02	7.5 to 14.8

Tableau 5. Amino Acid composition of Moringa oleifera seed (mg/g crude protein). (Manoj et al., (2022))

Amino Acid	Concentration (mg/g crude protein)
Lysine*	76.2
Histidine*	22.1
Argtinine*	62.3
Aspartic Acid	101.7
Threonine*	31.5
Serine	35.0
Glutamic Acid	137.8
Praline	32.6
Glycine	37.7
Alanine	30.0
Cystine	9.2
Valine*	38.1
Methionine*	9.9
Isoleucine*	32.0
Leucine*	77.8
Tyrosine	28.6
Phenylalanine*	51.4
TOTAL	**813.90**

Tableau 6.Percentage Essential, Non-Essential, Acidic, Basic, Neutral, Sulphur and Aromatic Amino Acid content. (Manoj et al., (2022))

Amino Acid	Percentage Concentration
% TEAA (with Histidine)	49.31
% TEAA (without Histidine)	46.59
% TNEAA (without Histidine)	50.69
% TNAA	50.8
% TAAA	29.4
% TBAA	19.7
% Cys in TSAA	48.2
% TArAA	9.83
Leu/ILe ratio	2.43
% Leu-Ile (diff.)	58.9
Isoelectric point (Iρ)	5.80
P-PER	2.76
EAAI	1.55

TEAA – *Total Essential Amino, Iρ* – Isoelectric Point
TNEAA – Total Non-Essential Amino Acid
TNAA – Total Neutral Amino Acid
TAAA – Total Acidic Amino Acid
TBAA – Total Basic Amino Acid
TSAA – Total Sulphur Amino Acid
TArAA – Total Aromatic Amino Acid
P-PER – Predicted Protein Efficiency Ratio
EAAI- Essential Amino Acid Index (EAAI)

The present study showed that M. oleifera leaf powders may be used for food and for preventative and curative medical purposes since they include phytochemicals, vitamins, amino acids, and mineral components. The environmental variables that affect the accumulation of chemical and mineral components in plants, such as climate, soil, altitude, age of growth, parasites, and harvesting time, were blamed for the variations in chemical composition (Udofia et al.,2020).

1.5.2. Nutritional value

Many researches and studies have confirmed the nutritional wealth that the Moringa oleifera plant carries in terms of benefits and nutritional or health values for the human body, including:

- Moringa leaves show about 25.5-31.03 mg of zinc/kg, which is the daily requirement for zinc in the diet. It is also known that it is a mineral that is very necessary for the growth of sperm cells, and is also very important for the synthesis of DNA and RNA. (Gopalakrishnan et al., 2016)
- Moringa powder is an effective treatment for anemia and is also used as an alternative to iron tablets. It has been reported that moringa contains more iron than spinach. (Gopalakrishnan et al., 2016)
- Moringa has been used by breastfeeding women because it contains hormone precursors (sitosterol, campysterol) that work to increase the production of estrogen and thus multiply the ducts of the mammary gland to produce milk. (Gopalakrishnan et al., 2016)
- It is eaten by obese people in their diet because it has a low caloric value.
- The Moringa plant has become famous in Africa and is used especially by infants and mothers to combat malnutrition due to its nutritional compounds and the huge amount of minerals for building the body (calcium, potassium, magnesium, iron, copper, vitamins such as beta carotene and folic acid...etc. (M. Mbikay., 2012)
- In fact, moringa is said to provide 7 times more vitamin C than oranges, 10 times more vitamin A than carrots, 17 times more calcium than milk, 9 times more protein than yogurt, 15 times more potassium than bananas, and 25 times more iron than iron from spinach (M. Godinoa et al.,2017)

1.6. Medicinal properties and traditional applications

1.6.1. Medicinal properties

- Moringa leaf juice has antibacterial activity against various tested strains

including Bacillus cereus, Staphylococcus aureus, Escherichia coli, Candida albicans, Candida primogenes. (Gopalakrishnan et al., 2016)

- in folk medicine, raw or ground molyvera seeds are used as boilers to treat stomach pain, ulcers, vision problems, joint pain, and to assist digestion (Leone et al.,2016).
- Olefeira is often referred to as a panacea and can be used to treat more than 300 diseases (Gopalakrishnan et al.,2016).
- Moringa Olifeira is used to treat malnutrition especially in infants and nursing mothers. The leaves are used to treat malaria, typhoid, parasitic diseases, urogenital problems, hypertension, arthritis, swelling, wounds, dermatology and diabetes, in addition to being heart-strengthening, contraceptive, lactating stimulant and immune system booster (Ragasa et al., 2015).
- M. oleifera can be used as an anti-cancer agent because it is natural, reliable and safe in constant concentrations. (Al-Asmari et al., 2015)
- Moringa is a memory activator as a result of the moringa's effectiveness in reducing the activity of pastel colin. (Al-Asmari et al., 2015)
- It has an anti-sore stomach activity so that it reduces and reduces the acidity of the stomach. (Al-Asmari et al., 2015)
- Brain-booster and a very strong neuroprotective factor. When blood flow to the brain is disturbed, oxidation occurs and the production of reactive oxygen types, moringa reduces these factors with its well-known antioxidant compounds. (Al-Asmari et al., 2015)

1.6.2. Traditional applications

When moringa was discovered in ancient times and before technology intervened, traditional humans used it randomly in the field of food and folk medicine and many simple applications of all parts of moringa shown in Table 06.

Tableau 7.Common Traditional method of preparation of morphological parts of the M. Oleifera tree.

Plant part	Traditional method of preparation
Root	**Prepared as decoctions.**
Bark	**Decoctions for creams or emollients.**
Gum	**Used to season food preparations.**
Leaf	**The leaves are cooked and used like spinach. Leaves are also commonly dried and crushed into a powder, and used in soups and sauces.**
Flower	**Flower extracts are used for preparations to enhance taste and color in dishes.**

Pod	**Young pods are sliced and boiled in water with salt. Mature pods are twisted open, are removed and fried in oil or cooked like pea, fresh or dried.**
Seed	**Seeds are prepared green, roasted or powdered, steamed and extracted as an oil.**
Seed oil	**Used in water treatment and purification.**

- Along with other therapeutic applications, The Ayurvedic Pharmacopoeia of India indicated the use of the dried root bark in goitre, glycosuria and lipid disorders (also dried seeds) (Mishra et al.,2011).
- Filipino women used moringa leaves mixed with chicken or shellfish soup to improve the taste.
- Used as dietary oil in Red Sea areas (Hana and Jamal., 2013) because moringa seed oil contains all fatty acids found in olive oil (Lalas and Toskanis., 2002).
- Moringa is also used in some areas for livestock feeding.
- Ancient Egyptians used moringa olivera flowers to make tea.

1.7. Hazardous or Adverse Effect

some studies have linked some chemicals contained in Moringa oleifera to serious liver, renal, hematological, and other disorders, therefore the plant is not completely safe. Potential mutagens such 4-(α-lramnopyranosyloxy)-benzylglucosinolate, which raise the percentage of micronucleated polychromatophilic erythroblasts, suggestive of some level of genotoxicity, may be found in roasted Moringa oleifera seeds (Asare et al.,2012).

High levels of saponins in the leaf may be detrimental to vegetarians because they decrease the absorption of divalent and trivalent elements like zinc and magnesium (Canett-Romero et al.,2014).

1.8. Recent scientific studies on pharmacological effects

1.8.1. Anti-diabetic effect

Type 1 diabetes involves inability to produce insulin, an important hormone for regulating blood sugar, while type 2 diabetes is characterized by insulin resistance and/or beta cell dysfunction, which hampers the body's response to insulin, Studies have shown that aqueous extracts of M. oleifera can alleviate streptozotocin (STZ)-induced type 1 diabetes and insulin-resistant type 2 diabetes in rat models (S.M. Divi, R. Bellamkonda, S.K.,2012).

STZ is known to cause beta cell damage through the generation of reactive oxygen species (ROS). Hyperglycemia exacerbates this process, as excess glucose enters the mitochondria of beta cells and stimulates the production of reactive oxygen species, leading to cell death and decreased insulin secretion, but flavonoids in moringa, such as quercetin, have antioxidant properties that may scavenge reactive oxygen species and protect beta cells from damage. This suggests that moringa mitigates oxidative stress that contributes to its antidiabetic effects, especially in managing hyperglycemia and maintaining beta cell function (N. Kamalakkannan, P.S.M., 2006).

However, although these results are promising, more research is needed to fully understand the mechanisms involved and to validate these results in human clinical trials.

1.8.2. Antitumor and anticancer effects

Moringa Oliveira (M. oleifera) has emerged as a potential alternative to treating cancer cell proliferation due to its natural origin and safety characteristics when taking specific doses. Research suggests that it may hinder the growth of cancer cells by acting as an anti- reproductive agent. It is believed that the mechanism behind this effect involves stimulating reactive oxygen types (ROS) within cancer cells, resulting in apoptosis (apoptosis) (I.L. Jung.,2014), More importantly, moringa appears to selectively stimulate reactive oxygen types (ROS) in cancer cells, while maintaining healthy cells. In addition, studies suggest that moringa extracts raise the level of glutathione-S-transferase, an enzyme that inhibits antioxidant activity. While many anti-cancer agents use ROS induction, they must also counter antioxidant enzymes. Interestingly, Telok et al. They show that moringa leaf extracts show antioxidant and anti- cancer properties, raising questions about the interaction between these opposing properties (C. Tiloke, A. Phulukdaree, A.A.,2013).

Compounds such as glucosinate, niazimycin and benzyl isothiocyanate found in moringa leaves are involved in their anti-cancer activity. Specifically, benzyl isothiocyanate (BITC) has been linked to intracellular ROS generation and subsequent cell death, also supporting moringa's potential as an anti-cancer agent. However, further research is needed to fully understand the complex mechanisms involved (Nakamura et al.,2002).

1.8.3. Effects on the reproductive system

Moringa extracts have shown an influence on anatomical processes of reproduction, embryonic growth and development due to the fact that fresh moringa leaves contain approximately 11300_23000 IU of vitamin A. Studies have also shown that leaf extract has a significant effect on increasing the weight of the testicle and sperm vesicles (Leone et al.,2015).

1.8.4. Cardiovascular activity

Research suggests that extracts from Moringa oleifera leaves may offer benefits for cardiovascular health. Studies in rats have shown potential to lower cholesterol levels and protect against hyperlipidemia caused by iron deficiency. Additionally, these extracts have demonstrated antihypertensive effects and may reduce heart rate and contractility. Specific compounds like niazinin A, B, and niazimicin are believed to contribute to these blood pressure-lowering properties. (Alia et al., 2022)

Furthermore, evidence suggests that leaf extracts may protect the heart against damage caused by isoproterenol-induced myocardial infarction. This cardioprotective effect is thought to be due to the extract's antioxidant properties, ability to prevent lipid peroxidation, and protection against structural damage in heart tissue, in another study, Moringa oleifera was found to have a positive impact on various tissues, reducing inflammation and lipid accumulation. (Alia et al., 2022)

1.9. Therapeutic potential in the context of liver diseases

In Sprague Dawley rats, leaf extract has demonstrated hepatoprotective properties against liver damage produced by carbon tetrachloride and acetaminophen.(MH Daba, MS Abdel-Rahman.,1998) (Nanjappaiah et Hugar., 2012) furthermore having a hepatoprotective effect in diabetic rats against liver damage caused by alloxan and antitubercular medications.(L Pari, NA Kumar., 2002) (Omodanisi et al.,2017) ,The 21-day plant-based diet shown a strong ability to mitigate hepatic damage.(Omodanisi et al.,2017) (MA Abd Eldaim et al., 2017) (OS Adeyemi et al.,2017), Ascorbic acid, flavonoids, kaempferol, alkaloids, quercetin, and benzyl glucosinolate were discovered to have hepatoprotective effect.

The therapeutic /hepatoprotective effects of MO extracts are probably due to inhibition of lipid peroxidation by-product as well as enhanced antioxidant enzymes.

Pari and Kumar, evaluated the hepatoprotective effect of ethanol extract of moringa leaves on liver damage induced by anti-tubercular drugs such as isoniazid (INH), rifampicin (RMP), and pyrazinamide (PZA) in rats and observed oral administration of the extract showed a significant protective action against hepatic disorders. .(Omodanisi et al.,2017)

In animal models, moringa oleifera leaf extract possesses hepatoprotective properties that help reduce oxidative stress and liver damage brought on by a high-fat diet... It decreased liver

enzyme levels and treated the early symptoms of fatty liver disease.) (Nanjappaiah et Hugar., 2012)

Moringa oleifera seed crude extracts show promise as a homeopathic treatment for hepatic disorders. While larger dosages (200–400 mg/L) lowered metabolic activity and liver enzyme levels (AST), suggesting the potential to attenuate liver damage, lower concentrations (50–100 mg/L) showed modest stimulatory effects on liver cells (Boluwatife O Sowunmi, Martin Gonzo.,2023).

The hepatoprotective qualities of moringa oleifera leaves are attributed to their antioxidant and phytochemical content, which includes flavonoids, glucosinolates, isothiocyanates, and phenolic acids. It can stop the development of liver failure in non-alcoholic fatty liver disease (NAFLD) (Aly et al.,2020).

Chapter 2

Overview of Nanoparticles

2.1. Definition of Nanoparticle

In 2008, the International Organization for Standardization (ISO) defined nanoparticles as discrete nano-objects with all three Cartesian dimensions measuring less than 100 nm. This definition extended to two-dimensional nano-objects (nanodiscs and nanoplates) and one-dimensional nano-objects (nanofibres and nanotubes). (King, S et al, 2024)

However, in 2011, the European Commission adopted a broader definition: A natural, incidental, or manufactured material containing particles, either unbound, aggregated, or agglomerated, where at least 50% of the particles in the number size distribution have one or more external dimensions between 1 nm and 100 nm. (King, S et al, 2024)

2.2. Classification of NPs

NPs are broadly categorized based on morphology, size, and chemical properties. Some well-known classes based on physical and chemical characteristics include:

2.2.1. Carbon-based NPs:

Fullerenes and carbon nanotubes (CNTs) are two essential sub-categories of carbon-based nanoparticles (NPs). Fullerenes consist of globular hollow cages, representing allotropic forms of carbon, and have garnered significant interest due to their electrical conductivity, high strength, unique structure, electron affinity, and versatility. These structures are composed of organized pentagonal and hexagonal carbon units, each exhibiting sp2 hybridization.

Conversely, CNTs are elongated tubular structures with diameters typically ranging from 1 to 2 nm. They resemble rolled-up graphite sheets, with the number of layers determining their classification as single-walled (SWNTs), double-walled (DWNTs), or multi-walled carbon nanotubes (MWNTs). (Astefanei et al., 2015)

2.2.2. Metal NPs:

Metal NPs, composed solely of metals, exhibit unique electrical properties due to their well-characterized localized surface plasmon resonance (LSPR) features. Notably, copper (Cu), silver (Ag), and gold (Au) nanoparticles display a broad absorption band within the visible region of the solar electromagnetic spectrum. These metal NPs find diverse applications across scientific disciplines due to their enhanced properties, which can be fine-tuned through facet, size, and shape-controlled synthesis methods. (Khan et al., 2019)

2.2.3. Ceramics NPs:

Ceramic nanoparticles (NPs) are minute particles composed of inorganic, non-metallic materials that undergo specific heat treatment and cooling processes to achieve desired

properties. They can be found in various morphologies, including amorphous, polycrystalline, dense, porous, and hollow forms. Ceramic NPs are renowned for their heat resistance and durability, making them suitable for applications such as coatings, catalysts, and batteries. (Sigmund et al., 2006)

2.2.4. Lipid-based NPs:

Lipid nanoparticles (NPs) are beneficial in various biological applications due to the presence of lipid moieties. These NPs are typically spherical and have a diameter ranging from 10 to 1000 nm. (Khan et al., 2019)

It's important to clarify the terminology: lipid NPs are distinct from polymeric NPs. Lipid NPs possess a solid lipid core encapsulated by a matrix of soluble lipophilic molecules. This structure allows for efficient encapsulation and delivery of therapeutic agents, particularly in drug delivery systems. The lipophilic nature of these NPs enhances their biocompatibility and interaction with biological membranes, making them valuable tools in various biomedical applications. (Khan et al., 2019)

2.2.5. Semiconductor NPs:

Semiconductor nanoparticles (NPs) possess characteristics of both metals and non-metals, resulting in unique physical and chemical properties that enable diverse applications. These NPs can absorb and emit light, making them valuable in enhancing the efficiency of solar cells and increasing the brightness of light-emitting diodes (LEDs). Additionally, their size and electronic properties facilitate the development of smaller, faster electronic devices like transistors. Semiconductor NPs also hold promise in the fields of bio-imaging and cancer therapy due to their ability to interact with biological systems and deliver targeted treatments. (Biju et al., 2008)

2.2.6. Polymeric NPs:

Polymeric nanoparticles (NPs) are organic nanoparticles typically ranging from 1 to 1000 nm in size. They can have active substances either surface-adsorbed onto their polymeric core or entrapped within their polymeric matrix. Due to their organic nature, they are often referred to as polymer nanoparticles (PNPs) in scientific literature. In essence, they closely resemble nanospheres or nanocapsules. (Khan et al., 2019; Zielińska et al., 2020)

2.3. Types of different metal-based NPs

Metal nanoparticles (NPs), synthesized from pure metal precursors, exhibit distinctive optoelectrical properties due to their well-characterized localized surface plasmon resonance (LSPR). Alkali and noble metal NPs, specifically copper (Cu), silver (Ag), and gold (Au),

display a broad absorption band within the visible range of the solar electromagnetic spectrum. The precise control of facet, size, and shape during metal NP synthesis is crucial in the development of cutting-edge materials for various technological applications. (Dreaden et al., 2012; Khan et al., 2019)

2.3.1. Silver nanoparticles (AgNPs)

Silver nanoparticles (AgNPs) are particles composed of silver with dimensions ranging from 1 to 100 nanometers. Their small size, high surface area-to-volume ratio, and ability to interact with light in the visible and near-infrared spectrum confer unique physical and chemical properties. These characteristics, notably their increased surface area, contribute to enhanced antimicrobial activity compared to ionic silver. (Shenashen et al., 2014)

AgNPs can be synthesized in various sizes and shapes, with chemical reduction being a common method. A typical synthesis involves the chemical reduction of a 12 mM aqueous silver nitrate (AgNO3) solution. This reaction, conducted under an argon atmosphere, combines 70 mL of AgNO3 solution with polyvinylpyrrolidone (PVP) (maintaining a molar ratio of PVP repeating unit to Ag of 34) and 21 mL of Aloe vera extract. The mixture is subjected to ultrasonic agitation for 45 minutes at room temperature, followed by heating at a rate of 2°C/min to 80°C, and maintained for 2 hours. This process results in a transparent solution containing suspended nanoparticles, which can be isolated through filtration. (Shenashen et al., 2014; Gloria et al., 2017)

2.3.2. Zinc nanoparticles (ZnONPs)

Zinc oxide (ZnO) nanoparticles (NPs), with sizes ranging from 1 to 100 nm, are wide band gap semiconductors characterized by a room temperature energy gap of 3.37 eV. Their catalytic, electrical, optoelectronic, and photochemical properties have garnered significant interest for various applications (Kumar S.S. et al., 2013). Notably, ZnO nanostructures are particularly well-suited for catalytic reaction processes due to their high surface area and reactivity. (Chen and Tang, 2007)

A multitude of methods can be employed for the synthesis of ZnO nanoparticles, including laser ablation, hydrothermal methods, electrochemical deposition, sol-gel techniques, chemical vapor deposition, thermal decomposition, combustion methods, ultrasound, microwave-assisted combustion, two-step mechanochemical-thermal synthesis, anodization, co-precipitation, electrophoretic deposition, and precipitation processes. (Madathil et al., 2007 ; Moghaddam et al., 2009 ; Ghorbani et al., 2015)

2.3.3. Copper nanoparticles (CuNPs)

Copper nanoparticles (CuNPs) are copper-based particles with dimensions ranging from 1 to 100 nm (Khan et al., 2019). Both copper (Cu) and gold (Au) have been known to exhibit fluorescence, with a peak centered on the metals' interband absorption edge when excited at 488 nm. Interestingly, the fluorescence peak energy remains consistent across different excitation wavelengths (457.9-514.5 and 300-400 nm), while the high-energy tail intensifies with increased photon energy. (Siwach and Sen, 2008)

A unique, physical, top-down approach known as exploding electrical wire (EEW) has been employed to synthesize Cu nanoparticles. This method involves passing a high-density current of 1010 A/m^2 through a thin copper wire, causing it to explode onto a copper plate within a microsecond timeframe. (Siwach and Sen, 2008)

2.3.4. Gold nanoparticles (AuNPs)

Gold nanoparticles (AuNPs) are nanometer-sized particles composed of gold. Their unique physical and chemical properties enable them to absorb and scatter light within the visible and near-infrared spectrum. (Rad et al., 2011; Compostella et al., 2017).

Anisotropic AuNPs were first observed by scientists around the turn of the 20th century. In his 1909 book, Zsigmondy noted that gold particles smaller than 40 nm were not always spherical and exhibited various colors due to their anisotropic nature (Li et al., 2014). His work with the ultramicroscope, which enabled the visualization of Au particle shapes, contributed to his 1925 Nobel Prize recognition. Notably, he observed the frequent crystallization of gold into a six-sided leaf shape. (Li et al., 2014)

Due to their optical, electrical, and molecular recognition properties, AuNPs are extensively researched for potential applications in diverse fields, including electron microscopy, electronics, nanotechnology, materials science, and biomedicine. (Rad et al., 2011)

2.3.5. Aluminum nanoparticles (AlNPs)

Aluminum nanoparticles (AlNPs) are nanoparticles composed of aluminum. Their high reactivity makes them attractive for various applications, including high-energy compositions, hydrogen generation through water reactions, and the synthesis of two-dimensional (2D) and three-dimensional (3D) alumina structures. (Lerner et al., 2016)

2.3.6. Iron nanoparticles (FeNPs)

Iron nanoparticles (FeNPs), with dimensions ranging from 1 to 100 nm, hold significant promise for various applications due to their unique properties (Khan et al., 2019). These applications include catalysis, drug delivery systems, sensors, energy storage and conversion,

photovoltaic and solar cells, water purification, and environmental remediation. Additionally, FeNPs are investigated for their potential as contrast agents in magnetic resonance imaging (MRI) to enhance tissue and organ visibility, as well as in magnetic recording media like hard disk drives. (Zhuang and Gentry, 2011; Jamkhande et al., 2019)

However, like all nanoparticles, the use of FeNPs raises potential health and safety concerns. These concerns stem from their diverse applications, including targeted drug delivery to specific sites within the body (such as cancer cells), use in MRI, and their potential for removing contaminants from water. (Farrell et al., 2003 ; Zhuang and Gentry, 2011)

2.4. Physicochemical properties of NPs

As previously mentioned, nanoparticles (NPs) possess unique physicochemical properties such as large surface area, mechanical strength, optical activity, and chemical reactivity, rendering them suitable for diverse applications. Key properties contributing to their versatility will be discussed in the following section. (Khan et al., 2019)

2.4.1. Electronic and optical properties

The optical and electronic properties of nanoparticles (NPs) are closely interconnected. For instance, noble metal NPs exhibit size-dependent optical properties, characterized by a strong UV-visible extinction band absent in the bulk metal spectrum. This band arises from the resonance between the incident photon frequency and the collective excitation of conduction electrons, known as localized surface plasmon resonance (LSPR). (Khan et al., 2019)

LSPR excitation results in wavelength-selective absorption with a high molar extinction coefficient, resonant Rayleigh scattering comparable to the efficiency of multiple fluorophores, and enhanced local electromagnetic fields near the NP surface, facilitating enhanced spectroscopies. The peak wavelength of the LSPR spectrum is influenced by the size, shape, and interparticle spacing of the NPs, as well as the dielectric properties of the NPs themselves and their surrounding environment, including the substrate, solvents, and adsorbates. (Khan et al., 2019)

Gold colloidal NPs are responsible for the ruby colors observed in stained glass, while silver (Ag) NPs typically appear yellow. The free electrons (d electrons in Ag and Au) on the surface of these NPs can move freely throughout the nanomaterial. The mean free path for Ag and Au is approximately 50 nm, exceeding the size of these NPs. Consequently, light interaction does not lead to bulk scattering but instead induces standing resonance conditions, resulting in the LSPR phenomenon. (Khan et al., 2019)

2.4.2. Magnetic properties

Magnetic nanoparticles (NPs) have captured the interest of researchers across various fields, including heterogeneous and homogeneous catalysis, biomedicine, magnetic fluids, data storage, magnetic resonance imaging (MRI), and environmental remediation, particularly water decontamination. Studies have shown that NPs exhibit optimal performance when their size is below a critical value, typically 10-20 nm. At this scale, the magnetic properties of NPs become dominant, making them invaluable for diverse applications. (Khan et al., 2019)

The magnetic behavior of NPs arises from the uneven distribution of electrons within the particles. The synthesis method also plays a crucial role in determining these properties. Various techniques, such as solvothermal synthesis, co-precipitation, micro-emulsion, thermal decomposition, and flame spray synthesis, can be employed to prepare magnetic NPs with tailored characteristics for specific applications. (Khan et al., 2019)

2.4.3. Mechanical properties

The unique mechanical properties of nanoparticles (NPs) have sparked interest in exploring their potential applications in various fields, including tribology, surface engineering, nanofabrication, and nanomanufacturing. To understand their mechanical behavior, several parameters, such as elastic modulus, hardness, stress and strain, adhesion, and friction, can be investigated. Additionally, factors like surface coating, coagulation, and lubrication can influence the mechanical properties of NPs. (Khan et al., 2019)

NPs exhibit distinct mechanical properties compared to microparticles and their bulk counterparts. In lubricated or greased contacts, the difference in stiffness between NPs and the contacting surface determines whether the NPs are indented into the surface or deformed under significant pressure. This understanding is crucial for predicting NP performance in contact situations. (Khan et al., 2019)

Effective control over the mechanical properties of NPs and their interactions with surfaces is essential for improving surface quality and enhancing material removal processes. Successful advancements in these fields require a comprehensive understanding of the fundamental mechanical properties of NPs, including their size-dependent characteristics, such as elastic modulus, hardness, movement laws, friction, and interfacial adhesion. (Khan et al., 2019)

2.4.4. Thermal properties

It is well-established that metal nanoparticles (NPs) possess higher thermal conductivities than their corresponding bulk materials in solid or liquid form. For instance, copper's thermal conductivity at room temperature is approximately 700 times greater than that of water and about

3000 times greater than that of engine oil. Even metal oxide NPs, such as alumina (Al_2O_3), exhibit higher thermal conductivity compared to water. Consequently, fluids containing suspended solid NPs, known as nanofluids, are expected to demonstrate significantly enhanced thermal conductivities relative to conventional heat transfer fluids. (Khan et al., 2019)

Nanofluids are produced by dispersing nanometer-scale solid particles into base fluids like water, ethylene glycol, or oils. Due to the increased surface area of nanoparticles, nanofluids are anticipated to display superior heat transfer properties compared to conventional fluids and those containing larger, microscale particles. The large total surface area of the nanoparticles also contributes to the stability of the suspension. Recent research has demonstrated that nanofluids composed of CuO or Al_2O_3 NPs dispersed in water or ethylene glycol exhibit significantly improved thermal conductivity. (Khan et al., 2019)

2.5. Green Synthesis of nanoparticles

2.5.1. Scientific background

The scientific community increasingly recognizes the imperative of transitioning from considering green science as an optional path to embracing it as the fundamental approach in research and development. With the growing knowledge of nanomaterial synthesis, scientists are actively exploring and developing methods that minimize environmental impact and prioritize human safety. (Huston, M., 2021)

The foundation of green chemistry was laid in the early 2000s by Anastas and Warner through their seminal work, "Green Chemistry," which introduced the 12 Principles of Green Chemistry (Anastas P., Warner J. 2000):

1. **Prevention:** Proactive measures should be taken to prevent waste generation.
2. **Atom Economy:** Maximize the incorporation of starting materials into the final product.
3. **Less Hazardous Chemical Synthesis:** Prioritize synthesis methods that utilize materials with minimal or no toxicity to the environment or humans.
4. **Designing Safer Chemicals:** Design chemicals that achieve their intended function while minimizing toxicity.
5. **Safer Solvents and Auxiliaries:** Avoid the use of solvents and auxiliary chemicals whenever possible.
6. **Design for Energy Efficiency:** Minimize energy consumption during synthesis.
7. **Use of Renewable Feedstocks:** Employ renewable feedstocks and avoid resource depletion.

8. **Reduce Derivatives:** Minimize the use of derivatives like blocking agents and protecting/deprotecting groups, as they generate additional waste.
9. **Catalysis:** Favor catalytic agents over stoichiometric reagents.
10. **Design for Degradation:** Design chemicals to break down into non-toxic derivatives at the end of their lifecycle.
11. **Real-time Analysis for Pollution Prevention:** Monitor synthesis processes in real-time to prevent the formation of toxic chemicals.
12. **Inherently Safer Chemistry for Accident Prevention:** Select reagents and processes that minimize the risk of hazardous accidents.

These principles provide a framework for developing sustainable and environmentally responsible approaches in chemical synthesis and nanomaterial production.

Adherence to the 12 Principles of Green Chemistry is crucial for minimizing the release of hazardous materials into the environment and reducing human exposure to these chemicals. To facilitate the adoption of these principles, Gałuszka et al. proposed the mnemonic "SIGNIFICANCE" in their 2012 review of green analytical chemistry (Gałuszka et al.2013):

- **S** - Select direct analytical techniques
- **I** - Integrate analytical processes and operations
- **G** - Generate minimal waste and ensure proper treatment
- **N** - Never waste energy
- **I** - Implement automation and miniaturization of methods
- **F** - Favor reagents obtained from renewable sources
- **I** - Increase operator safety
- **C** - Carry out in-situ measurements
- **A** - Avoid derivatization
- **N** - Note the sample number and size should be minimal
- **C** - Choose multi-analyte or multi-parameter methods
- **E** - Eliminate or replace toxic reagents

This mnemonic serves as a helpful reminder of the key considerations for implementing green chemistry practices in analytical chemistry and beyond. By adhering to these principles,

scientists can contribute to a more sustainable and environmentally responsible approach to research and development.

A significant emphasis in green chemistry, highlighted by both Anastas and Warner and Gałuszka et al., is the utilization of agricultural waste as reducing and capping agents in nanoparticle synthesis. This waste often comprises various plant materials like onion peels, banana peels, honey, and other byproducts. (Yap et al., 2020. Tăbăran et al., 2020. Moulton et al., 2010. Krishnaswamy K., Orsat V, 2017. Lu Y., Ozcan S, 2015)

Furthermore, while many nanomaterials are traditionally synthesized using organic solvents, a greener alternative is the use of water (H_2O). Even slightly heated water can facilitate nanomaterial formation. Additionally, when water is heated to a supercritical state (above its critical temperature and pressure but below the solid phase), its properties change, enabling it to act as a solvent in the reaction (Wang Z., 2018. Stephenson et al., 2004. Soppimathet al., 2001). Other compounds suitable for use as supercritical fluids in nanomaterial synthesis include ethanol and carbon dioxide. (Stephenson et al., 2004. Lane M.K.M., Zimmerman J.B, 2019)

This approach aligns with the principles of green chemistry by reducing the reliance on hazardous chemicals and promoting the use of renewable resources, ultimately contributing to more sustainable and environmentally friendly nanomaterial production processes. (Huston, M., 2021)

The efficacy of nanomaterials in various applications is heavily influenced by their diverse facets, including morphology, size, and composition. For example, silver nanoparticle-coated nanosheets are highly valued for their electrical catalytic properties in electronics, yet unsuitable for biomedical imaging techniques like MRI (Shen H., 2015). This highlights the crucial role of these factors in determining nanomaterial functionality.

Nanomaterials are typically classified into three general morphologies: 0D, 1D, and 2D. These "dimensions" refer to any part of the nanomaterial exceeding 100 nanometers, sometimes extending into the micrometer range. (Huston, M., 2021)

- **0D nanomaterials:** These are nanoparticles that can adopt various shapes, ranging from triangles and hexagons to spheres and polymeric forms. They find applications in drug delivery, medical imaging, and other biomedical fields, as well as in optical and electronic technologies.

- **1D nanomaterials:** These typically take the form of nanorods, nanowires, or nanotubes. Their composition and formation vary slightly; for example, nanotubes are usually made of carbon and formed from rolled-up graphene sheets.

- **2D nanomaterials:** These materials have two dimensions exceeding 100 nanometers and include graphene, nanofilms, and nanocoatings.

Importantly, each of these nanomaterial types can be synthesized using green substrates and techniques, aligning with the principles of sustainable and environmentally friendly production processes. The versatility of nanomaterials and the ability to tailor their properties through green synthesis methods open up a wide range of possibilities for future technological advancements.

2.6. Definition of Green Synthesis of nanoparticles

The synthesis of nano-sized materials employing "green" processes is relatively cost-effective and does not harm the surrounding environment, as non-toxic chemicals are used throughout the entire process. Therefore, using stabilizers and reducing agents of biological origin, such as microbial entities, fauna, and various other resources, is a sustainable way to produce nano-sized materials. Although being cost-effective and environmentally friendly are key factors motivating the green synthesis of nano-sized materials, the "stability" of the produced material has attracted the attention of researchers worldwide. (Singh et al. 2023)

The methods involved in green synthesis are relatively diverse. Typically, living entities involved in the synthesis react with different metallic salts and reduce them to nano-sized materials, which can be utilized for different purposes following appropriate characterization. Both microbe- and plant-mediated approaches are employed to synthesize nano-sized materials:

1. **Microbe-Mediated Synthesis:**
    - Microbe-mediated synthesis involves the sophisticated biochemical machinery of microbes, leading to well-defined nanoparticles of different chemical compositions, shapes, and sizes.
    - However, scaling up microbial preparations can sometimes be challenging. (Singh et al. 2023)
2. **Plant-Mediated Synthesis:**
    - This drawback of microbial synthesis can be overcome by using plant-based extracts, which amplify production rates.
    - Plant extracts are more efficient than microbes in terms of production rate, reducing metal ions faster, and producing very stable nano-sized materials.
    - Plants contain various compounds (e.g., alkaloids, flavonoids, phenol, tannin, alcohol) capable of reducing metallic ions to nanoparticles with decent stability.

Current evidence suggests that the benefits of plant-based synthesis arise from the synergy of these compounds. (Singh et al. 2023)

A general scheme of the "green synthesis of nano-sized materials" is illustrated in Figure 1.

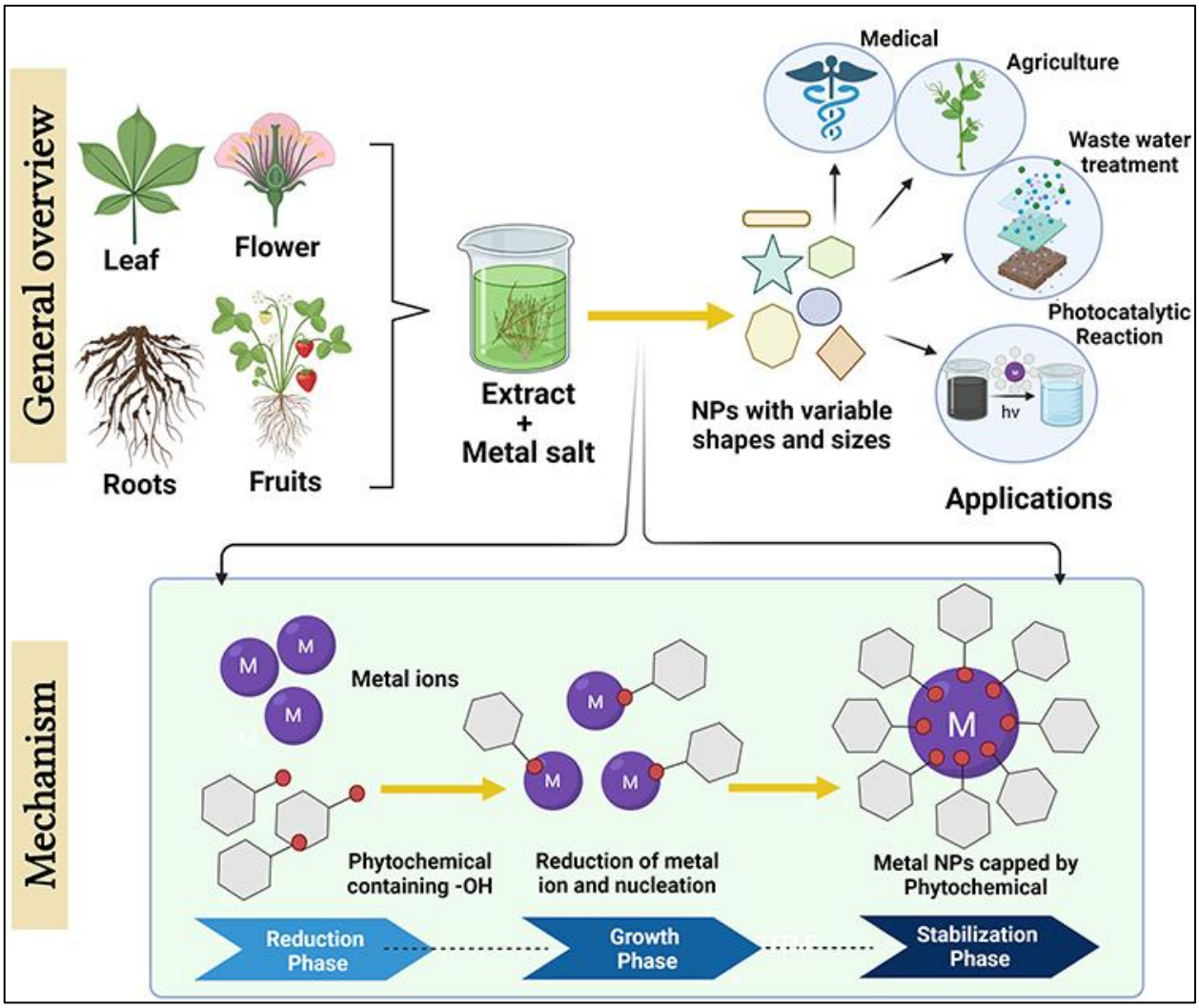

Figure 3: Schematic illustration of the method and mechanism involved in green synthesis of nanoparticles using plants as reducing agents (Singh et al. 2023)

2.7. ZnO Nanoparticles

Zinc oxide nanoparticles (ZnO NPs) have garnered significant attention from researchers and scientists over the past 4–5 years due to their wide range of applications in the biomedical field, as well as in optics and electronics. ZnO nanoparticles are particularly appealing because they are inexpensive to synthesize, safe, and can be produced using straightforward methods. These nanoparticles possess a high exciton binding energy of 60 meV and a large bandgap of 3.37 eV. Consequently, they exhibit various semiconducting properties such as high catalytic activity, wound healing, anti-inflammatory effects, and ultraviolet filtering properties. These

attributes make them extensively used in various cosmetics, such as sunscreen (Jadoun et al, 2020)

In addition to their use in cosmetics, ZnO nanoparticles have numerous biomedical applications, including antifungal, antibacterial, drug delivery, antidiabetic, and anticancer properties. Numerous studies have reported the synthesis and utilization of ZnO nanoparticles using plants, microorganisms, and other sources. Plant parts such as flowers, roots, seeds, and leaves have been employed for the synthesis of ZnOnanoparticles (Jadoun et al, 2020)

2.7.1. Synthesis of ZnO Nanoparticles Using Plant Extracts

ZnO nanoparticles can be synthesized by mixing a clear solution of plant extract with a 0.5 mM solution of hydrated zinc sulfate, zinc oxide, or zinc nitrate. The mixture is then boiled for a desired time and at a specific temperature to ensure effective mixing. Parameters such as time, temperature, and pH can be optimized during this process. A change in color typically indicates the formation of ZnO nanoparticles. These nanoparticles are characterized using various techniques for spectral, morphological, and thermal analysis. For instance, energy-dispersive X-ray analysis (EDAX) and scanning electron microscopy (SEM) provide different results compared to X-ray diffraction (XRD).

- **Examples of ZnO Nanoparticle Synthesis**

1. **Azadirachta indica (Neem) :**
    - The leaves of Azadirachta indica (Neem) from the Meliaceae family have been widely used for the synthesis of ZnO nanoparticles (Bhuyan et al. 2015).
2. **Vitex negundo :**
    - Both the flowers and leaves of the Vitex negundo plant have produced ZnO nanoparticles with an average size of 38.17 nm, as determined by the Debye–Scherrer equation using XRD (Ambika and Sundrarajan 2015).
3. **Functional Groups Involvement :**
    - FTIR studies confirm the involvement of functional groups such as alcohols, alkanes, carbonates, amides, carboxylic acids, and amines in nanoparticle synthesis.

2.7.2. Microbial Synthesis of ZnO Nanoparticles

2.7.2.1. Bacillus licheniformis :

ZnO nanoflowers synthesized by Bacillus licheniformis were uniform in size and demonstrated highly enhanced photostability and photocatalytic activity for methylene blue (MB) dye degradation, achieving 83% dye degradation. Three repeated cycles of the experiment

at different time intervals showed 74% degradation, highlighting the photostability of the ZnO nanoflowers (Auld 2001).

2.7.2.2. Lactobacillus Plantarum :

Lactobacillus plantarum was used to synthesize ZnO nanoparticles, which were found to be moderately stable with a zeta potential value of −15.3 mV (Selvarajan and Mohanasrinivasan 2013).

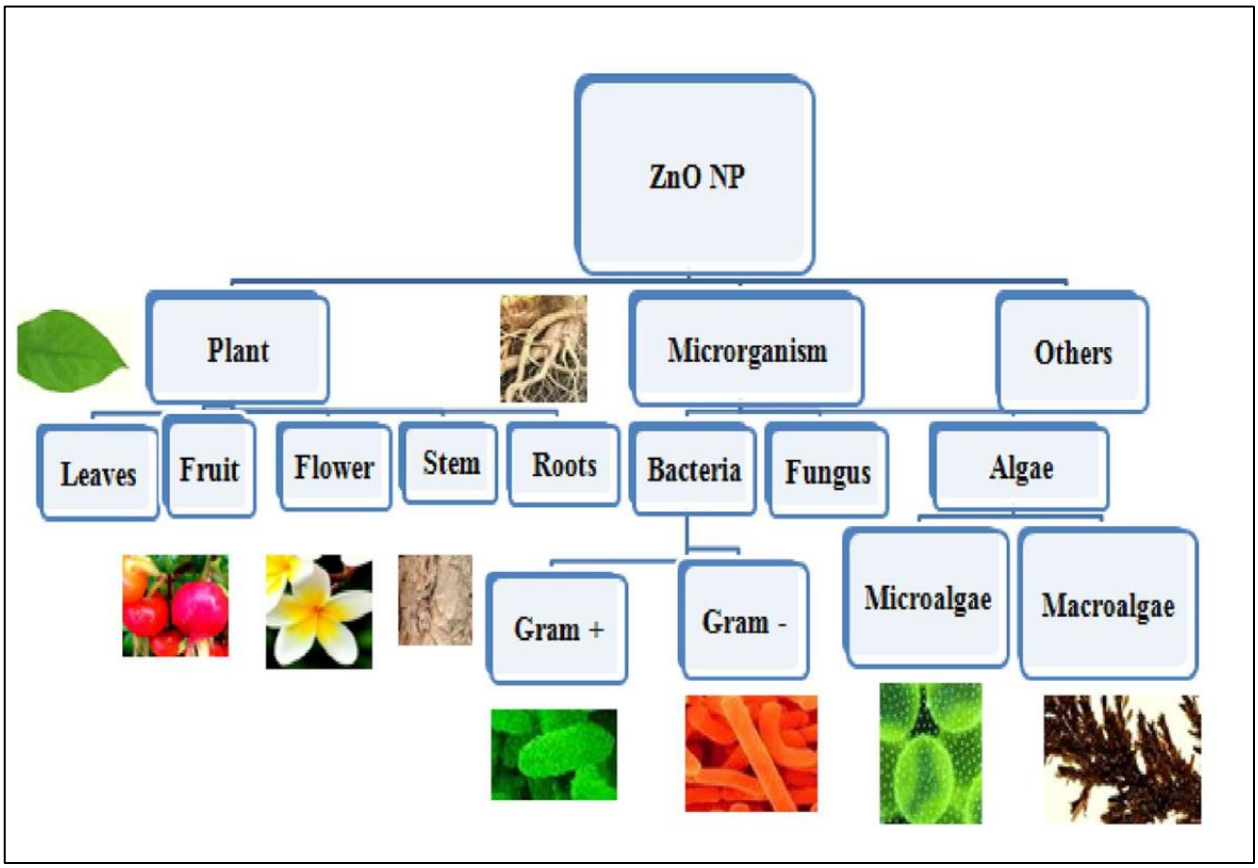

Figure 4: Biosynthesis of zinc oxide nanoparticles (Jadoun et al. 2020)

2.8. Selenium Nanoparticles (SeNPs)

Elemental selenium (Se) holds significant importance in physics, chemistry, and biology. Selenium exists in both crystalline and amorphous polymorphic structures. The crystalline forms include monoclinic selenium (m-Se), which is red and contains rings of Se8, and trigonal selenium (t-Se), which is black and the most stable form at room temperature. Non-crystalline forms include red amorphous (a-Se), black amorphous, and vitreous selenium. Selenium plays a critical role in human biology, being part of selenoproteins and selenocompounds, and is essential for reproduction, DNA synthesis, thyroid hormone metabolism, and protection from infections and oxidative damage. However, the margin between its beneficial and toxic doses is narrow. The recommended daily intake of selenium is 60 μg for women and 70 μg for men, with

toxicity occurring at intakes above 400 µg, leading to selenosis. In recent years, the advent of nanotechnology has expanded the applications of selenium, particularly in the form of selenium nanoparticles (SeNPs) (Bisht et al. 2022).

SeNPs are economical to synthesize compared to other metal nanoparticles like gold (Au) and silver (Ag), and they can be integrated with biological agents to enhance their properties. The high surface-to-volume ratio of SeNPs at the nano-level leads to enhanced biological activity. SeNPs exhibit promising potential as antioxidants, cancer therapeutic agents, and drug carriers. They have been shown to possess significant anticancer, antioxidant, antimicrobial, and anti-biofilm properties. For instance, Vahdati et al. demonstrated the synergistic antimicrobial effect of SeNPs and lysozymes. Additionally, SeNPs have been used in the therapy of Huntington's disease with promising results. Beyond biomedical applications, SeNPs possess unique semiconducting, photoelectric, and X-ray-sensing properties, making them useful in photocells, photocopying, photometers, and xerography. They also play a role in renewable energy devices and have environmentally important mercury-capturing properties. (Bisht et al. 2022)

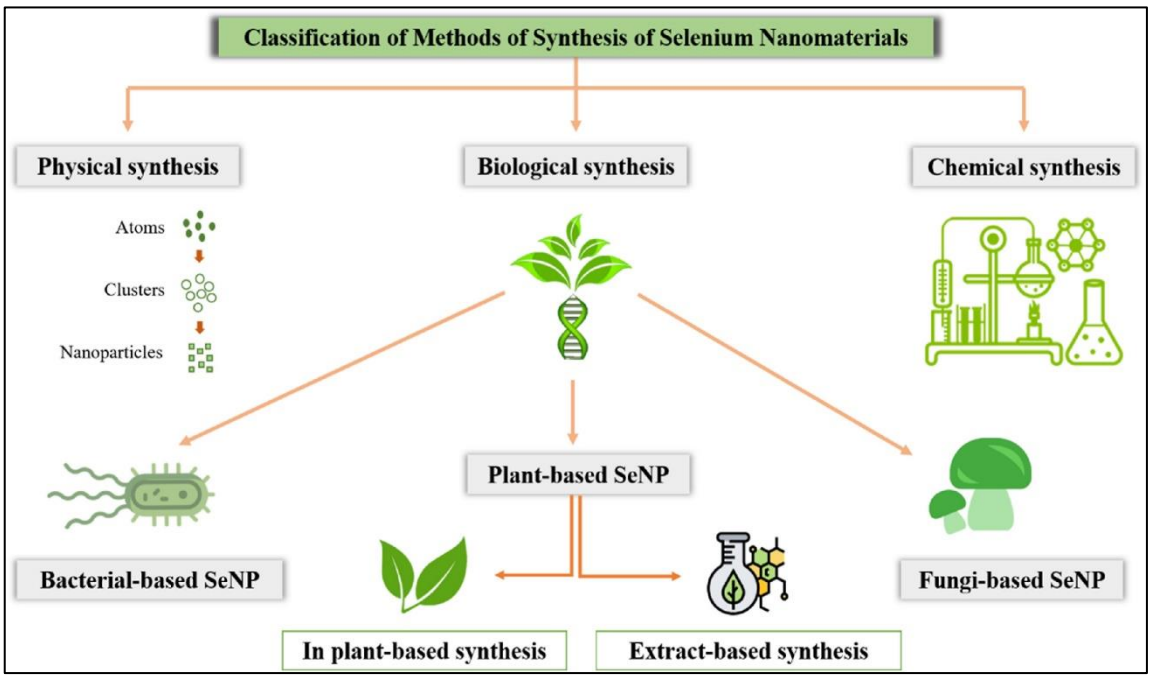

Figure 5: The different methods of synthesis and sources of synthesis of Selenium nanoparticles (Karthik, 2024)

2.8.1. Green synthesis of Selenium Nanoparticles (SeNPs)

SeNP green synthesis is a simple, one-step process that does not require toxic chemicals, high temperatures, or complex equipment. Green synthesis can be realized in two ways: directly

in living organisms or with the help of bioreagents extracted from them. Precursors such as sodium selenite/selenate, selenous acid, and selenium dioxide are used for SeNP synthesis by adding them to a "bioreactor" like bacteria or fungi culture fluid, or plant extract. The addition of these precursors to the bioextract results in a red, red–orange, or orange solution, indicating the reduction of selenium compounds and the formation of colloidal SeNPs. Subsequent stabilization and capping processes prevent nanoparticle agglomeration. (Mikhailova, 2023)

The reduction of selenium salt to elemental selenium (Se0) occurs due to various biopolymers capable of performing this role. In bacteria, enzymes such as thioredoxin reductase, nitrite reductase, or other membrane reductases are assumed to be responsible for SeNP synthesis. These bacterial reductases can reduce the water-soluble oxyanion SeO_4^{2-} to SeO_3^{2-}, and then to insoluble elemental selenium Se0 in a two-stage reaction. In plants, a variety of proteins, terpenoids, vitamins, flavonoids, tannins, polysaccharides, and other biologically active substances may be responsible for both the reduction process and SeNP stabilization and capping, preventing their agglomeration in aqueous solution. (Mikhailova, 2023)

Capping agents, essential components of nanoparticles, are particularly attractive for study due to their therapeutic significance. These biocompounds often enhance the medical effect of SeNPs and reduce their toxicity. This is especially true for plant-derived SeNPs, as medicinal herbs used in their production are known for their beneficial effects on the body. (Mikhailova, 2023)

2.8.2. SeNPs Biosynthesis by Plants

The diversity of plant-based selenium nanoparticles is vast. Medicinal plants from traditional systems like Chinese medicine and Ayurveda, as well as commonly consumed plants, serve as "biofactories." For instance :

- **Roots :** Blumea axillaris
- **Peel :** Solanum melongena (eggplant)
- **Wheat Seedlings :** Triticum aestivum
- **Leaves :** Azadirachta indica (neem), Petroselinum crispum (parsley)
- **Stem :** Banana
- **Flowers :** Calendula officinalis (marigold)

The specific mechanism of SeNP synthesis in plants varies, with various biomolecules—proteins, enzymes, flavonoids, terpenoids, sterols, polysaccharides, vitamins, phenolic

compounds, organic acids, and lignin—participating in nanoparticle synthesis and packaging. These biomolecules act as reducing agents and electron donors for metal ions, converting them into nanoparticles, preventing aggregation, and promoting the formation of smaller particles (Mikhailova, 2023)

2.8.3. The health effects of selenium and zinc nanoparticles

The health effects, particularly the hepatoprotective effects, of nanoparticles of selenium (Se) and zinc oxide (ZnO) nanoparticles have been studied extensively. Here's an overview of their potential impacts:

2.8.3.1. Selenium Nanoparticles (Se NPs)

- **Hepatoprotective Effects:** Studies have shown that selenium nanoparticles possess hepatoprotective properties by reducing oxidative stress and inflammation in the liver. Se NPs can scavenge free radicals and enhance antioxidant enzyme activity, thereby protecting liver cells from damage caused by toxins or diseases. (Zhang, 2016)
- **Anti-inflammatory Activity:** Selenium nanoparticles exhibit anti-inflammatory effects that can alleviate liver inflammation and prevent the progression of liver diseases. Zhou, 2019
- **Antioxidant Effects:** Se NPs have strong antioxidant properties, which contribute to their hepatoprotective effects by neutralizing reactive oxygen species (ROS) and reducing lipid peroxidation in hepatocytes. (Zhou, 2019)

2.9.3.2. Zinc Oxide Nanoparticles (ZnONPs):

- **Hepatoprotective Effects:** Zinc oxide nanoparticles have been reported to exhibit hepatoprotective effects against liver damage induced by various toxins or drugs. ZnO NPs mitigate oxidative stress, enhance antioxidant defenses, and promote liver regeneration. (Hussain, 2005)
- **Anti-inflammatory and Immunomodulatory Actions:**

ZnO nanoparticles possess anti-inflammatory properties that can suppress inflammatory responses in the liver. They also modulate immune responses, which can contribute to liver protection. (Sriram, 2012)

- **Regulation of Apoptosis and Cell Signaling:**

ZnO NPs influence cellular pathways involved in apoptosis (cell death) and signal transduction, which play roles in liver cell survival and regeneration. (Sriram, 2012)

Chapter 3

Overview of Deltamethrin

3.1. Identity of Deltamethrin

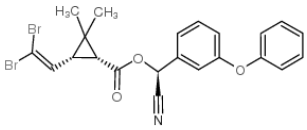	**Common Name**	**Deltamethrin**		
	CAS Number	52820-00-5	**Molecular Weight**	505.19900
	Density	1.595g/cm3	**Boiling Point**	535.8ºC at 760mmHg
	Molecular Formula	C22H19Br2NO3	**Melting Point**	101-102ºC
	MSDS	N/A	**Flash Point**	277.8ºC

- **Synonyms and trade names:**

Butoflin, Butox, Cislin, Decamethrin, Decis, FMC 45498, K-Obiol, K-Othrine, NRDC 161, RU 22 974, WHO 1998 (OMS 1998).

CAS registry no: 52918-63-5

Relative molecular mass: 505.24

Deltamethrin is a synthetic dibromo-pyrethroid. Of the eight possible stereoisomers, it contains only the d-cis isomer. Technical grade deltamethrin is more than 98% pure.

It is mainly formulated as emulsifiable concentrates (25-100 g/litre), ultra-low volume concentrates (1.5-30 g/litre), wettable powders (25-50 g/litre), flowable powders (7.5-50 g/litre), or dust powders (0.5-2 g/kg).

3.2. Physical and Chemical Properties

The technical product referred to is deltamethrin, which is an odorless white crystalline powder. It exhibits almost no solubility in water but can dissolve in various organic solvents.

Deltamethrin demonstrates stability to light, heat (up to 6 months at 40°C), and air. However, it is unstable in alkaline media.

Physical and chemical properties of deltamethrin, as provided in the International Chemical reference (WHO, 1989):

- Appearance: Odorless white crystalline powder

- Solubility: Almost insoluble in water, but soluble in many organic solvents

- Stability: Stable to light, heat (up to 6 months at 40°C), and air; unstable in alkaline media

These properties are essential for understanding the handling, storage, and applications of deltamethrin in various industries, particularly in agriculture and pest control.

3.3. Uses

Deltamethrin finds its primary application in cotton, constituting 45% of its usage, as well as in various crops like coffee, maize, cereals, fruits, vegetables, and hops, along with stored products. Additionally, it is utilized in animal health, vector control, and public health sectors. Deltamethrin comes in various formulations including emulsifiable concentrate, ultra-low-volume concentrate, wettable powder, suspension concentrate, or dust powder, either independently or in conjunction with other pesticides. (WHO, 1989)

3.4. Effects on Experimental Animals and In Vitro Test Systems

3.4.1. Single Exposures

Rats were administered intraperitoneal injections of 14C-labelled deltamethrin at doses sufficient to induce motor symptoms of toxicity such as tremor and choreoathetosis. Blood and brain samples were collected and analyzed for their total radiolabel content. Additionally, ethyl acetate extraction was performed to determine levels of extractable parent deltamethrin and 3-phenoxybenzyl-derived acid, as well as residual radiolabel post-extraction. A clear correlation was observed between symptom onset and deltamethrin levels in the blood and brain. The study revealed that specific threshold levels of parent deltamethrin in these tissues were necessary for symptom development and that symptoms persisted as long as this threshold was maintained (Rickard & Brodie, 1985).

3.4.2. Acute Oral Toxicity in Non-Aqueous Mediums

In non-aqueous mediums, the acute oral toxicity of deltamethrin ranges from high to moderate, with LD50 values of 19 - 34 mg/kg for mice and 31 - 139 mg/kg for rats. However, when suspended in water, its toxicity significantly decreases, with LD50 values surpassing 5000 mg/kg for rats. Classified as a Type II pyrethroid, clinical symptoms of deltamethrin poisoning include tremors, salivation, and convulsions, with rapid onset and disappearance within several days in survivors. Electroencephalogram readings indicate generalized spike and wave discharges preceding choreo-athetosis. (WHO, 1989)

3.4.3. Skin and Eye Irritation

Single applications of technical deltamethrin did not induce any irritant effects on intact or abraded rabbit skin. However, transient irritations were observed in rabbit eyes, both with and without rinsing. Deltamethrin did not exhibit skin sensitization in guinea pigs. (WHO, 1989)

3.4.4. Chronic Toxicity in Rats

In rats orally dosed with deltamethrin up to 10.0 mg/kg body weight per day for 13 weeks, hyperexcitability was observed at 6 weeks in males receiving the highest dose, along with lower body weight gain in males receiving 2.5 and 10 mg/kg. (WHO, 1989)

3.4.5. Long-Term Feeding Studies in Mice and Rats

In a 24-month study where mice were fed deltamethrin up to 100 mg/kg diet, tumor incidence remained unaffected, with 100 mg/kg diet as the no-observed-effect level for systemic toxicity. Rats fed deltamethrin at levels of up to 50 mg/kg diet for 2 years showed no compound-related tumors, with 50 mg/kg diet as the no-observed-effect level for systemic toxicity. (WHO, 1989)

3.4.6. Mutagenicity Testing

Deltamethrin did not demonstrate mutagenicity in various in vivo and in vitro test systems, including DNA repair, gene mutation, chromosomal aberration, sister chromatid exchange, micronucleus formation, and dominant lethal tests. (WHO, 1989)

3.4.7. Teratology Studies

Teratology studies on pregnant rats and mice receiving deltamethrin orally at levels of up to 10 mg/kg body weight per day during major organogenesis showed no teratogenic or reproductive effects, except for a dose-related decrease in mean fetal weight in the mouse study and slightly delayed ossification in the rat study. (WHO, 1989)

3.4.8. Reproduction Studies

In a 3-generation, 2-litter reproduction study where rats were fed deltamethrin at levels of up to 50 mg/kg diet, no reproductive effects were noted. There are indications that toxicity potentiation may occur when deltamethrin is combined with certain organophosphorus compounds. (WHO, 1989)

3.5. Effects on Human Beings

3.5.1. Skin Sensations and Occupational Exposure

- Deltamethrin exposure can lead to skin sensations in workers.
- Neglect of safety precautions in occupational settings have resulted in non-fatal cases of poisoning.
- Symptoms such as numbness, itching, tingling, and burning of the skin, along with vertigo, are commonly reported.
- Occasionally, transient popular or blotchy erythema has been observed.

- Most symptoms resolve within 5 - 7 days with no long-term adverse effects reported. (WHO, 1989)

3.5.2. Cases of Ingestion Poisoning

- Three non-fatal cases of deltamethrin poisoning have been documented following ingestion of several grams of the product. (WHO, 1989)

3.6. Variability in Toxicity Levels of Deltamethrin: Insights from LD50 Values

Deltamethrin exhibits varying degrees of toxicity depending on the dosage administered. Studies have shown that the acute oral toxicity of deltamethrin in different species, such as mice and rats, can be quantified by its LD50 values. For instance, in non-aqueous solutions, LD50 values range from 19 to 34 mg/kg for mice and 31 to 139 mg/kg for rats, indicating a moderate to high toxicity level. However, when deltamethrin is suspended in water, its toxicity significantly decreases, with LD50 values exceeding 5000 mg/kg for rats. This substantial contrast in LD50 values underscores the importance of considering the formulation and delivery method when assessing the potential toxicity of deltamethrin. Furthermore, studies have explored the correlation between deltamethrin dosage and the onset of symptoms, such as tremor and choreoathetosis, revealing that specific threshold levels of deltamethrin in the blood and brain are required for symptom development and persistence (Rickard & Brodie, 1985).

3.7. Toxicology of Deltamethrin

3.7.1. Deltamethrin-mediated oxidative damage

Oxidative stress occurs when there is an imbalance between the production of reactive oxygen species (ROS) and reactive nitrogen species (RNS) and the ability of the body to detoxify or neutralize their harmful effects. These species include superoxide anion ($O_2^{\bullet -}$), hydrogen peroxide (H_2O_2), hydroxyl radical ($HO^{\bullet}$), hypochlorous acid (HOCl), hydroperoxyl radical ($HOO^{\bullet}$), nitric oxide (NO), and peroxynitrite.

Deltamethrin, an insecticide, has been shown to induce oxidative stress by generating ROS and RNS. Studies have demonstrated that deltamethrin increases ROS production in various cell types, including PC12 cells and murine thymocytes. Similarly, it induces cell death and ROS production in rat primary hepatocytes. In vivo studies on rainbow trout have also shown a significant increase in ROS production following deltamethrin exposure. Moreover, deltamethrin treatment has been linked to increased NO production, which contributes to oxidative damage. Administration of deltamethrin in rats resulted in elevated activities of nitric oxide synthase

(NOS) and poly (ADP-ribose) polymerase (PARP) in the brain. Neurotoxicity induced by deltamethrin in rats has been associated with increased NO production. Deltamethrin has been found to promote NOS activity, further exacerbating oxidative stress. Studies on Anatolian water buffaloes showed increased plasma NO levels after deltamethrin treatment. The oxidative stress induced by deltamethrin can lead to damage to lipids, DNA, and proteins, ultimately resulting in cell death and apoptosis. However, the detailed mechanism by which deltamethrin increases ROS and RNS production requires further investigation. Overall, the evidence suggests a strong relationship between deltamethrin exposure, oxidative stress, and various adverse health effects, including cellular damage and neurotoxicity.

3.7.2. Factors Influencing Deltamethrin Toxicity

Factors influencing deltamethrin toxicity can vary widely and may include dosage, route of exposure, duration of exposure, individual susceptibility, and environmental conditions.

Dosage: The toxicity of deltamethrin is often dose-dependent, meaning higher doses typically result in more severe toxic effects. Exposure to high doses of deltamethrin can lead to acute poisoning symptoms such as tremors, convulsions, and respiratory distress.

Route of Exposure: The route through which deltamethrin enters the body can significantly influence its toxicity. Deltamethrin can be absorbed through ingestion, inhalation, or dermal contact. Ingestion of deltamethrin-containing products can result in systemic toxicity, while inhalation or dermal exposure may lead to localized or systemic effects depending on the dose and duration of exposure.

Duration of Exposure: The duration of exposure to deltamethrin also plays a critical role in its toxicity. Acute exposure to high doses may result in immediate symptoms of poisoning, while chronic exposure to lower doses over an extended period can lead to cumulative toxicity and health effects such as neurotoxicity or reproductive toxicity.

Individual Susceptibility: Individual factors such as age, genetics, pre-existing health conditions, and metabolic differences can influence an individual's susceptibility to deltamethrin toxicity. Children, elderly individuals, and individuals with compromised liver function may be more vulnerable to the toxic effects of deltamethrin.

Environmental Conditions: Environmental factors such as temperature, humidity, and presence of other chemicals can affect the absorption, distribution, metabolism, and excretion of deltamethrin in the body. Additionally, environmental persistence of deltamethrin residues can lead to continued exposure and potential health risks for humans and other organisms. (David 2016)

3.8. Liver

The liver plays a crucial role in maintaining digestion and overall health through a variety of essential functions. It produces bile to aid in fat digestion, regulates bilirubin levels to prevent jaundice, and stores blood while synthesizing clotting factors necessary for coagulation. Metabolically, it processes nutrients for energy and detoxifies harmful substances, contributing significantly to the body's detoxification process. Additionally, the liver stores vital minerals and vitamins and participates in immune defense mechanisms. Its multifaceted contributions highlight its indispensable role in sustaining bodily functions and promoting well-being.

3.8.1. Liver histology

The liver's fundamental structural unit is the liver lobule, which takes on a hexagonal shape similar in size to a sesame seed. It comprises hepatocyte plates arranged around a central vein, with portal triads located at each corner. Within the liver lobule, one finds liver sinusoids, Kupffer cells, bile canaliculi, and the Space of Disse. Portal triads consist of a hepatic portal arteriole, a hepatic portal venule, and a bile duct. Blood circulates through sinusoids toward the central vein, while bile moves in the opposite direction. Hepatocytes are responsible for processing nutrients, while Kupffer cells play a role in removing worn-out blood cells and bacteria, contributing to the liver's vital functions

3.8.2. Cellular architecture of the liver

The liver is the largest internal organ in the human body and plays a crucial role in metabolism, detoxification, and storage of nutrients. Its unique cellular architecture enables it to perform these diverse functions efficiently.

The basic functional unit of the liver is the liver lobule, a hexagonal structure consisting of hepatocytes (liver cells) arranged in plates radiating from a central vein. These plates are separated by sinusoids, which are blood-filled spaces lined with endothelial cells and Kupffer cells (specialized macrophages). Blood flows from the portal vein and hepatic artery into the sinusoids, where it comes into contact with hepatocytes for metabolic exchange.

Portal triads, located at the corners of the lobule, contain branches of the hepatic artery, portal vein, and bile duct. The hepatic artery supplies oxygenated blood to the liver, while the portal vein carries nutrient-rich blood from the digestive system. The bile duct collects bile produced by hepatocytes and transports it to the gallbladder for storage and concentration.

The acinus is another functional unit of the liver, representing the smallest unit of hepatic parenchyma supplied by a terminal branch of the hepatic artery and portal vein. It is divided into

three zones based on the distance from the blood supply: zone 1 (periportal), zone 2 (intermediate), and zone 3 (perivenous).

This complex cellular architecture allows for efficient blood flow, nutrient exchange, and bile production, enabling the liver to perform its vital functions.

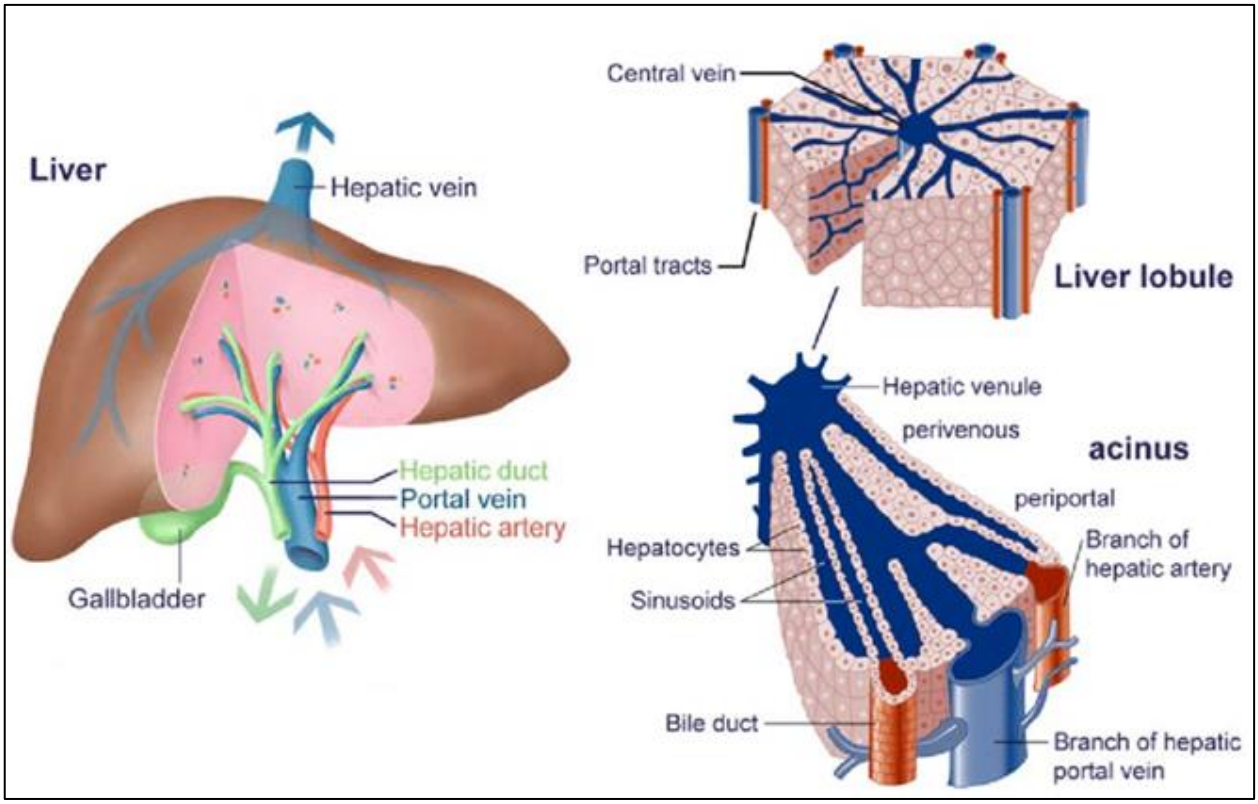

Figure 6: Liver structure and functional subunits (by Jeffrey J Chalmers)

3.8.3. Liver Lobules

The liver acts as the primary destination for venous blood originating from the intestines, which arrives via the vena porta. It is organized into periportal regions surrounding incoming blood vessels and perivenous regions around outgoing vessels. The periportal area is intricate, consisting of a collagen matrix that accommodates incoming blood vessels, bile ducts, nerves, and lymphatic vessels. Additionally, this region hosts various cell types, including fibroblasts, hematopoietic cells, inflammatory cells, as well as epithelial and endothelial cells, along with smooth muscle cells (Butura A. (2008), Grisham JW (1983)) .

Within the liver lobule, the primary structural components are hepatocytes and sinusoids, which are interconnected by a collagen matrix. Kupffer cells and stellate cells are situated in the tissue space between hepatocytes and sinusoids, while terminal bile ductules link to bile canaliculi between hepatocytic plates (Grisham JW (1983)) . The walls of hepatic sinusoids are

lined by sinusoidal endothelial cells, Kupffer cells, and stellate cells, sometimes accompanied by liver-specific natural killer (NK) T cells Kmiec (Z.(2001)) .

Hepatocytes constitute the main parenchymal mass, making up approximately 60% of the liver cell count in rats, with non-parenchymal cells and extracellular spaces constituting the remainder (Hendriks HF et al. (1990)) . The liver comprises diverse cell types, including hepatocytes, endothelial cells, Kupffer cells (resident macrophages), and stellate cells.

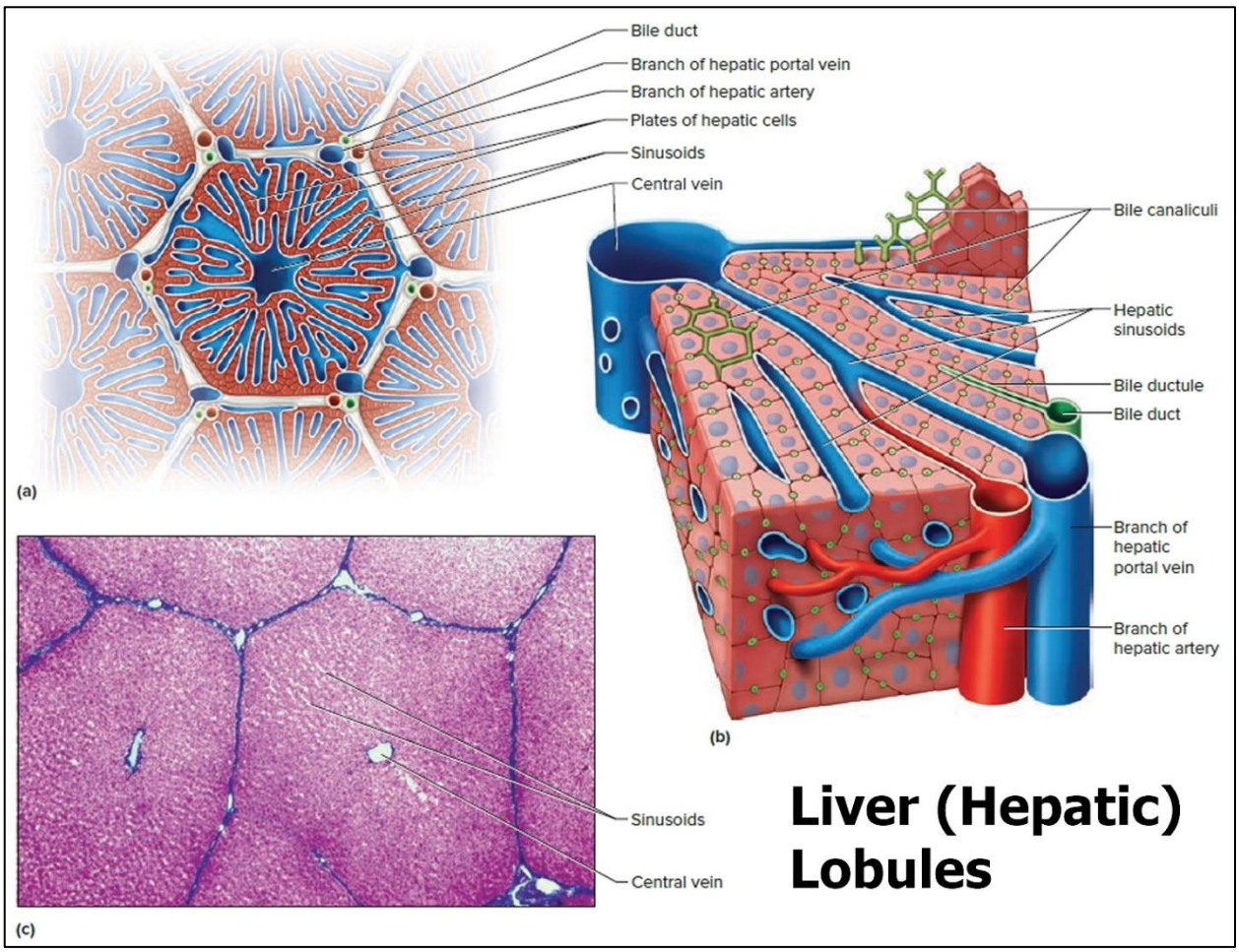

Figure 7: Liver lobules ((a) Cross section of a hepatic lobule. (b) Enlarged longitudinal section of a hepatic lobule. (c) Light micrograph of hepatic lobules in cross section. Health Jade Team on July 8, 2019)

3.8.4. Hepatocytes

Hepatocytes, comprising 60% of liver cells, are pivotal for liver function. They extract toxins and nutrients from blood, facilitating lipid, carbohydrate, and protein metabolism. Hepatocytes synthesize serum proteins, bile, and detoxify substances. Their function varies based on location within the liver lobule, with periportal hepatocytes primarily involved in

gluconeogenesis and perivenous hepatocytes dominant in glycolysis and hydroxylation reactionsButura A. (2008), [17] Smith MT, Wills ED (1981), Gebhardt R, Mecke D.(1983) .

3.8.5. Endothelial Cells

Sinusoidal endothelial cells line hepatic sinusoids, facilitating filtration and possessing high endocytic capacity. They potentially contribute to viral clearance and antigen presentation [19, 12]. [19] Breiner KM et al. (2001), Kmiec Z.(2001) .

3.8.6. Kupffer Cells

Liver-resident Kupffer cells are the largest tissue macrophage population, constantly activated by gut-derived particles. They secrete inflammatory mediators and phagocytose cells via receptors for immunoglobulins and complement [20, 21, 22]. [20] Knook DL et al., (1982), Kmiec Z. (2001), Smedsrod B et al. (1985), Munthe-Kaas AC et al.(1976) .

3.8.7. Stellate Cells

Stellate cells store vitamin A, regulate extracellular matrix turnover, and contractility. Under stress, they activate into myofibroblast-like cells, increasing extracellular matrix production and contributing to fibrotic responses [23, 24]. [23] Knook DL et al. (1982), Friedman SL. (2008)

3.9. Functions of the liver

The liver performs a wide array of functions, which can be categorized into several main groups: bile secretion, bilirubin metabolism, vascular and hematologic functions, nutrient metabolism, metabolic detoxification, and storage of minerals and vitamins.

Tableau 8. Summary Of Major Functions of The Liver

Secretion of Bile
Metabolism of Bilirubin
Vascular and Hematologic Functions • Important blood reservoir
Metabolism of Nutrients • Fat - fatty acid oxidation, synthesis of cholesterol/lipoproteins and production of ketoacids • Protein – Amino acid production, turnover of proteins

- Carbohydrate – converts galactose/fructose to glucose, gluconeogenesis and contains 100g of glycogen for release

Metabolic Detoxification

- Toxins
- Hormones
- Drugs

Storage of Minerals and Vitamins

- Iron
- Copper
- Vitamins ADEKB12
- Glycogen

Endocrine functions

- Activation of vitamin D
- Conversion of thyroxine (T4) to T3
- Secretes angiotensinogen
- Metabolises hormones

Immunological/ Protective Functions Reticuloendothelial Component

- Filters the portal blood from bacteria
- Important in antigen presentation
- Phagocytosis via kupffer cells
- Removes haemolysis products Inactivation of Toxins and Drugs
- Phase I (oxidation, reduction and hydrolysis)
- Phase II (conjugation/ cytochrome P450 system)

3.10. Effect of deltamethrin in Liver

The histological examination of the liver in rats treated with deltamethrin revealed several notable findings：

3.10.1. Dilated and congested central veins

The central veins, which are crucial vessels in liver circulation, were observed to be dilated and congested. This indicates impaired blood flow within the liver.

3.10.2. Necrosis and mononuclear cell infiltration

Some areas of the central vein exhibited necrosis, characterized by tissue death, and infiltration of mononuclear cells. This suggests inflammatory processes and tissue damage.

3.10.3. Loss of hepatocyte architecture

Hepatocytes, the main functional cells of the liver, lost their normal architecture. This indicates cellular damage and dysfunction.

3.10.4. Vacuolization in hepatocyte cytoplasm

Vacuoles, which are abnormal fluid-filled structures, appeared in the cytoplasm of hepatocytes. This is indicative of cellular stress or metabolic dysfunction.

3.10.5. Cell degeneration and cellular debris

The liver sections showed evidence of cell degeneration and the presence of cellular debris, suggesting ongoing tissue damage and turnover.

3.10.6. Congestion and dilation in central veins (Group C)

Similar to group B, group C exhibited congestion and dilation of central veins. Additionally, cell degeneration and vacuolization were observed in hepatocytes.

3.10.7. Mild variations in hepatic architecture (Group D)

Group D showed milder alterations compared to groups B and C. This included mild dilation in central veins and less severe effects on hepatocytes, fat vacuoles, sinusoids, and central veins.

Overall, the histological analysis suggests that deltamethrin exposure leads to liver damage characterized by vascular congestion, necrosis, inflammation, hepatocyte degeneration, and vacuolization. The severity of these effects appears to be dose-dependent, with higher doses causing more pronounced histopathological changes. (Pooname et al., 2014)

Part 2

Practical Part

Chapter 1

Materials and methods

4.1. Materials and methods

4.2.1. Biological materials

The biological materials used in this context include:

- **Moringa:**

This refers to parts of the Moringa tree used for analysis or experimentation. The leaves were picked from the home garden in the house of (CH. A), located in the Al-Hood Al-Gharbi neighborhood, Guemar Municipality, El-Oued Province, as described in the document. (The coordinates of the site: 33.52538087267938, 6.7782930928672105. https://maps.app.goo.gl/miPBKoWqBaYZdYLt8)

Figure 8: An image from Google Maps showing the location of the tree used in the study

- **Blood and organs from rats for histo-hemobiochemical analysis**

– Liver (hepatic tissue)

– Blood

The study parameters were carried out at the laboratory of the Faculty of Natural and Life Sciences at Echahid Hamma Lakhdar University in El-Oued. Blood analyses were conducted at El Rimal Clinic in El Oued and at the medical analysis laboratories EL-Mordjan and Belkhir.

4.2.1. Non-biological material

The equipment used in the laboratory consists of equipment, chemicals, and material.

- **Devices**

Devices	Career Objective
Centrifuge	Separates components of a mixture based on density by spinning at high speeds.

Magnetic agitator	Stirs liquids using a rotating magnetic field and a magnetic stir bar placed inside the liquid.
Spectrophotometer	Measures the intensity of light absorbed or transmitted by a sample at specific wavelengths, used for quantitative analysis.
Oven	Heats or dries substances at controlled temperatures.
Hood (Fume Hood)	Provides ventilation to remove hazardous fumes and vapors generated during experiments, protecting the user.
Electronic scale	Measures the mass of objects accurately.
PH Meter	Measures the acidity or alkalinity of a solution.

- **Materials**

Solvents (for Extraction)	Dissolve specific chemical components from a mixture, allowing for separation and isolation.
EDTA Tube	Contains EDTA (ethylenediaminetetraacetic acid), an anticoagulant that prevents blood clotting, used for hematological tests.
Heparin Tube	Contains heparin, another anticoagulant, typically used for blood chemistry and certain genetic tests.
Culture Media	Provides nutrients for growing microorganisms (bacteria, fungi) in controlled laboratory conditions.
Incubators	Maintain optimal temperature and humidity conditions for growing cell cultures or microorganisms.
Inoculating Loops or Needles	Transfer small amounts of microorganisms to culture media for growth.
Autoclave	Sterilizes equipment and materials using high-pressure steam to kill microorganisms.
Pipettes and Bunsen Burners	Pipettes transfer precise volumes of liquid, while Bunsen burners provide a flame for sterilization and heating.
Mueller-Hinton Agar	A specific type of culture medium commonly used for antibiotic susceptibility testing.
Autoanalyzer Mindray BC-	Automated hematology analyzer that measures

2800	various blood cell parameters.

- **Chemical materials**

Chemical	Chemical Formula	Functional Objective (Task)
Ethanol	CH3-CH2-OH	Solvent, fixative, denaturant
Methanol	CH3OH	Solvent, fixative, denaturant
Sodium citrate	Na3C6H5O7	Anticoagulant, buffering agent, food preservative
Methylene blue	C16H18ClN3S	Stain, redox indicator, antiseptic
Phosphate buffered Saline	Mixture of salts	Washing buffer, diluent, isotonic solution
Saline serum	0.9% NaCl in water	Electrolyte replacement, vehicle for drug delivery
Ascorbic acid (Vitamin C)	C6H8O6	Antioxidant, cofactor for enzymes
Potassium ferricyanide	K3[Fe (CN)6]	Oxidizing agent, redox indicator
Salicylic acid	C7H6O3	Anti-inflammatory, analgesic, plant hormone
NaCl (Sodium chloride)	NaCl	Electrolyte, isotonic solution, preservative

4.3. Methodology of work

4.3.1. Preparation of Moringa Leaves

Moringa leaves were harvested from the home garden in the "Al Hood" area of El Oued State on November 16, 2023, and brought to the laboratory. The leaves were removed from the branches, keeping only the leaves, then washed with tap water three times and with distilled water twice, and left to drain. Then, the leaves were spread on the work surface in the laboratory

and left to dry for 3 to 5 days until completely dry. Afterwards, the leaves were ground in an electric blender Moulinex until they became powder. Then, the powder was sifted through a sieve with a thickness of 0.5 to 1 mm. The powder was then stored in bottles, with each bottle containing 40 grams of powder for later use.

- **Preparation of Pure Moringa Leaf Extract:**

In a 1-liter Erlenmeyer flask, the contents of one bottle of powder (40g) were emptied, followed by the addition of 1 liter of water (40g/liter). The flask was then placed on a hot plate and a magnetic stirrer for continuous stirring and homogenization of the solution. The temperature of the mixture was maintained at 80 degrees Celsius for 30 minutes while ensuring continuous stirring throughout the 30 minutes. After 30 minutes, the obtained solution was filtered to remove impurities using Whatman Filter paper, resulting in a pure solution.

4.3.2. Preparation of ZnO-NPs

Begin by placing 400 ml of previously prepared pure Moringa leaf extract on a hot plate with continuous stirring.

Prepare a zinc acetate solution by dissolving 4 grams of zinc acetate in 200 ml of distilled water. Slowly add this solution drop by drop to the pure Moringa leaf extract.

Dissolve 3 grams of sodium hydroxide pellets (NaOH) in 150 ml of distilled water. Distill the sodium hydroxide solution slowly and carefully over the previous solution while maintaining the pH level of the solution until it reaches 11. The color of the solution should change from dark brown to bright yellow.

Maintain the temperature at 80°C with continuous stirring for 30 minutes.

After half an hour, allow the final mixture to cool, then transfer it to a crystallizer and place it in an oven at 60°C until completely dried.

Afterward, collect the solid precipitate from the bottom of the crystallizer. Wash the obtained powder by rinsing it with distilled water three times in a centrifuge at 5000 rpm for 20 minutes, followed by rinsing once with ethanol and once with methanol, then rinsing it again with distilled water for the final time to ensure the removal of any compounds soluble in water or alcohol.

Let the obtained precipitate dry in the oven for 5 to 7 hours.

Then, take the dried powder to the furnace and heat it at 550°C for 5 hours to eliminate any organic compounds.

4.3.3. Preparation of Se-NPs

In a round-bottom flask, place 400 ml of previously prepared pure Moringa leaf extract and place it on a hot plate equipped with a magnetic stirrer.

Prepare a Gray selenium solution by dissolving 1.6 grams of selenium oxide in 200 ml of distilled water. Obtain a semi-homogeneous solution with a dark gray color and slowly add it to the first solution.

Next, prepare a sodium hydroxide (NaOH) solution by dissolving 3 grams of NaOH in 150 ml of distilled water. Gradually add it to the previous mixture until obtaining a final overall mixture with a pH of 11.

Leave the mixture at 80°C with continuous stirring for a total of two hours.

Afterward, observe the color change of the solution from dark gray to dark green, with the appearance of a red layer on the surface.

Transfer the mixture to a crystallizer to dry at 60°C for 3 days. Then, vacuum filter the precipitate and wash it has done with ZnO-NPs. Let it dry, and prepare it for burning as well.

4.3.4. Preparation of ZnO-Se doping via Moringa Oleifera

In Bisher, we place 400 ml of previously prepared pure Moringa leaf extract on a heated plate equipped with a magnetic stirrer.

Just like in the previous preparation of zinc acetate solution, with the same steps and concentration, we slowly add it to the first solution.

On the other hand, we prepare a Gray selenium solution by dissolving 7.4 mg of selenium oxide in 200 ml of distilled water and slowly add it to the previous solution.

Thus, we obtain a final solution consisting of pure Moringa leaf extract, selenium oxide solution, and zinc acetate solution.

On another side, we dissolve 4 grams of sodium hydroxide pellets in 200 ml of distilled water and add it to the mixture to adjust the mixture's pH to 11.

We leave it at 80°C for 30 minutes, then let it cool down and proceed with it as we did with ZnO-NPs and Se-NPs.

4.4. Nanoparticles characterization

4.4.1. UV-Vis Spectroscopy

Spectrophotometry is a quantitative analytical method that involves measuring the absorbance (or optical density) of a chemical substance in a liquid solution using a light source that is approximately monochromatic.

This method allows, for example, the determination of a substance's concentration by measuring the relative absorption of light compared to that of a substance with a known concentration.

- **Principle**

The principle of ultraviolet and visible absorption spectrometry is based on the absorption of radiation by molecules in the range of 190 to 800 nm, which corresponds to the ultraviolet (190-400 nm) and the visible (400-800 nm) regions of the spectrum (A. de l'Afsset, R.d.E 2010).

4.4.2. Fourier Transform Infrared Spectroscopy (FT-IR)

FT-IR spectroscopy is a technique used to obtain the infrared absorption or emission spectrum of a solid, liquid, or gas. This technique relies on analysing the vibrational patterns of particles, which include stretching and bending patterns. The vibrational frequencies depend on the atoms involved and the type of bond considered. Therefore, the vibrational patterns and their associated frequencies allow the identification of different chemical bonds.

- **Principle**

A molecule can be represented as a set of atoms bonded together by chemical bonds. Under the influence of thermal agitation, molecules undergo translational, rotational, and vibrational movements concerning their chemical bonds. These vibrations occur at different frequencies, depending on the nature of the bonds and their environment. It is noteworthy that most molecular vibration frequencies correspond to the infrared region of the electromagnetic radiation spectrum. Thus, when a molecule is irradiated with electromagnetic waves in this range, absorption of the incident wave occurs whenever the frequency of the incident wave matches one of the molecule's vibrational frequencies (A. de l'Afsset, R.d.E 2010).

4.4.3. X-Ray Diffraction (XRD)

- **Principle**

The X-ray diffraction technique is a method used to determine the crystalline phases of a sample and to identify the arrangement of atoms and their interatomic distances. This technique involves observing the interaction of X-rays with matter. When matter is bombarded with X-rays, radiation is emitted in all directions with waves that are in phase and of the same wavelength. This scattering causes interference between the waves scattered by each atomic plane, forming a diffracted wave whose characteristics depend on the crystalline structure of the material. The resulting diffractogram is recorded as a spectrum. Spectra can be obtained from a solid fragment or a small quantity of powder (Shin et al., 2008).

- **Operating Procedure**

The powders obtained from nanoparticles prepared using plant extract were deposited on a glass slide and then analyzed by XRD. The analysis was performed using an Expert Prof Panalytical diffractometer. This diffractometer is equipped with a Zn-SeNPs tube, utilizing the divergence slit and antiscatter programs. The voltage generator operates at 40 kV, and the tube current is set to 30 mA.

4.4.4. Scanning electron microscopy (SEM)

Scanning electron microscopy (SEM) is a powerful imaging technique used to visualize the surface morphology and topography of a sample. It involves scanning a focused beam of electrons across the sample's surface, which interacts with the atoms in the sample, generating various signals that can be detected and used to form an image. (Goldstein et al., 2018)

- **Principles**

SEM operates based on the interaction between the electron beam and the sample. When the primary electron beam strikes the sample, it can generate several types of signals, including secondary electrons (SE), backscattered electrons (BSE), and characteristic X-rays. SE signals provide information about the sample's topography, while BSE signals reveal information about the sample's composition. Characteristic X-rays can be used for elemental analysis. (Egerton, 2011)

- **Image Formation**

The SEM image is formed by collecting and processing the signals generated by the electron beam-sample interaction. The SE signal is typically used to create topographical images with high resolution and contrast. The BSE signal can be used to create compositional images that reveal differences in elemental distribution. (Reimer, 1998)

SEM is widely used in various fields, including materials science, biology, geology, the semiconductor industry, and forensic science. (Goldstein et al., 2018)

4.5. Biological Activity

4.5.1. Evaluation of antioxidants Activity

4.5.1.1. DPPH Radical Scavenging Effect

- **Principle**

The DPPH free radical scavenging method is widely used to evaluate the antioxidant activity of plant extracts. Antioxidants reduce the DPPH radical (2,2-diphenyl-1-picrylhydrazyl), which has a violet color, to a yellow compound (2,2-diphenyl-1-picrylhydrazine). In this

technique, the antioxidant effect can be easily evaluated by monitoring the decrease in DPPH absorption, and the reaction is monitored at 517 nm. (Brandwilliams et al., 1995; Musa et al., 2016; Krimat et al., 2017)

- **Procedure**

Prepare the extracts to be tested.

Prepare the DPPH solution by dissolving 4 mg of DPPH powder in 100 mL of 90% methanol. Store in the refrigerator for 2 hours (can be stored for 4 to 5 days when prepared at 2-5°C in darkness)- Mix 100 µL of the Zn-SePNs concentrate (prepared at 0.1%) with 3.9 mL of the DPPH solution at room temperature. After 30 minutes of incubation in darkness, measure the absorbance using a spectrophotometer at 517 nm.

- **Calibration Curve**

Simultaneously, during the preparation of this experiment, we conduct a parallel experiment with ascorbic acid at various concentrations, with the first concentration serving as the control (Pourrut, 2008). Mix different concentrations of ascorbic acid (100 µL) with 3.9 mL of prepared DPPH solution, then incubate for 30 minutes at room temperature and measure the absorbance using a spectrophotometer at 515 nm (Afshari et al., 2015). The results are expressed as percentage inhibition (I%) (Schaich et al., 2015).

The formula for calculating the percentage inhibition (I%) is:

Abs test

$$I\% = [(Abs\ control - Abs\ test) / Abs\ control] \times 100$$

- I%: percentage of inhibition
- Abc: absorbance
- Ac: absorbance of control
- At: absorbance of test

4.5.1.2. FRAP technique

- **Principle**

The ferric reducing power of the nanoparticles samples was determined using the Oyaizu method (1986). This method relies on the color change of the sample from green to blue, reflecting the reducing capacity of the compounds present. The presence of reducing agents (antioxidants) leads to the reduction of the Fe3+/ferricyanide complex (ferric form) to its ferrous form. Absorbance is measured at 700 nm, as described by Ferreira et al. (2007).

- **Operating Mode for Ferric Reducing Power Assay:**

1. **Preparation of Reaction Mixture:**
    - Add 1 mL of prepared concentrated connate extract to a test tube.
    - Add 2.5 mL of phosphate buffer (2M, pH 6.6) to the test tube.
    - Add 2.5 mL of potassium ferricyanide (1% in water) to the test tube.
2. **Incubation:**
    - Thoroughly mix the contents of the test tube.
    - Incubate the mixture in a 50°C water bath for 20 minutes.
3. **Precipitation and Centrifugation:**
    - Add 2.5 mL of trichloroacetic acid (10%) to the test tube.
    - Centrifuge the mixture at 3000 rpm for 10 minutes.
4. **Preparation of Colorimetric Solution:**
    - Carefully separate 2.5 mL of the supernatant from the centrifuged mixture and transfer it to a new test tube.
    - Add 2.5 mL of distilled water to the test tube.
    - Add 0.5 mL of iron chloride (0.1%) to the test tube.
    - Mix well and incubate the mixture in a 50°C water bath for 10 minutes.
5. **Spectrophotometric Measurement:**
    - After incubation, measure the absorbance of the final solution at 700 nm using a spectrophotometer.

Note: This protocol is based on the methods described in Ouchemoukh et al. (2012) and Nabavi et al. (2012).

4.5.2. In Vitro Anti-Inflammatory Activity

- **Principle**

The in vitro anti-inflammatory activity of selenium nanoparticles is assessed using the protein denaturation inhibition method. This technique measures the ability of a molecule to prevent protein denaturation (Chandra et al., 2012).

- **Operating Procedure**

1. Preparation:

- Prepare dry test tubes and add 0.1 ml of the preserved Bovine serum albumin (BSA)to each.

2. Buffer Addition:

- Add 1.4 ml of phosphate-buffered saline (PBS) with a pH of 6.4 to each tube.

3. Sample Addition:

- Add 1 ml of the concentrated extract to the test tubes.

4. Control and Standards:

- Prepare additional tubes by replacing the extracts with varying concentrations of sodium diclofenac, and prepare a control tube with distilled water.

5. Incubation:

- Incubate all tubes at 37°C for 15 minutes.

- Follow this with a second incubation at 70°C for 5 minutes.

6. Centrifugation:

- Allow the tubes to cool to room temperature and then centrifuge them at 2000 rpm for 5 minutes.

7. Measurement:

- Read the absorbance using a spectrophotometer at around 660 nm (Chandra et al., 2012).

8. Calculation:

- Calculate the percentage inhibition of protein denaturation using the following formula:

$$\text{Percentage Inhibition} = \left(\frac{A_{\text{control}} - A_{\text{sample}}}{A_{\text{control}}}\right) \times 100$$

4.5.3. Anti-hemolytic activity

- **Mechanism of Hemolytic Assay**

Generally, the complement system mainly functions by cracking the target cells through the formation of the cytolytic membrane attack complex (MAC). Based on this property, the hemolysis assay has been developed as the major approach for total complement system activity assessment.

Usually, serum isolated from immunized rabbits and SRBC is used in vitro for hemolytic assay. Specific antibodies, namely hemolysin, will be produced after the sheep red blood cells (SRBC) are injected into rabbits as antigens. When SRBC is added to the tube with isolated serum, the hemolysin immediately reacts with the antigen on the surface of SRBC forming antigen-antibody complex. If a complement sample with normal activity is added to the tube, the complement will attack the antigen-antibody complex on the surface of SRBC, leading to the SRBC lysis and hemolysis. Common hemolysis assays are CH50 and AH50 (i.e., diluted serum

complement concentration at 50% lysis of SRBC), which are respectively used for assessment activities of complement classic pathway and complement alternative pathway. (Fornaguera, Cristina, and Conxita Solans. 2017)

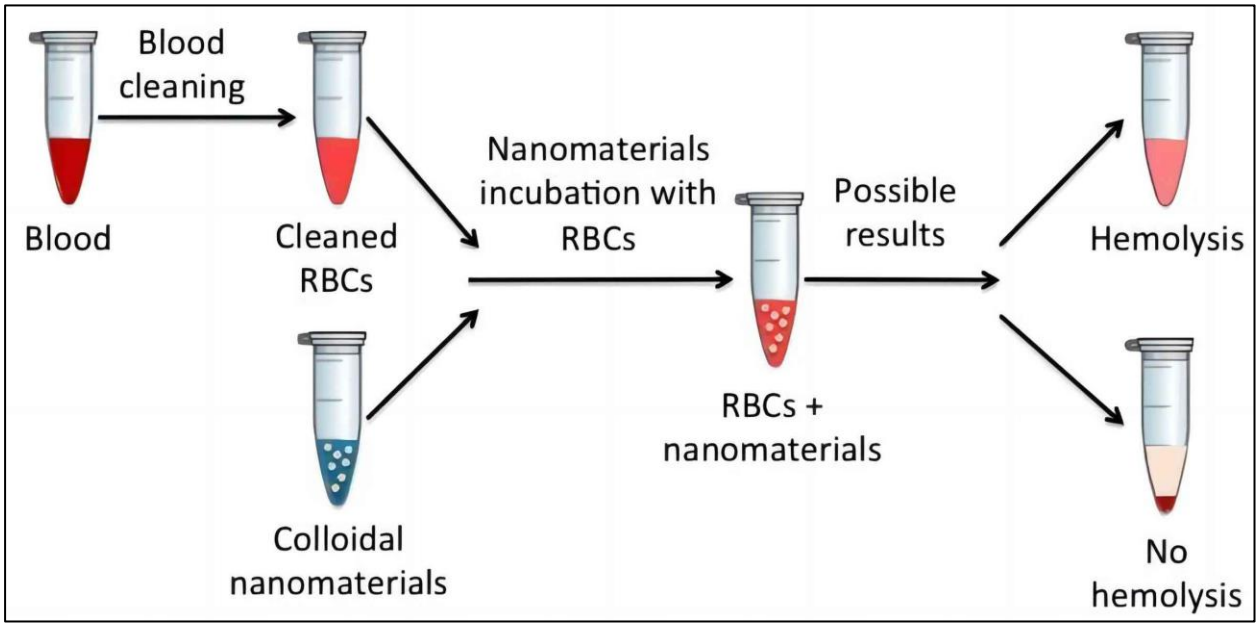

Figure 9: Hemolysis assay process. (Fornaguera, Cristina, and Conxita Solans. 2017)

- **Operating mode**

1. **Prepares erythrocyte hemolytic 10%**

When taking a blood sample, add EDTA anticoagulant to the tube and mix very well and very sensitively; Add this tube to a 2000 centrifuge for 10 minutes to separate the plasma and hemolysis. After separation, add a few milliliters of PBS phosphate buffer (7.4;0.9Nacl) and sensitized mixture and add the mixing tube to a 2000 rpm centrifuge for 10 min. And respite from this stage in 3fiot (Rani et al.,2014).

Place 1ml of suspension in a tube and add 9ml PBS.

2. **Induction by hypotonic NaCL**

Prepare the dry tubes by adding 100ul erythrocyte hematocrit 10% and adding 5ml NACL in different concentrations, after incubation in normal ambient temperature for 30 min.

After centrifuging at 3000 rpm for 10 minutes and reading in a 540 nm wavelength spectrophotometer, negative control adds the concentration of NACL 9 mg/ml and positive control exchanges the NACL with distilled water (Louerrad et al., 2016).

3. **Effect on hemolysis induced by NaCL**

Prepare dry tubes by adding 100ul erythrocyte hematocrit 10% and 100ul sample concentration conne. After incubating for 10 minutes at room temperature; and adds 5 ml NACL (3.5 mg/ml) and incubates for a second time for 30 minutes at a temperature of 37°C in an incubator. After centrifuging all the tubes in a 3000-rpm centrifuge for 10 minutes. After reading the supernatant in 540 nm (Louerrad et al.,2016).

All hemolysis tests calculate percentage in the following formula (Shobana and Vidhya.,2016)

Hemolysis percentage% = (abs test/abs control) *100

4.5.4. Antibacterial Activity Assay

Well method assay

- **Preparation of Materials and Bacterial Cultures**

Bacterial strains including Staphylococcus saprophyticus, Staphylococcus aureus, Pseudomonas aeruginosa, Escherichia coli (E. coli), and Proteus mirabilis were sourced from reputable Type Culture Collections. Each strain was cultured aerobically in nutrient broth for 24 hours at 37°C to achieve mid-logarithmic growth phase, ensuring uniformity in bacterial density prior to experimental use

- **Antibacterial Activity Assay**

Different concentrations (2.5%, 5%, 10%, and 20% w/v) of various nanoparticles synthesized using Moringa Oleifera (ZnO nanoparticles, Se nanoparticles, and ZnO-Se doped nanoparticles) and pure Moringa Oleifera extract were prepared .

1. **Preparation of agar well**

Agar well (6 mm diameter) was impregnated with 20 µL of each nanoparticle suspension or Moringa extract.

2. **Inoculation and Cultivation**

Nutrient agar plates were inoculated with standardized bacterial suspensions of *Staphylococcus saprophyticus, Staphylococcus aureus, Pseudomonas aeruginosa, Escherichia coli (E. coli),* and *Proteus mirabilis*.

3. **Application of agar well**

The impregnated discs were placed on the surface of the inoculated agar plates using sterile forceps, ensuring even distribution across the plates.

4. Determination of Minimum Inhibitory Concentration (MIC)

After incubation for 24 hours at 37°C, the plates were examined for zones of inhibition (ZOI) around each agar well, indicating the antibacterial efficacy of the tested substances against the respective bacterial strains.

5. Measurement of Zones of Inhibition

The diameter of clear zones around each agar well was measured using a calibrated ruler, and the average diameter was recorded.

6. Analysis of Results

The minimum inhibitory concentration (MIC) was determined as the lowest concentration of each test substance that produced a zone of inhibition against the target bacteria.

	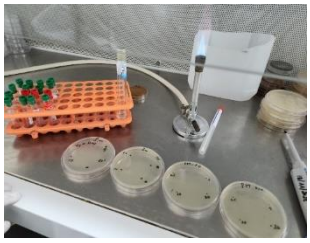
Bacterial culture in Chromogenic agar	Preparation Bacterial in Mueller-Hinton agar
	
Bacterial inoculation in Mueller-Hinton agar	Application of nanoparticles

4.5.5. Activated Partial Thromboplastin Time (aPTT) Analysis

The Semi-Auto Coagulation Analyzer Mindray C2000-2 performs aPTT analysis using nanoparticle technology at concentrations of 5, 10 and 20 mg/ml to assess blood coagulation

function. aPTT measures the time it takes for blood to clot after the activation of the intrinsic coagulation pathway.

- **In this analysis:**

Nanoparticles (at 5, 10 mg/ml and 20 mg/ml concentrations) are introduced into the blood sample along with the coagulation reagent containing cephalin and other activators.

The nanoparticles interact with blood components involved in the coagulation process, triggering the intrinsic pathway.

The time taken for clot formation is measured by the analyzer, providing aPTT results in seconds.

4.5.6. Prothrombin Time (PT) Analysis

The Semi-Auto Coagulation Analyzer Mindray C2000-2 utilizes nanoparticles as an anticoagulant agent during Prothrombin Time (PT) testing to maintain sample fluidity and prevent clotting within the analyzer's system. In this innovative approach:

Nanoparticles (at concentrations of 5 mg/ml ,10 mg/ml and 20 mg/ml) are introduced into the blood sample along with the PT reagent containing tissue factor and calcium ions.

The nanoparticles act as anticoagulants, inhibiting the initiation of clotting cascades within the analyser while allowing for the activation of the extrinsic coagulation pathway by tissue factor.

The Prothrombin Time (PT) is measured as the time it takes for clot formation after the addition of tissue factor, reflecting the functional activity of key clotting factors in the plasma. Nanoparticle-based anticoagulation ensures accurate and reliable PT measurements, facilitating the assessment of coagulation function without interference from unintended clot formation.

4.6. In vivo tests

4.6.1. Animal design

We procured male rats from the animal laboratory within our faculty. At the time of purchase, the rats exhibited weights ranging from 130 to 160 grams and displayed overall good health with no observable diseases or disorders. Each rat was individually identified and assigned a unique identification number for tracking throughout the study. The rats were housed in appropriate animal facilities under controlled environmental conditions, including regulated temperature and humidity, with a standard light-dark cycle. They were provided with ad libitum

access to water and a standard laboratory diet. Prior to commencing the experimental procedures, the rats underwent an acclimatization period of month and half to adapt to their new environment. During this period, they were closely monitored for any signs of stress or abnormal behaviour. Detailed records of individual rat identifiers are presented in the accompanying table for reference and tracking purposes throughout the study.

Tableau 9.animal identification

Groups	Animal	Identification
Group 1	T1	Witness 1
	T2	Witness 2
Group 2	M1	Witness e 1
	M2	Witness 2
Group 3	ZnO 1	Rat 1 treated by ZnO nanoparticles via Moringa Oleifera
	ZnO 2	Rat 2 treated by ZnO nanoparticles via Moringa Oleifera
Groupe4	Se 1	Rat 1 treated by Se nanoparticles via Moringa Oleifera
	Se 2	Rat 2 treated by Se nanoparticles via Moringa Oleifera
Group 5	Dop 1	Rat 1 treated with ZnO-Se doping via Moringa Oleifera
	Dop 2	Rat 2 treated with ZnO-Se doping via Moringa Oleifera
Group 6	XP 1	Rat 1 treated with pure extraction of Moringa Oleifera
	XP 2	Rat 2 treated with pure extraction of Moringa Oleifera
Group 7	Pr ZnO	Rat 2 treated in before deltamethrin injection with ZnO nanoparticles via Moringa Oleifera
	Pr Se	Rat 2 treated in before deltamethrin injection

		with Se nanoparticles via Moringa Oleifera
	Pr Dop	Rat 2 treated in before deltamethrin injection with ZnO-Se doping via Moringa Oleifera

4.6.2. Animal treatment

After a two and a half months adaptation period, the rats' weights reached 220 and 260 grams. The study included three treatment periods using deltamethrin.the rats were divided into different groups, all of which received an intraperitoneal injection of 1 ml of deltamethrin. Subsequently, we observed various disorders. After 2 days, they received another injection of 0.3 ml, followed by an additional 0.3 ml injection after 3 days. During the treatment period, which lasted 21 days, the rats were administered prepared nanoparticles with a concentration of 10 ml/mg via oral gavage at 1 ml per day. Autopsy procedures were conducted as follows: one day prior to autopsy, feeding was withheld from the rats. The animals were euthanized by cutting the jugular vein to collect an adequate quantity of blood. Blood samples were placed in EDTA tubes for hematological analysis and heparin tubes for biochemical analysis. After the autopsy, liver and testis samples were collected and fixed in formalin for histological examination. For protective group oral gavage of nanoparticles were for 8 days then the injection of deltamethrin for 5 days.

Animal adaptation

Animal identification

	
Animal injection	Nanoparticles gavage
	
Anesthetizing	Slaughtering the rat and blood sampling
	
Animal dissection	Organ's sampling

4.6.3. Measurement of Hematological Parameters

Hematological parameters (hemoglobin, red blood cells, white blood cells, platelets) are determined using the Coulter method employing the Autoanalyzer Mindray BC-2800 specific to FNS (complete blood count formula).

Parameters Measured:

- **Red Blood Cell (RBC) Count:** The number of red blood cells in a volume of blood.
- **White Blood Cell (WBC) Count:** The number of white blood cells in a volume of blood.

- **Hemoglobin (Hb):** The protein in red blood cells that carries oxygen.
- **Hematocrit (Hct):** The proportion of blood volume occupied by red blood cells.
- **Platelet Count (PLT):** The number of platelets in a volume of blood.

Measurement of Biochemical Parameters:

- **ASAT (AST, Aspartate Aminotransferase) Analysis**

The Biochemical Autoanalyzer Mindray BS-360 E automates the measurement of ASAT levels in blood samples using enzymatic techniques. ASAT, present in liver cells, heart, and muscle tissues, serves as an important indicator of liver and cardiac health. Elevated ASAT levels in the blood can signify liver damage, heart conditions, or muscle injury. The analyzer employs specific enzymatic reactions tailored to ASAT, enabling accurate quantification of its concentration in the sample. By utilizing these enzymatic techniques, clinicians can assess liver and cardiac function more effectively, aiding in the diagnosis and management of related conditions.

- **ALAT (ALT, Alanine Aminotransferase) Analysis**

The Biochemical Autoanalyzer Mindray BS-360 E performs ALAT analysis through enzymatic methods designed for precise measurement. ALAT, primarily found in liver cells, is released into the bloodstream during liver injury or inflammation. Elevated ALAT levels are indicative of liver disorders such as hepatitis or fatty liver disease. The analyzer utilizes enzymatic reactions specific to ALAT, allowing for accurate determination of its concentration in the blood sample. This enables healthcare providers to evaluate liver function efficiently, supporting the diagnosis and monitoring of liver-related conditions.

- **Total Bilirubin Analysis:**

The Biochemical Autoanalyzer Mindray BS-360 E enables the measurement of total bilirubin levels in blood samples using photometric techniques. Bilirubin is a pigment produced from the breakdown of hemoglobin in red blood cells and is metabolized by the liver. Elevated total bilirubin levels can indicate liver dysfunction, bile duct obstruction, or hemolytic disorders. The analyzer utilizes photometric methods to measure the absorbance of light by bilirubin in the sample, allowing for accurate quantification of its concentration. This automated analysis assists healthcare providers in assessing liver function and diagnosing conditions affecting bilirubin metabolism. By employing photometric techniques, the Biochemical Autoanalyzer Mindray BS-

360 E delivers reliable results crucial for the diagnosis and management of liver and blood-related disorders.

- **Bilirubin D (Direct Bilirubin) Analysis:**

The Biochemical Autoanalyzer Mindray BS-360 E facilitates the measurement of direct bilirubin (Bilirubin D) levels in blood samples using enzymatic and photometric techniques. Direct bilirubin represents the fraction of bilirubin that is conjugated in the liver and directly excreted into bile. Elevated direct bilirubin levels can indicate liver dysfunction, bile duct obstruction, or other hepatobiliary disorders. The analyzer employs enzymatic reactions specific to direct bilirubin, followed by photometric detection to quantify its concentration accurately in the sample. This automated analysis assists healthcare providers in assessing liver and bile duct function, aiding in the diagnosis and management of conditions affecting bilirubin metabolism. By utilizing enzymatic and photometric techniques, the Biochemical Autoanalyzer Mindray BS-360 E delivers precise results essential for evaluating hepatobiliary health and guiding patient care decisions

- **Indirect Bilirubin (Unconjugated Bilirubin) Analysis:**

The Biochemical Autoanalyzer Mindray BS-360 E facilitates the measurement of indirect bilirubin levels in blood samples using photometric techniques. Indirect bilirubin represents the fraction of bilirubin that is unconjugated and bound to albumin, circulating in the bloodstream before being processed by the liver. Elevated indirect bilirubin levels can be associated with conditions such as hemolytic disorders, where there is increased breakdown of red blood cells, leading to excess unconjugated bilirubin production. The analyzer utilizes photometric methods to measure the absorbance of light by indirect bilirubin in the sample, allowing for accurate quantification of its concentration. This automated analysis assists healthcare providers in assessing bilirubin metabolism and diagnosing conditions affecting red blood cell breakdown or liver function. By employing photometric techniques, the Biochemical Autoanalyzer Mindray BS-360 E delivers reliable results crucial for the evaluation and management of conditions related to unconjugated bilirubin levels.

- **Gamma-Glutamyl Transferase (GGT) Analysis:**

The Biochemical Autoanalyzer Mindray BS-360 E enables the measurement of Gamma-Glutamyl Transferase (GGT) levels in blood samples using enzymatic and photometric techniques. GGT is an enzyme found in various tissues, with high concentrations in the liver. Elevated GGT levels can indicate liver disease, bile duct obstruction, or alcohol-related liver

damage. The analyzer utilizes enzymatic reactions specific to GGT, followed by photometric detection, to accurately quantify its concentration in the sample. This automated analysis assists healthcare providers in evaluating liver function and diagnosing conditions affecting bile ducts and hepatobiliary health. By employing enzymatic and photometric techniques, the Biochemical Autoanalyzer Mindray BS-360 E delivers reliable results crucial for the diagnosis and management of liver-related disorders

- **Alkaline Phosphatase (ALP) Analysis:**

The Biochemical Autoanalyzer Mindray BS-360 E facilitates the measurement of alkaline phosphatase (ALP) levels in blood samples using enzymatic and photometric techniques. ALP is an enzyme found in various tissues, with particularly high concentrations in the liver, bones, and bile ducts. Elevated ALP levels can indicate liver or bone disorders, bile duct obstruction, or certain cancers. The analyzer utilizes enzymatic reactions specific to ALP, followed by photometric detection, to accurately quantify its concentration in the sample. This automated analysis assists healthcare providers in evaluating liver and bone health and diagnosing conditions affecting these tissues. By employing enzymatic and photometric techniques, the Biochemical Autoanalyzer Mindray BS-360 E delivers reliable results crucial for the diagnosis and management of liver and bone-related disorders.

4.6.4. Sample Preparation for Histological Study

For the histological study, livers and testis from all groups are collected promptly to avoid autolysis, which occurs shortly after the animal's death. After rinsing the samples with distilled water followed by 0.9% NaCl, they are immediately fixed in a 30% formalin solution. The technique used involves the following steps:

- **Fixation**

Samples (organ fragments) are fixed in formalin and placed in special cassettes with perforated walls to allow fluid passage.

- **Dehydration:**

Dehydration of samples using an automatic device that progressively passes the samples through baths of increasing ethanol concentrations (70%, 95%, and 100%).

- **Embedding and Processing:**

The tissues are then immersed in baths of liquid paraffin. After impregnation with paraffin, the tissues undergo embedding, where the tissue is enclosed in a paraffin block that solidifies for sectioning. This step utilizes inclusion devices with a reservoir of liquid paraffin

kept molten by a heating system, a small faucet, and a refrigerated metal plate for rapid solidification of the paraffin block containing the tissue. Thin sections of a few microns (average 5 µm) are made possible using special devices called microtomes. These sections are spread onto glass slides, flattened, and affixed to the slide using heated gelatinous water.

- **Staining**

For staining, the Hematoxylin-Eosin (H&E) technique is used, which requires acidic alcohol (100 ml of 70% ethyl alcohol + 50 ml of HCl)، ammoniacal water (100 ml distilled water + 2 ml ammonia), and Eosin solution (100 ml 3% aqueous Eosin solution, 125 ml 95% ethyl alcohol, 375 ml distilled water, and 2 drops of acetic acid). The staining process involves:

Deparaffinization and hydration of slides in tap water followed by rinsing in distilled water.

Immersion in Harris Hematoxylin solution (15 minutes) to stain basophilic structures (nuclei) violet-blue.

Treatment with acidic alcohol (1-2 dips), followed by tap water with microscope examination to check differentiation.

Immersion in ammoniacal water, then in Eosin solution (15 seconds to 2 minutes) to stain acidophilic structures (cytoplasm) pink. Each step is separated by rinsing with tap water.

- **Microscopic Observation**

The prepared slides are dried and observed under an optical microscope, with images captured using a camera.

Chapter 2

Results and discussion

2.1. Preparation yield and characterization

This table shows the composition of the pure extract and the yield of the preparation

Molécule	**Pure moringa leaf extract**
Weight (g)	20
Appearance	Powder
Color	Dark brown

Yield of the preparation calculated by the following relationship:

(Weight of synthesized products / Dry product weight) * 100

Dry product weight: 40 g

Weight of synthesized products: 20 g

20/40*100= 50%

This table shows the composition of the zinc oxide nanoparticle from moringa leaf extract and the yield of the preparation

Molécule	**Zinc oxide**
Formula	ZnO
Weight (g)	1.7
Appearance	Powder
Color	Yellowish white

Yield of the preparation calculated by the following relationship:

(Weight of synthesized products / Dry product weight) * 100

Dry product weight: 40 g

Weight of synthesized products: 1.7 g

1.7/40*100= 3.5 %

This table shows the composition of the Selenium nanoparticle from moringa leaf extract and the yield of the preparation

Molécule	**Grey of Selenium**
Formula	Se
Weight (g)	0.4

Appearance	Powder
Color	Red

Yield of the preparation calculated by the following relationship:

(Weight of synthesized products / Dry product weight) * 100

Dry product weight: 40 g

Weight of synthesized products: 0.4 g

0.4/40*100= 1 %

This table shows the composition of the doping nanoparticle from moringa leaf extract and the yield of the preparation

Molécule	**Zinc oxide**	**Gray of Selenium**
Formula	ZnO	Se
Weight (g)	4	0.18
Appearance	Powder	
Color	White	Gray

Yield of the preparation calculated by the following relationship:

(Weight of synthesized products / Dry product weight) * 100

Dry product weight: 40 g

Weight of synthesized products: 1.9 g

1.9/40*100= 4.75 %

2.2. Characterization

2.2.1. UV-Vis Analysis of ZnO NPs from Moringa Leaf Extract

The UV-Vis absorption spectrum of the synthesized ZnO NPs provides key insights:

- Absorption Peak: The prominent peak at 376 nm signifies the characteristic absorption of ZnO nanoparticles due to the electronic transition from the valence band to the conduction band. This corresponds to the bandgap energy of the ZnO NPs.

- Blue Shift: The absorption peak is blue-shifted compared to the bulk ZnO bandgap of 375 nm. This shift is indicative of the quantum confinement effect, which occurs in nanoparticles due to their small size. It demonstrates that the synthesized ZnO NPs are indeed in the nanometer range.

- Sharp Band at 376 nm: The sharpness of the band at 376 nm indicates the homogeneity and narrow size distribution of the synthesized nanoparticles. It also suggests efficient reduction of Zn ions by the Moringa leaf extract, highlighting the effectiveness of this green synthesis approach.

- **The findings align well with existing literature:**

- Degefa et al. (2021): This study also employed green synthesis to produce ZnO NPs using plant extracts. Their findings, along with the work of others, support the use of natural extracts like Moringa oleifera for nanoparticle synthesis.

- Hazaa et al. (2020): Although this study focused on silver nanoparticles, it underscores the versatility of plant extracts in synthesizing various types of nanoparticles. It also emphasizes the importance of characterization techniques like UV-Vis spectroscopy in understanding the properties of the synthesized nanoparticles.

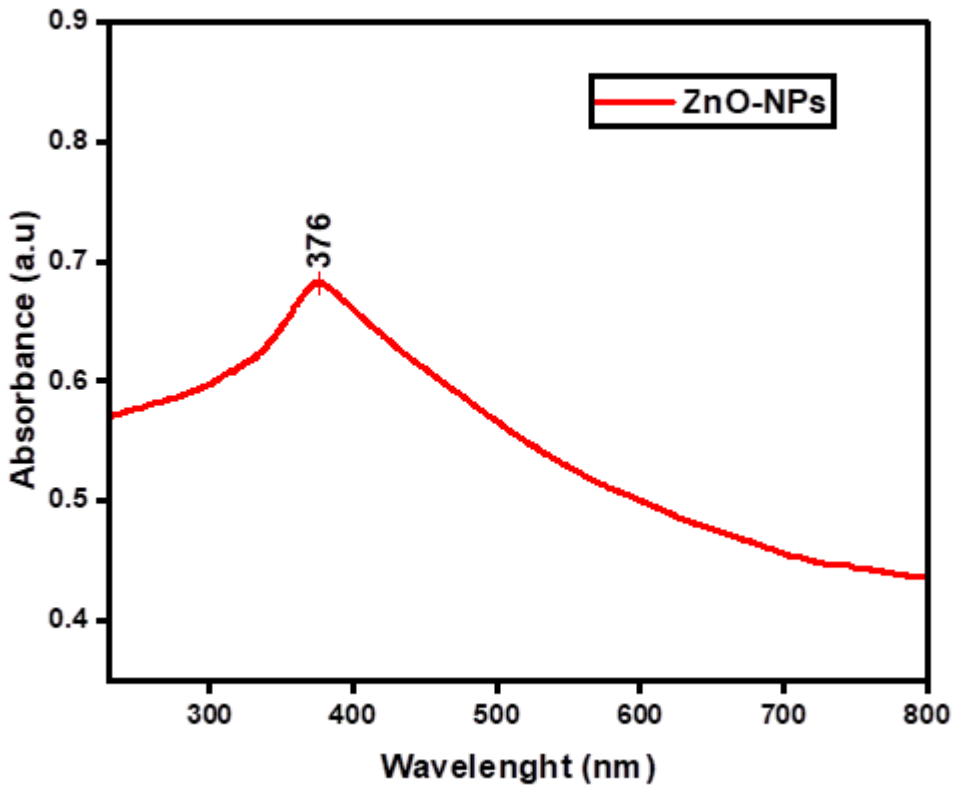

Figure 10: UV-Vis absorption spectrum of the synthesized ZnO NPs.

2.2.2. UV-Vis Analysis of Se NPs from Moringa Leaf Extract

The UV-Vis absorption spectrum of the synthesized SeNPs reveals a prominent absorption maximum at 201 nm. This is a significant finding for several reasons:

- Quantum Confinement: The blue shift (hypsochromic shift) of the absorption peak compared to bulk selenium (which absorbs at longer wavelengths) is a clear indication of the quantum confinement effect. This phenomenon arises when the size of a material is reduced to the nanometer scale, leading to changes in its electronic structure and optical properties.

- Particle Size Estimation: The degree of the blue shift is inversely related to the size of the nanoparticles. This means that smaller particles exhibit a larger blue shift. While the exact size cannot be determined from the UV-Vis spectrum alone, the strong absorption at 201 nm suggests the formation of SeNPs with sizes in the nanometer range.

- Optical Properties: The blue shift highlights the unique optical properties of SeNPs compared to bulk selenium. This makes them promising candidates for applications that rely on light absorption and emission, such as solar cells, photodetectors, and biomedical imaging.

- We findings are in good agreement with previous research on SeNPs:

- Cittrarasu et al. (2021): This study also used a green synthesis approach to produce SeNPs, employing Ceropegia bulbosa extract. They observed an absorption peak at 277.5 nm, which, while at a longer wavelength than our result, still demonstrates the characteristic blue shift due to quantum confinement.

- Alagesan & Venugopal (2019): This study reported a bandgap energy of 2.75 eV for SeNPs. the 2.4 eV value we obtained from a Tauc plot analysis is consistent with this previous finding. The bandgap energy is related to the absorption wavelength, and both studies suggest a significant blue shift compared to bulk selenium.

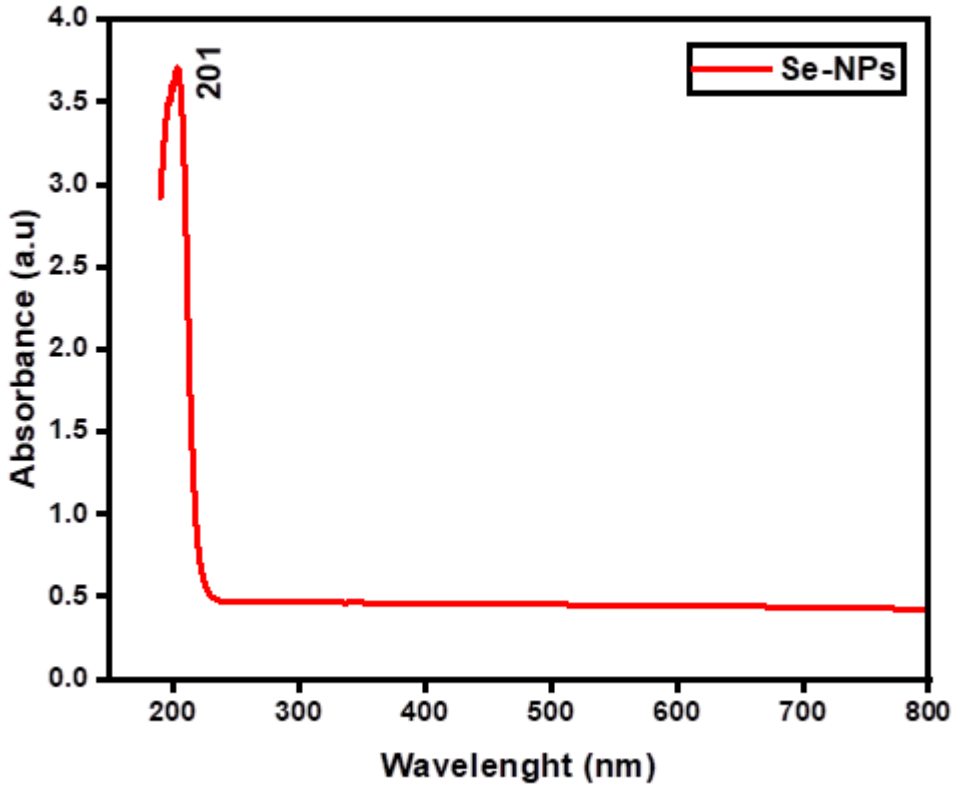

Figure 11: UV-Vis absorption spectrum of the synthesized SeNPs

2.2.3. UV-Vis Analysis of Doping Zn-Se NPs from moringa leaf extract

The UV-Vis absorption spectrum you provided offers valuable insights into the synthesized nanoparticles:

- **Two Distinct Peaks**

The spectrum shows two well-defined peaks, one at 281 nm and another at 378 nm. This suggests the presence of two distinct types of nanoparticles in the sample.

- 281 nm Peak: This peak corresponds to the characteristic absorption of selenium nanoparticles (SeNPs). The absorption of SeNPs typically occurs in the ultraviolet range.

- 378 nm Peak: This peak is consistent with the characteristic absorption of zinc oxide nanoparticles (ZnO NPs). This absorption is due to the bandgap transition of ZnO, which falls within the near-UV range.

ZnO NPs: The 378 nm peak for ZnO NPs is slightly blue-shifted compared to the bulk ZnO bandgap of around 375 nm. This blue shift is a typical characteristic of quantum confinement effects observed in nanoparticles. Several studies have reported similar blue shifts

for ZnO NPs synthesized using various methods, including green synthesis with plant extracts (Ali et al., 2021; Singh et al., 2018).

SeNPs: The 281 nm peak for SeNPs is within the expected range for these nanoparticles. However, the exact position of the peak can vary depending on the size and morphology of the SeNPs. Previous research on SeNPs synthesized using plant extracts, such as Ceropegia bulbosa (Cittrarasu et al., 2021), has reported similar absorption peaks in the UV range.

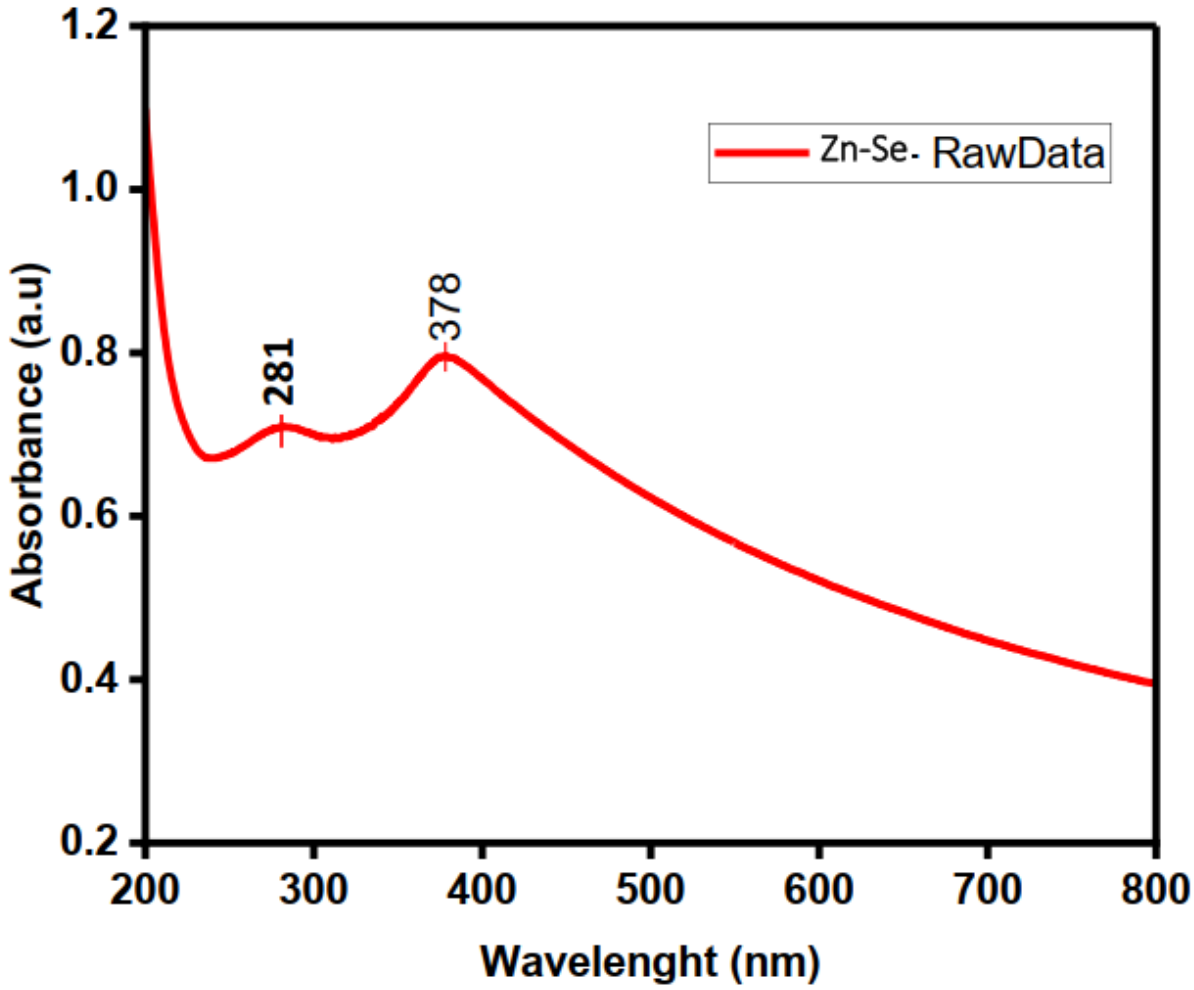

Figure 12: UV-Vis absorption spectrum of the synthesized Doping Zn-Se NPs

2.3. Fourier Transform Infrared Spectroscopy (FT-IR)

2.3.1. Infrared (IR) spectrum of pure moringa leaf extract

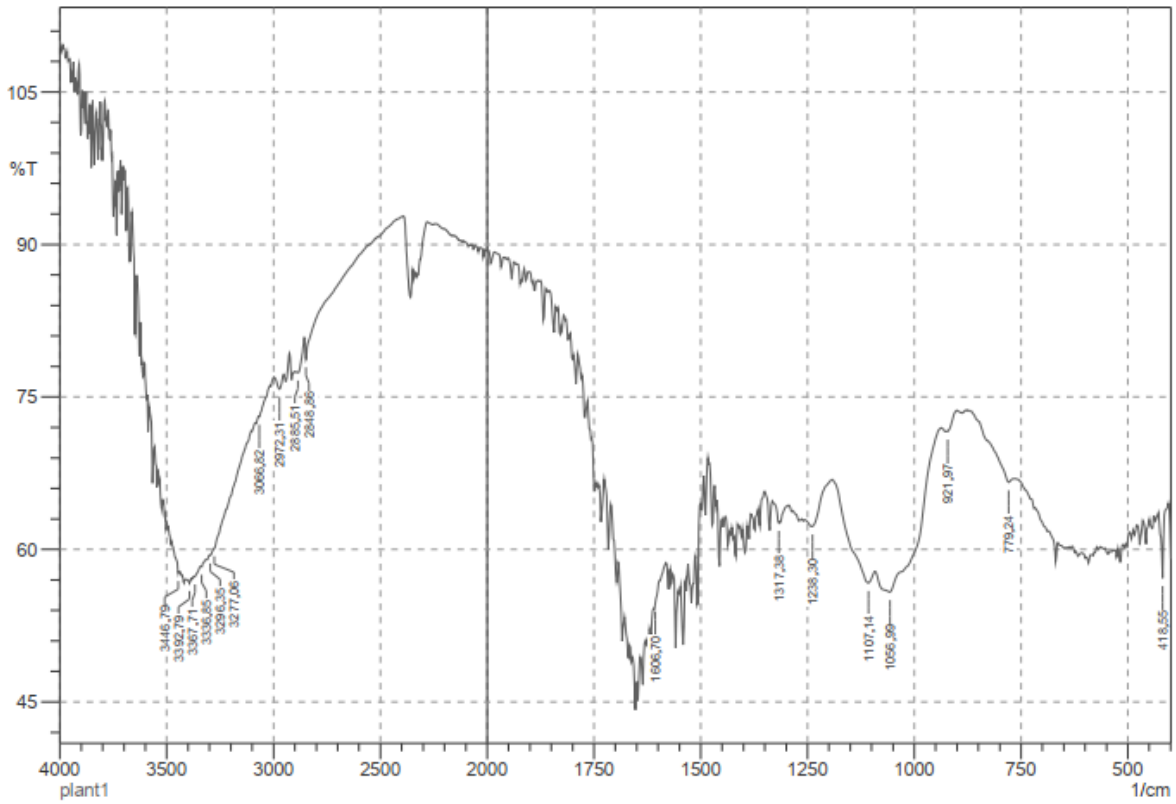

Figure 13: FT-IR spectra of synthesized pure moringa leaf extract

Large Band around 3200-3500 cm^{-1}: This large and intense band is characteristic of O-H stretching vibrations, indicating the presence of hydroxyl groups (-OH) in the extract. This is commonly attributed to phenols, alcohols, and carboxylic acids.

Previous studies on moringa leaf extracts have consistently reported a strong presence of phenolic compounds like flavonoids and phenolic acids, which contribute to this broad O-H band. (Leone, A., et al. (2015)., Saini, R. K., et al. (2014))

Peaks around 2800-3000 cm^{-1}: These peaks correspond to C-H stretching vibrations from aliphatic (straight-chain) hydrocarbons. This is consistent with the presence of fatty acids and other aliphatic compounds found in moringa leaves. (Mbikay, M. (2012))

Peak around 1735 cm^{-1}: This peak is indicative of C=O stretching vibration, suggesting the presence of carbonyl groups (C=O), typically found in esters, ketones, or aldehydes. Moringa leaf extracts have been reported to contain various aromatic compounds with carbonyl functionalities. (Anwar, F., et al. (2007))

- Fingerprint Region (1500-500 cm^{-1}): This region shows several overlapping peaks due to various bending vibrations (C-H, O-H) and stretching vibrations (C-O, C-N, CC). While difficult to assign specific peaks definitively, the overall pattern is consistent with the complex mixture of organic compounds found in moringa leaf extracts, including carbohydrates, amino acids, and other phytochemicals. (Fuglie, L. J. (2001))

The observed IR spectrum aligns well with previous studies on moringa leaf extracts. The presence and relative intensities of the major peaks corroborate the findings of other researchers who have analyzed the IR spectra of moringa leaves from various geographical locations. (Leone, A., et al. (2015), Saini, R. K., et al. (2014), Mbikay, M. (2012), Anwar, F., et al. (2007), Fuglie, L. J. (2001))

2.3.2. Infrared (IR) spectrum of Zinc Oxide NPs (ZnO NPs) from moringa leaf extract

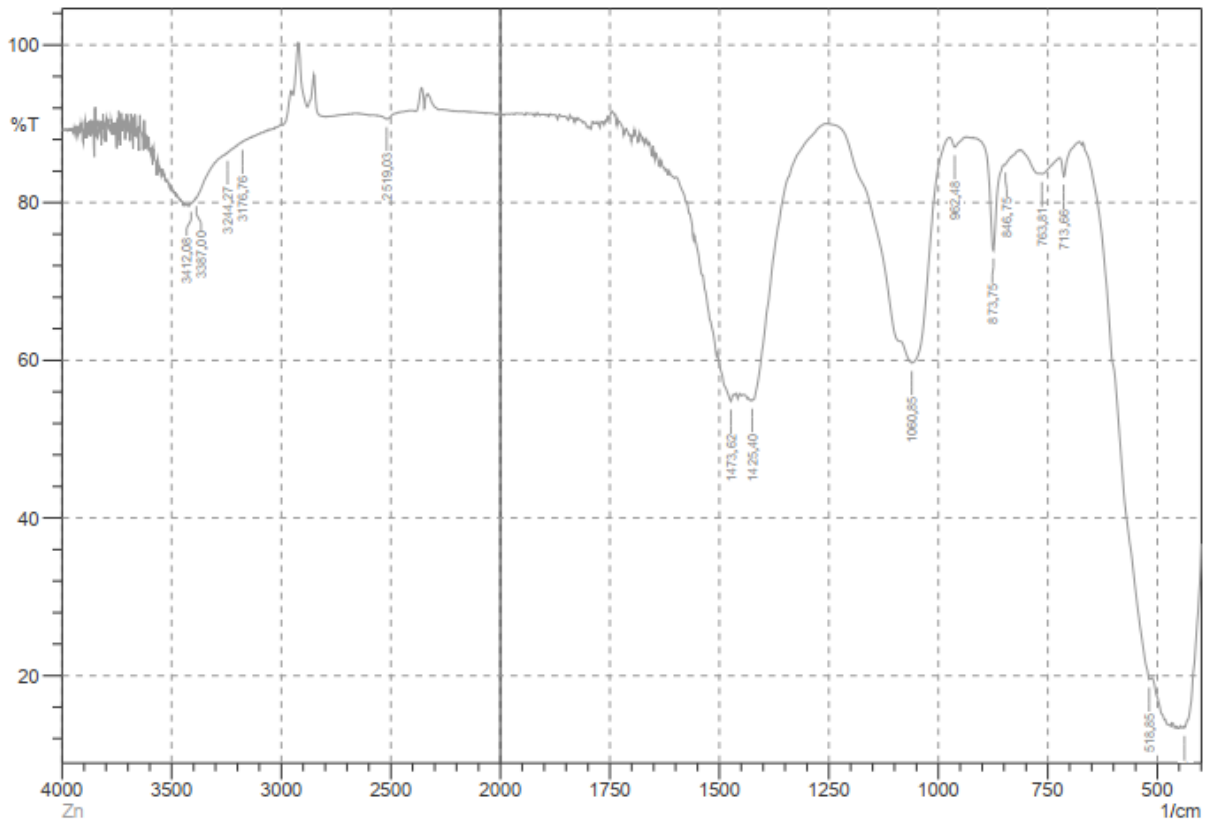

Figure 14: FT-IR spectra of synthesized pure moringa leaf extract

Large Peak around 3200-3500 cm^{-1}: This prominent large peak is characteristic of OH stretching vibrations. This suggests the presence of hydroxyl groups (OH), likely due to surface moisture adsorbed onto the ZnO nanoparticles or residual organic compounds from the moringa leaf extract. This observation aligns with findings in previous studies, where a broad peak in this

region was attributed to the presence of hydroxyl groups on the surface of ZnO NPs synthesized using plant extracts (Sangeetha, G., et al. (2011), Ambika, S., & Sundrarajan, M. (2015)).

Peaks around 1500-1650 cm^{-1}: These peaks can be attributed to various bending vibrations, including C-H bending (possibly from residual organic compounds) and OH bending from water molecules. This observation is consistent with studies that reported the presence of organic residues on ZnO NPs synthesized using plant extracts (Ramesh, P. S., et al. (2015), Gunalan, S., et al. (2012)).

Peaks around 1380-1450 cm^{-1}: These peaks could be assigned to the stretching vibrations of C=O and C-O bonds, indicating the presence of carbonyl and carboxyl groups, respectively. These functional groups are commonly found in organic molecules present in plant extracts.

Strong Peak around 516 cm^{-1}: This intense peak is the most characteristic feature of ZnO nanoparticles. It corresponds to the Zn-O stretching vibration, confirming the formation of ZnO. The position of this peak aligns with previous studies that reported a Zn-O peak around 500 cm^{-1} for ZnO NPs synthesized using various methods (Baruah, S., & Dutta, J. (2009), Rajabi, H. R., et al. (2019)).

The observed IR spectrum is consistent with findings from previous studies on ZnO NPs synthesized using plant extracts, particularly moringa leaf extract (Yugander, S., & Rajaram, R. (2015)). The broad O-H peak, peaks in the 1500-1650 cm^{-1} region, and the characteristic Zn-O peak are all commonly observed in such spectra. This suggests that the synthesis method employedhere is effective in producing ZnO NPs with similar surface characteristics and functional groups as reported in the literature.

2.3.3. Infrared (IR) spectrum of Selenium NPs (Se NPs) from moringa leaf extract

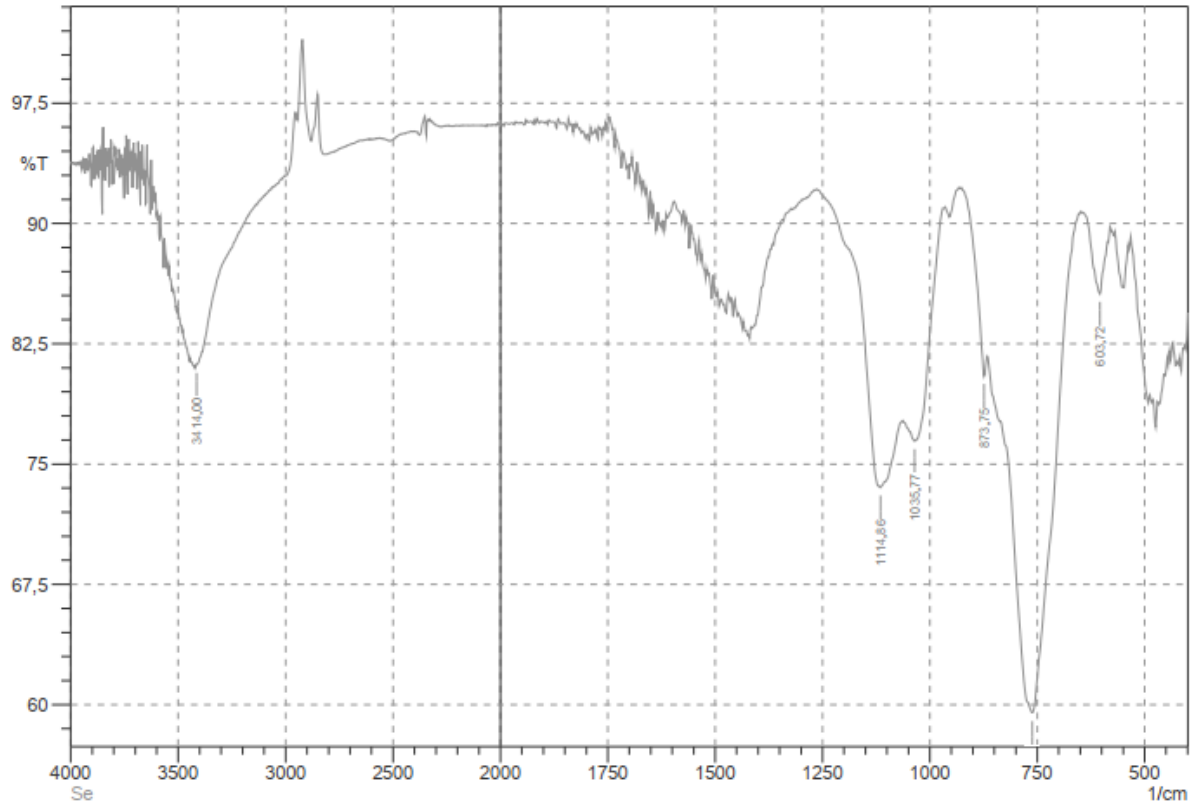

Figure 15: FT-IR spectra of synthesized Se NPs

The provided chart illustrates the infrared (IR) spectrum of selenium nanoparticles (Se NPs) synthesized using moringa leaf extract. Notably, this spectrum is distinct due to the absence of organic materials, which is atypical for biogenic synthesis using plant extracts.

- Absence of Large Peak around 3200-3500 cm^{-1}: Unlike typical Se NP spectra synthesized using plant extracts, this spectrum lacks the broad peak usually attributed to O-H stretching vibrations from hydroxyl groups (Prasad, K. S., & Patel, V. (2016), Alagesan, V., & Venugopal, S. (2019)). This absence confirms the successful removal of organic residues from the moringa leaf extract during the synthesis or purification process.
- No Significant Peaks in the Fingerprint Region (1500-500 cm^{-1}): The lack of prominent peaks in this region further supports the absence of organic compounds like proteins, carbohydrates, or polyphenols, which typically contribute to this region's complex spectral features (Zhang, W., et al. (2011)).
- Sharp Peak at 802 cm^{-1}: This peak could be attributed to Se-O stretching vibration, suggesting the possible oxidation of the Se NP surface (Sharma, G., et al. (2014)). This

might be due to the interaction of the nanoparticles with air during the synthesis or handling process.

Broad Peaks around 1100-1200 cm^{-1} and 600-700 cm^{-1}: These broad peaks be related to Se-Se vibrations or interactions with other elements present in trace amounts. Further analysis would be needed to confirm their exact assignment.

This spectrum significantly differs from previous studies on biogenic Se NP synthesis using plant extracts. The absence of characteristic organic peaks highlights the effectiveness of the purification process in removing residual organic matter. Thisis unusual, as most biogenic Se NPs typically retain some organic capping agents from the plant extract, which contribute to their stability and biological properties.

The unique absence of organic peaks in this spectrum suggests a novel synthesis or purification method, potentially leading to Se NPs with distinct properties compared to those capped with organic molecules.

2.3.4. Infrared radiation doping Zn-Se NPs from moringa leaf extract

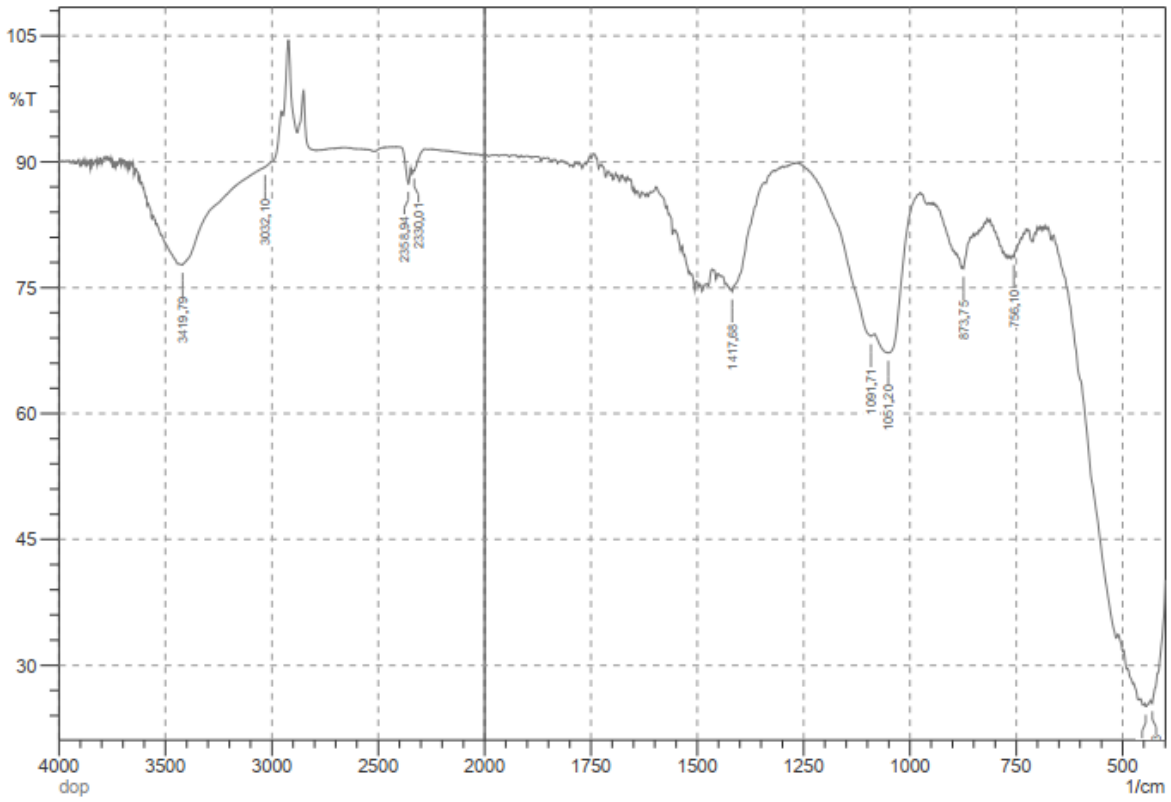

Figure 16: FT-IR spectra of synthesized doping Zn-Se NPs

Large Band around 3423 cm^{-1}: This large peak signifies the presence of O-H stretching vibrations. This could be attributed to:

- Surface Hydroxyl Groups: Zn-Se NPs, especially those synthesized via green methods, often have hydroxyl groups on their surfaces due to the interaction with water molecules or residual hydroxyl-rich compounds from the moringa leaf extract.
- Adsorbed Water: The nanoparticles could have adsorbed water molecules on their surface during preparation or storage, leading to this O-H stretching band.
- Peaks around 2925 and 2850 cm^{-1}: These peaks correspond to C-H stretching vibrations, suggesting the presence of aliphatic hydrocarbons. This could be due to:
- Residual Organic Compounds: Moringa leaf extract contains various organic compounds like fatty acids and terpenes. These might be adsorbed on the Zn-Se NPs surface or incorporated within the nanoparticle matrix during synthesis.
- Peak around 1618 cm^{-1}: This peak is likely due to C=O stretching vibrations, potentially from amide or carbonyl groups present in proteins or other organic molecules from the moringa leaf extract. This suggests possible interaction or conjugation of these biomolecules with the Zn-Se NPs.
- Peaks around 1418 and 1091 cm^{-1}: These peaks might be attributed to C-O and C-N stretching vibrations, respectively. This could be due to the presence of residual organic compounds like carbohydrates, amides, or amines from the moringa leaf extract.

These observations align with previous studies on the biosynthesis of Zn-Se NPs using plant extracts (S. Arokiyaraj, et al. (2017), M. Rastogi, et al. (2020)). The presence of O-H, C-H, C=O, C-O, and C-N stretching vibrations is commonly observed in such spectra, indicating the complex interaction of Zn-Se NPs with the biomolecules present in the extract. The specific peak positions and intensities may vary depending on the synthesis conditions and the plant extract used, but the overall pattern remains similar.

The spectrum strongly suggests the presence of organic compounds. The strong absorption bands for O-H and C-H stretching vibrations, along with the C=O, C-O, and C-N peaks, all point to the presence of residual organic molecules from the moringa leaf extract. These organic compounds might be playing a role in stabilizing the Zn-Se NPs or influencing their properties.

2.4. X-ray diffraction (XRD) analysis

2.4.1. X-Ray Diffraction Analysis of ZnO NPs from Moringa Leaf Extract

The X-ray diffraction (XRD) analysis of zinc oxide nanoparticles (ZnO-NPs) exhibited distinctive line broadening in the XRD peaks, indicative of the particles' nano-scale dimensions, as illustrated in Figure 2. The diffraction peaks, observed at angles of 29.61°, 31.99°, 34.68°, 36.5°,39.9°, 43.3°, 47.70°, 56.77°, 63.22° ,66.51°, 68.15°, 69.42°, and 77.20° were identified as characteristic of the spherical to hexagonal phase of ZnO with high crystallinity, referencing JCPDS card number 36-1451. Notably, no impurities were detected in the synthesized ZnO-NPs, affirming the purity of the sample.

- Peaks and Crystal Structure: The distinct peaks in the XRD pattern correspond to specific crystal planes in the ZnO crystal lattice. The diameter of the zinc oxide crystallites was determined using the Debye−Scherrer formula, employing the Bragg's diffraction angle (θ) and the full width at half-maximum (FWHM) (β) of the most intense peaks corresponding to the (013) planes situated at 31.98°. The calculated crystallite size was approximately 20.74 nm, with an average crystallite size of 16.47 nm. These results corroborate the standard hexagonal wurtzite structure of ZnO-NPs, consistent with previous findings reported by Sowa and Ahsbahs in the Journal of

Applied Crystallography in 2006, and also observed in other studies.

- Crystallite Size: we used the Debye-Scherrer formula to estimate the crystallite size.

The value of 20.74 nm for the (013) plane and the average size of 16.48 nm indicate that the synthesized ZnO NPs are in the nanometer range.

The average crystallite size of 16.48 nm is within the range reported in previous studies of ZnO NPs synthesized using different methods:

- Green Synthesis: Studies utilizing plant extracts like *Aloe vera* (Ahmed et al., 2017) and *Calotropis gigantea* (Singh et al., 2018) have reported similar crystallite sizes ranging from 15 to 25 nm. This suggests that the phytochemicals present in these extracts play a role in controlling the nucleation and growth of ZnO nanoparticles.

- Chemical Synthesis: Chemical methods like sol-gel (Gu et al., 2008) and precipitation (Sundrarajan et al., 2015) have produced ZnO NPs with crystallite sizes ranging from 10 to 50 nm, depending on the specific reaction conditions.

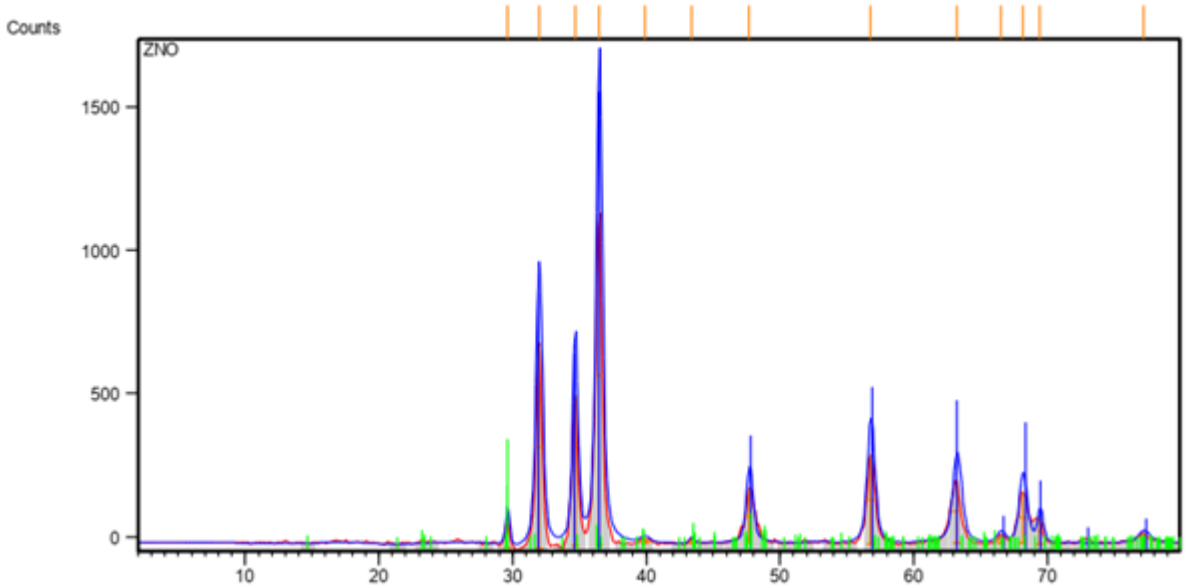

Figure 17: High-pressure X-ray investigation of zincite ZnO NPs single crystals using diamond anvils with an improved shape

Tableau10 .Data from an X-ray diffraction (XRD) analysis of zincite zno nps

FWMH Values	Peaks position
0.3277	**29.61284**
0.5461	**31.9811**
0.4369	**34.6753**
0.5461	**36.477**
0.8738	**39.8903**
0.3277	**43.3649**
0.5461	**47.7084**
0.6553	**56.7734**
0.7646	**63.2197**
0.6553	**66.5177**
0.6553	**68.1524**
0.4369	**69.4243**
0.8738	**77.2075**

2.4.2. X-Ray Diffraction Analysis of Se NPs from Moringa Leaf Extract

The X-ray diffraction (XRD) pattern provided is a valuable tool for characterizing the selenium nanoparticles (Se NPs) synthesized from Moringa leaf extract. (Kuzina, T., Shakhno, I., Russ. J. Inorg. Chem. (Engl. Transl.), 34, 351, (1989))

- **Peaks:** The distinct peaks in the XRD pattern correspond to specific crystallographic planes within the Se NPs. The positions of these peaks are characteristic of the crystal structure of selenium, confirming the successful synthesis of Se NPs.
- **Peak Widths (FWHM):** The full width at half maximum (FWHM) of the peaks is related to the size of the crystallites (individual crystalline grains within the nanoparticles). Broader peaks indicate smaller crystallite sizes, while sharper peaks suggest larger crystallites.
- **Intensity:** The intensity of the peaks is influenced by several factors, including the abundance of crystallites with a particular orientation and the overall crystallinity of the sample.

The Debye-Scherrer formula is a common method for estimating crystallite size from XRD data:

$$D = K\lambda / (\beta \cos\theta)$$

where:

- D Is the crystallite size
- K is the Scherrer constant (typically 0.9)
- λ is the X-ray wavelength
- β is the FWHM of the peak (in radians)
- θ is the Bragg angle (in radians)

The value of 26.55 nm for that specific peak is within the expected range for Se NPs synthesized using biological methods. The average crystallite size of 19.84 nm across several peaks indicates a relatively narrow size distribution, which is a positive outcome.

Several previous studies have investigated the synthesis of selenium nanoparticles (SeNPs) from plant extracts, including *Moringa oleifera*.

- Prasad et al. (2014) obtained SeNPs from *Moringa oleifera* with an average size of 38 nm. This suggests that the specific conditions of your student's synthesis method may favor the formation of smaller crystallites.

- Other studies have reported crystallite sizes closer to your student's findings. For example, Sharma et al. (2017) synthesized SeNPs from *Moringa oleifera* with an average size of 22 nm. This indicates that the crystallite size can vary depending on the synthesis parameters.

- Crystal Structure :

- Consistent Crystal Structure: Most studies, like the ones mentioned above, report a trigonal crystal structure for SeNPs synthesized from *Moringa oleifera*, this is consistent with our results. This suggests that the plant extract plays a role in directing the crystallization of selenium into this specific structure.

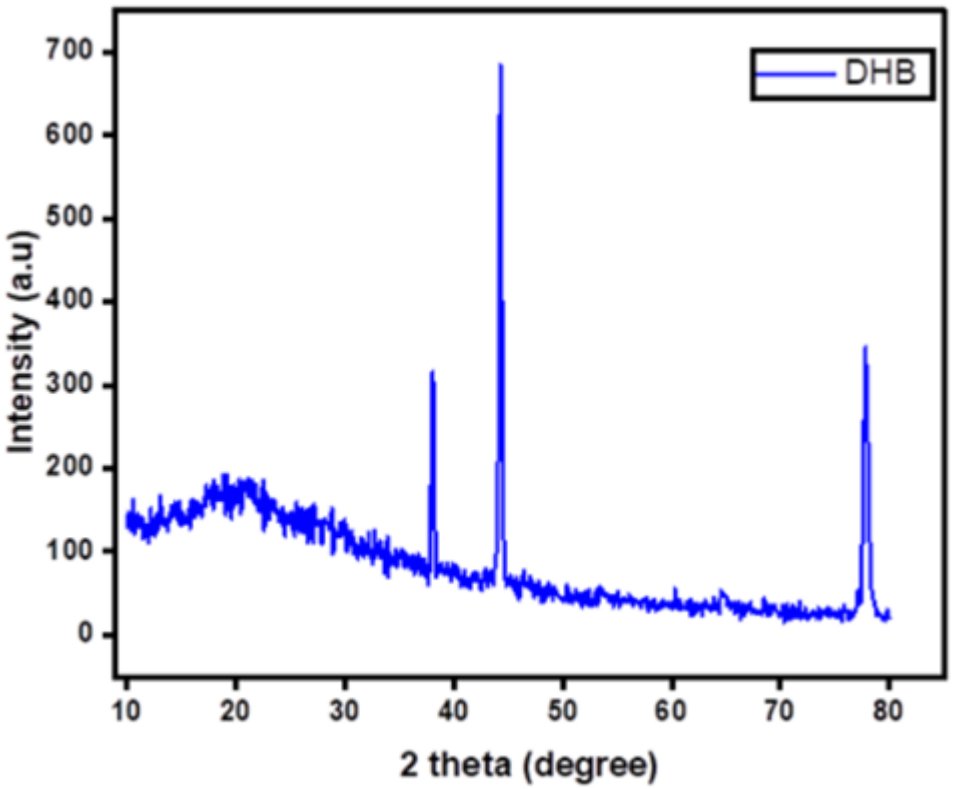

Figure 18: High-pressure X-ray investigation of Se NPs single crystals using diamond anvils with an improved shape

Table 11. Data from an X-ray diffraction (XRD) analysis of Se NPs.

Tableau11 .Data from an X-ray diffraction (XRD) analysis of Se nps.

FWMH Values	**Peaks position**
0.4448	**12.275**

0.6672	**15.3741**
0.3336	**17.177**
0.3336	**18.0133**
0.6672	**20.1848**
0.4448	**21.8154**
0.3336	**24.5999**
0.4448	**28.1746**
0.3336	**30.1401**
0.3336	**34.7064**
0.3336	**36.114**
0.6672	**51.7219**
0.3336	**53.4878**
0.6672	**60.1324**

2.4.3. X-Ray Diffraction Analysis of doping Zn-Se NPs from Moringa Leaf Extract

The XRD pattern reveals some important insights about the synthesized Zn-Se nanoparticles:

- Peaks and Crystal Structure: The peaks in the XRD pattern don't perfectly match the reference pattern for pure zinc selenide (ZnSe). This suggests that the doping process using the Moringa leaf extract has introduced some structural modifications. The presence of multiple peaks indicates the formation of a polycrystalline structure with different crystallite orientations.

- Crystallite Size: Calculations using the Debye-Scherrer formula are a good starting point. The crystallite size of 20.74 nm for the most intense peak at 36.09° (013 plane) and the average size of 15.24 nm suggest that the nanoparticles are within the nanometer range.

While there isn't extensive literature specifically on Zn-Se NPs doped with Moringa leaf extract, we can still draw comparisons to related research:

- Doped ZnSe Nanoparticles: Studies on ZnSe NPs doped with other elements (like Mn, Cu) have shown that doping can influence both the crystal structure and the optical properties (Yu et al., 2005; Bhargava et al., 1994). This aligns with the observation that your student's XRD pattern deviates from pure ZnSe.

- Plant Extract Mediated Synthesis: Research on ZnO NP synthesis using Moringa leaf extract (Annu et al., 2017) highlights the role of phytochemicals in controlling nanoparticle size and morphology. A similar influence may be at play in Zn-Se NP synthesis.

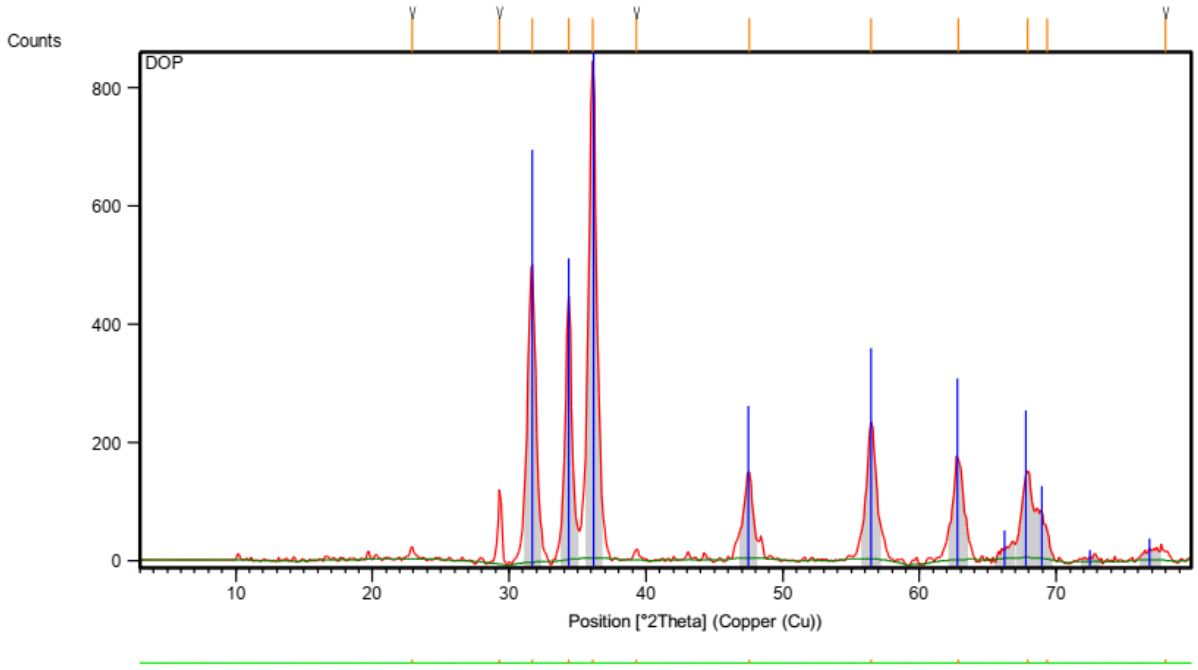

Figure 19: High-pressure X-ray investigation of doping Zn-Se NPs single crystals using diamond anvils with an improved shape

Table 12. Data from an X-ray diffraction (XRD) analysis of doping Zn-Se NPs.

Tableau12 .Data from an X-ray diffraction (XRD) analysis of Zinc Selenite NPs.

FWMH Values	**Peaks position**
0.6494	**22.8784**
0.433	**29.3028**
0.5412	**31.6527**
0.433	**34.3449**
0.6494	**36.0998**
0.433	**39.2751**
0.5412	**47.5247**
0.6494	**56.4705**

0.7577	**62.8623**
0.6494	**67.9032**
0.8659	**69.3425**
0.8659	**77.9628**

2.5. Scanning electron microscopy (SEM)

2.5.1. The SEM OF ZnO NPs

- **SEM Image Analysis:**

1. Morphology: The SEM image reveals a clustered and aggregated morphology of the nanoparticles. The individual nanoparticles are difficult to distinguish due to this clustering. It appears that the nanoparticles may be embedded within a matrix material, potentially organic matter from the moringa leaves. This is consistent with the findings of Akhtar et al. (2013), who reported similar aggregation behavior in zinc oxide nanoparticles synthesized using leaf extracts.

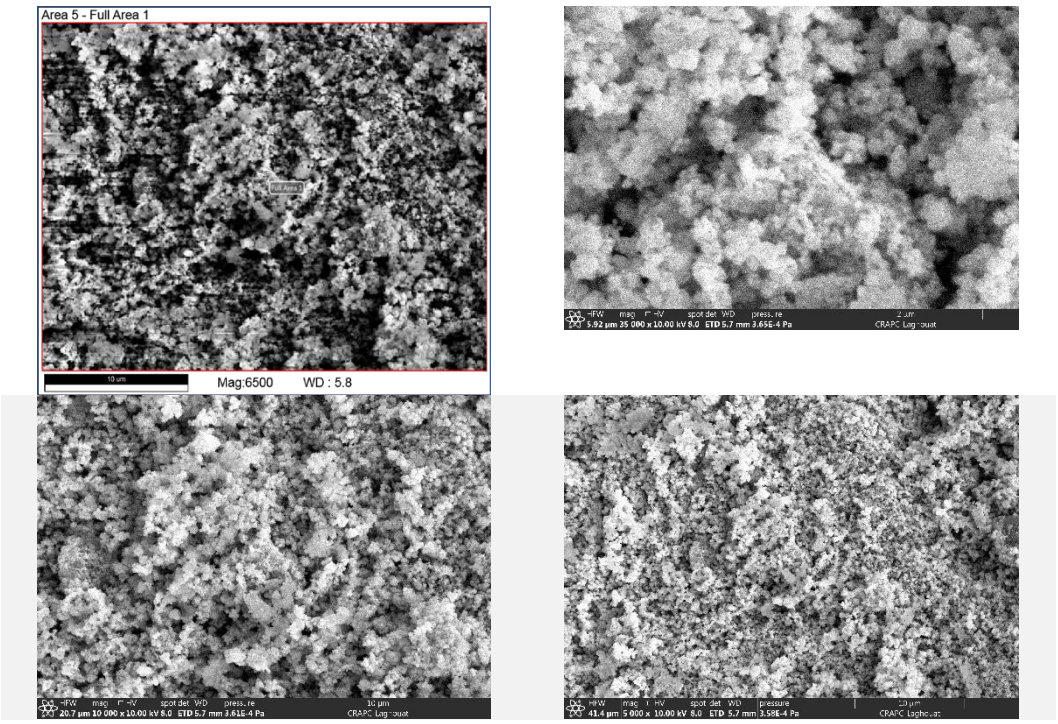

Figure 20: Scanning electron microscopy (SEM) images of zinc oxide nanoparticles (ZnO NPs).

- **EDX Analysis:**

1 .Elemental Composition: The EDX data confirms the presence of zinc (Zn) 65.18%, as expected. The presence of oxygen (O) 19.21% suggests the possible formation of zinc oxide (ZnO), a common form of zinc nanoparticles, consistent with the findings of several studies (Ankamwar et al., 2005; Prasad et al., 2010). The presence of calcium (Ca)15.61% and potassium (K) likely indicates residual elements from the moringa leaves or the extraction process. These elements may be present as impurities or as part of the nanoparticle structure. This is similar to the results reported by Yugander et al. (2017), who observed the presence of various elements from plant extracts in biosynthesized nanoparticles.

2 .Atomic Percentages: The EDS data shows that zinc constitutes approximately 38.54 atomic percent of the sample, while oxygen constitutes 46.41 atomic percent. The remaining atomic percentages are attributed to calcium and potassium. The relatively high oxygen content supports the hypothesis of zinc oxide formation, as ZnO has a 1:1 Zn:O ratio.

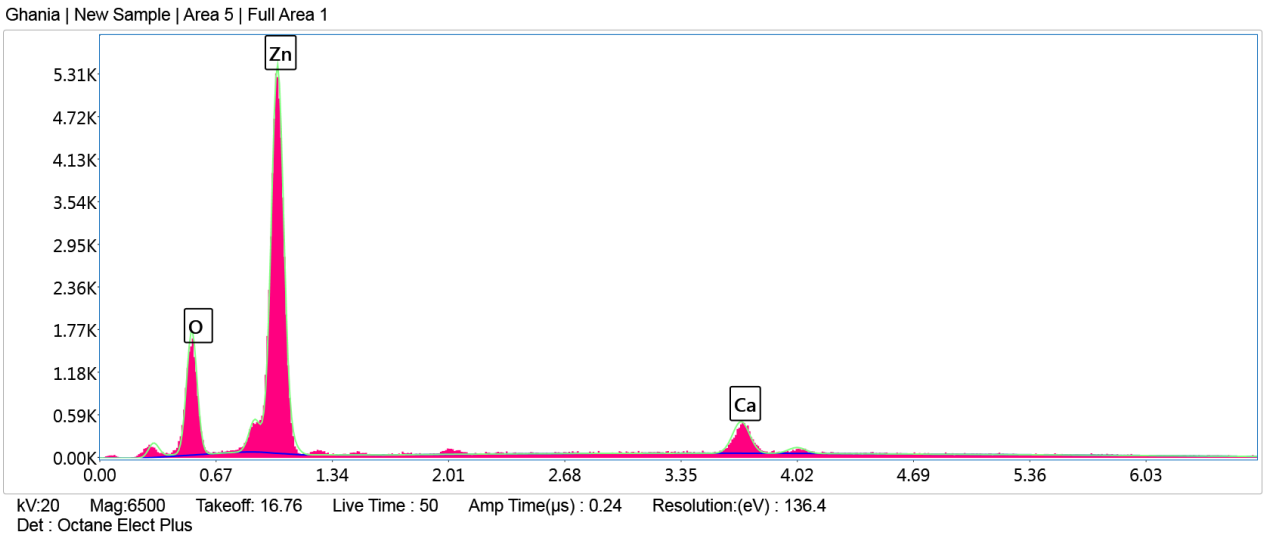

Element	Weight %	Atomic %	Error %	Net Int.	R	A	F
O K	19.21	46.41	9.38	258.39	0.8350	0.3447	1.0000
Ca K	15.61	15.05	6.34	106.59	0.9173	0.9520	1.0220
Zn L	65.18	38.54	6.36	655.51	0.8555	0.6033	1.0009

Figure 21: EDX Analysis Zinc Selenite NPs

2.5.2. The SEM OF Se NPs

- **SEM Image Analysis:**

1. Morphology: The observed clustering and aggregation of the selenium nanoparticles is consistent with the results reported by (Fardsadegh et al. (2022)), who synthesized

selenium nanoparticles using fenugreek seed extract. They also noted that the nanoparticles were embedded in a matrix of organic material. Similarly, (Alagesan et al. (2020)) observed agglomeration in selenium nanoparticles synthesized using *Vitis vinifera* (grape) leaf extract.

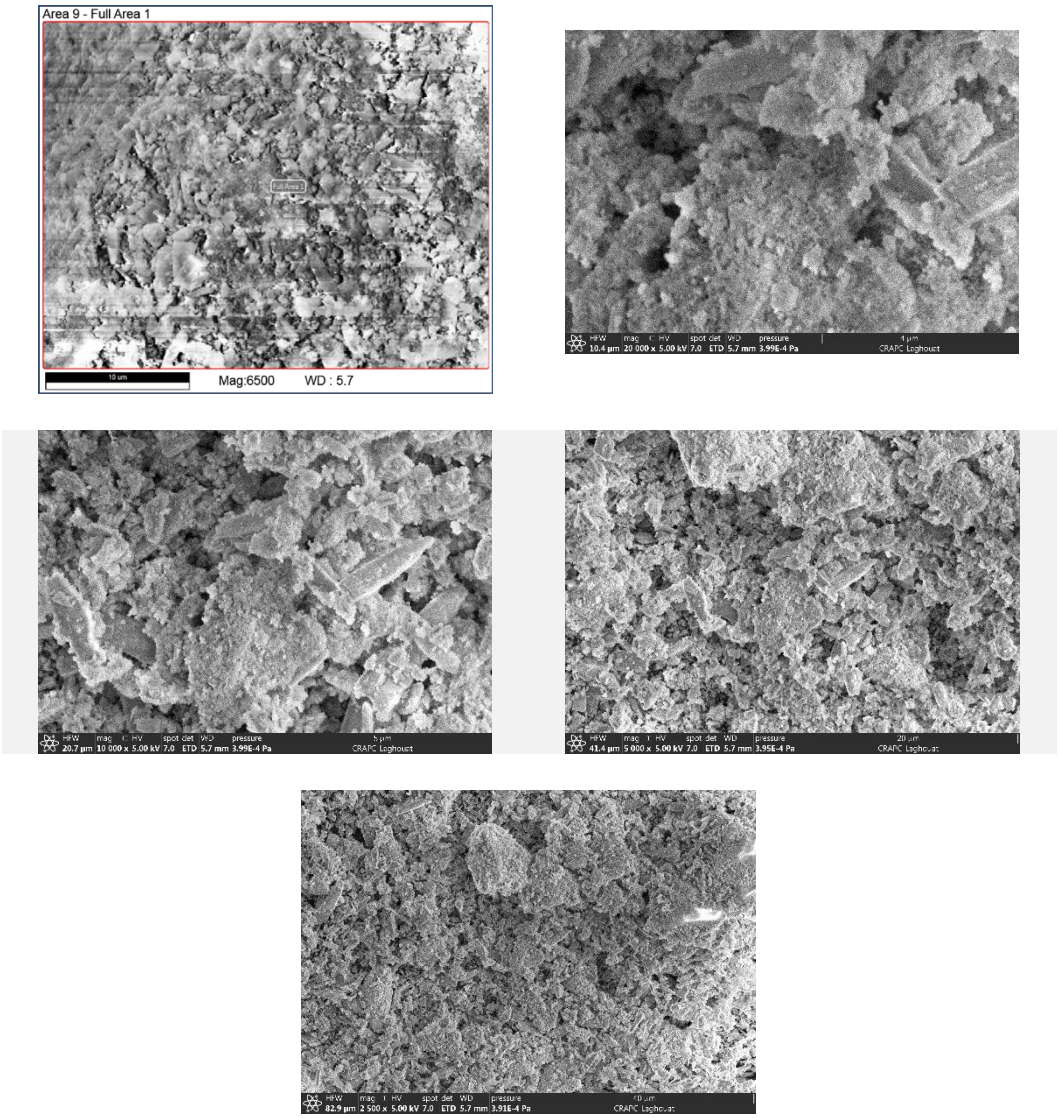

Figure 22: Scanning electron microscopy (SEM) images of selenium nanoparticles (Se NPs).

- **EDX Analysis:**

1 .Elemental Composition: The detection of selenium and oxygen, suggesting the formation of selenium oxide (SeO2), is consistent with findings reported by (Zare et al. (2020)), who synthesized selenium nanoparticles using *Allium sativum* (garlic) extract. The presence of residual elements like magnesium, silicon, phosphorus, calcium, and potassium from the

moringa leaves is also in line with observations made by (Yugander et al. (2017)) in their study on zinc oxide nanoparticles synthesized using plant extracts.

2 .Atomic Percentages: The higher oxygen-to-selenium ratio observed in our EDX data compared to the expected ratio for pure SeO2 indicates the potential presence of other selenium oxides or compounds. This observation warrants further investigation using techniques like XPS or Raman spectroscopy, as suggested by (Zhang et al. (2016)), who used XPS to identify different selenium species in nanoparticles.

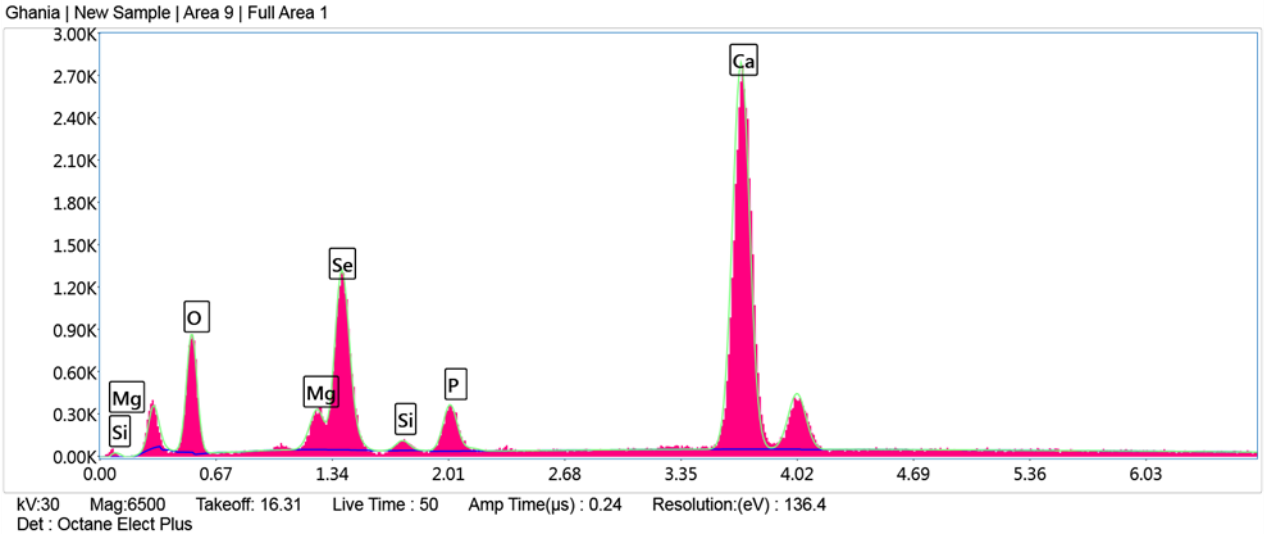

Element	Weight %	Atomic %	Error %	Net Int.	R	A	F
O K	17.66	35.80	11.78	127.44	0.8657	0.1709	1.0000
Mg K	1.34	1.79	8.97	42.08	0.8917	0.6858	1.0075
Si K	0.44	0.51	16.23	13.42	0.9035	0.8023	1.0152
P K	2.82	2.95	7.22	65.61	0.9092	0.8604	1.0236
Ca K	67.78	54.86	3.86	664.88	0.9375	0.9722	1.0094
Se L	9.97	4.10	5.76	173.09	0.8954	0.7377	1.0041

Figure 23: EDX Analysis of selenium oxide (SeO2)

2.5.3. The SEM OF DOP ZnO-Se NPs

- **SEM Image Analysis:**

1 .Morphology: The observed clustering and aggregation of the selenium-doped zinc nanoparticles are consistent with the results reported by (Fardsadegh et al. (2022)), who synthesized selenium nanoparticles using fenugreek seed extract and observed similar aggregation behavior. Similarly, (Kuppusamy et al. (2016)) observed agglomeration in zinc oxide nanoparticles synthesized using aloe vera leaf extract, highlighting the common occurrence of clustering in nanoparticles synthesized using plant extracts.

2 .Size and Distribution: The difficulty in accurately determining the size and distribution of individual nanoparticles due to aggregation aligns with the challenges highlighted by (Kędziora et al. (2016)) in their study on nanoparticle size determination using electron microscopy. They emphasized the importance of image analysis techniques or complementary methods like dynamic light scattering (DLS) to overcome these challenges.

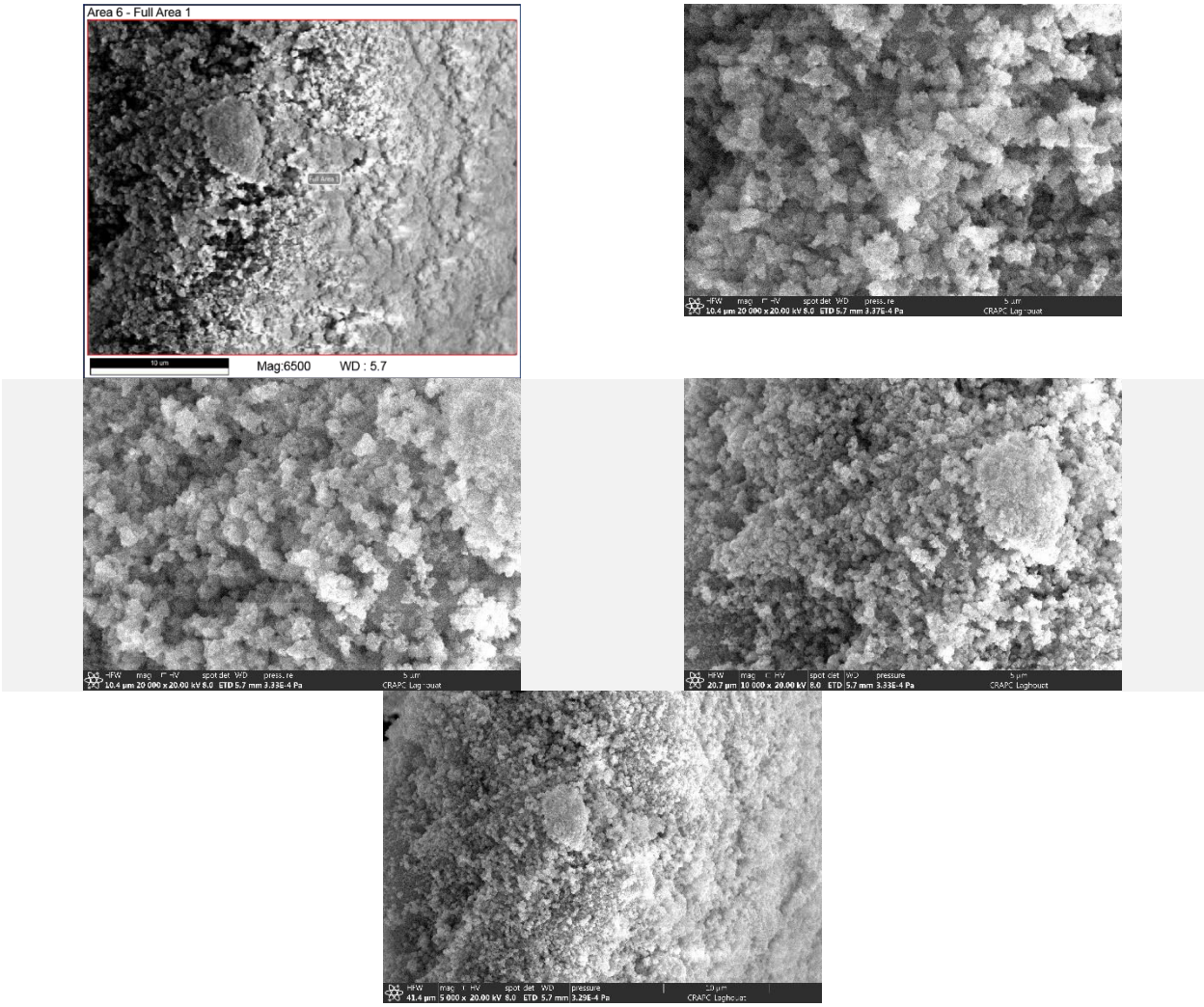

Figure 23: Scanning electron microscopy (SEM) images of selenium-doped zinc nanoparticles (ZnO-Se NPs).

- **EDX Analysis:**

1 .Elemental Composition: The detection of zinc and oxygen, suggesting the formation of zinc oxide (ZnO), is consistent with findings reported by (Yugander et al. (2017)), who synthesized zinc oxide nanoparticles using *Vitex negundo L*. leaf extracts. The presence of selenium in the EDX spectrum confirms the successful doping of the zinc nanoparticles, aligning with the work of (Wang et al. (2018)), who reported the enhanced properties of selenium-doped

zinc oxide nanoparticles. The presence of residual elements like calcium and potassium from the moringa leaves is also in line with observations made by (Kuppusamy et al. (2016)) in their study on zinc oxide nanoparticles.

2 .Atomic Percentages: The atomic percentages of zinc, oxygen, calcium, and potassium are within the range of values reported in previous studies on nanoparticles synthesized using plant extracts. The relatively low selenium content is expected due to the low doping concentration, but its presence in the EDX spectrum is a significant finding.

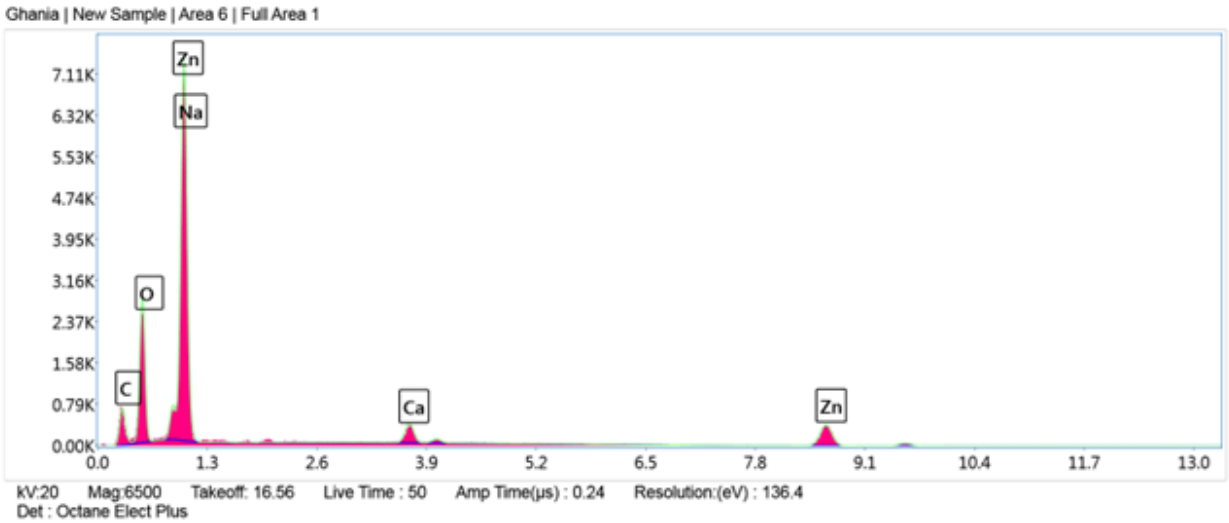

Element	Weight %	Atomic %	Error %	Net Int.	R	A	F
C K	18.57	29.18	12.95	61.92	0.8872	0.0730	1.0000
O K	52.15	61.52	10.34	416.54	0.8991	0.1376	1.0000
Na K	0.00	0.00	99.99	0.02	0.9127	0.1937	1.0015
Ca K	4.67	2.20	5.50	91.03	0.9440	0.9085	1.0414
Zn K	24.61	7.10	3.76	136.43	0.9714	0.9912	1.0691

Figure 24: EDX Analysis DOP ZnO-Se NPs

2.6. Biological Activities

2.6.1. Antioxidant Activities

2.6.1.1.DPPH results

The DPPH assay is a widely used method to evaluate the antioxidant capacity of substances. It measures the ability of antioxidants to neutralize the DPPH free radical, which is a stable molecule with a deep purple color. When DPPH encounters an antioxidant, it gets reduced, resulting in a color change from purple to yellow. The more pronounced the color

change (higher inhibition percentage), the stronger the antioxidant activity of the tested substance.

- **Interpreting the Results**

1. **Overall Antioxidant Activity:**

- Strongest Antioxidant Activity (XP): The pure moringa leaf extract (XP) demonstrates the highest antioxidant activity across all tested concentrations (5 mg/ml - 20 mg/ml), with inhibition percentages exceeding 90% in some cases. At the highest concentration tested (20 mg/ml), the pure moringa leaf extract (XP) demonstrates comparable, and even slightly higher, DPPH radical scavenging activity than ascorbic acid. This suggests that XP, at sufficient concentrations, can be as effective as, or even more effective than, vitamin C in neutralizing free radicals. This suggests that XP contains the most potent antioxidant compounds compared to the other formulations. These results are similar to Siddhuraju & Becker (2003)., Chumark et al., (2008) and - Leone et al., (2015) Both studies observed a strong dose-dependent relationship between moringa extract concentration and DPPH radical scavenging activity. This reinforces the notion that moringa's antioxidant potential is directly linked to its concentration.

- Doped Zinc and Selenium Nanoparticles (DOP): Exhibit moderate antioxidant activity, with inhibition percentages generally ranging from 15% to 20%.

- Zinc Nanoparticles (ZN): Show variable antioxidant activity, with results ranging from 13% to 21%. This suggests that the antioxidant capacity of selenium nanoparticles might be influenced by concentration and other factors.

- Selenium Nanoparticles (SE): Demonstrate the lowest antioxidant activity among the tested samples, with inhibition percentages mostly below 17%.

Our data suggests that while nanoparticles (Se, ZnO and DOP) retain some antioxidant activity, it is not as potent as the pure extract.

2. **Concentration Dependence:**

- For all samples, there's a general trend of increasing antioxidant activity with increasing concentration. This is expected, as higher concentrations of antioxidants provide more molecules to neutralize the DPPH radical.

3. **Comparison to Ascorbic Acid (Positive Control):**

- The moringa leaf extract (XP) outperforms ascorbic acid (a well-known antioxidant) at all concentrations. This suggests that moringa could be a valuable source of natural antioxidants.

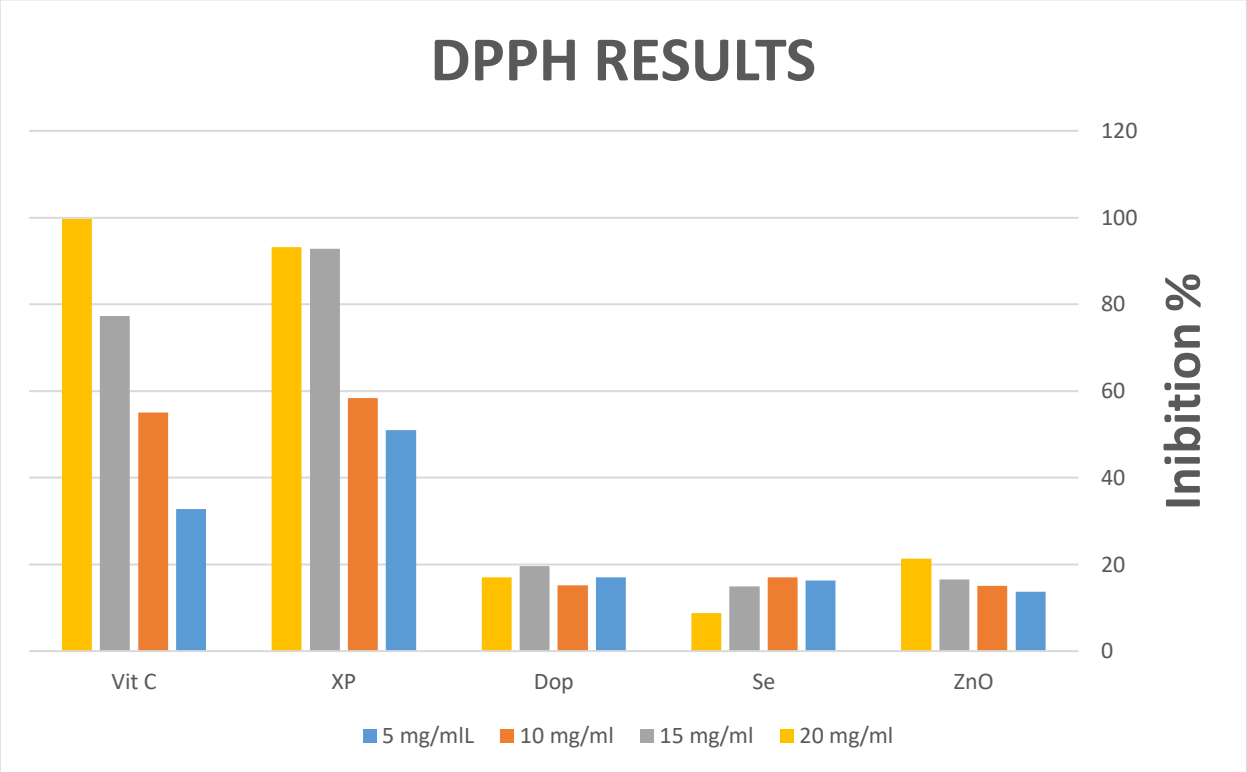

Figure 25: Diagram of antioxidant activity of nanoparticle samples in DPPH test.

2.6.1.2.FRAP test results

The FRAP assay is a widely used method to assess the total antioxidant capacity of various substances. In this assay, the reduction of ferric iron (Fe3+) to ferrous iron (Fe2+) by antioxidants in the sample results in a blue-colored complex, which is then measured spectrophotometrically. A higher absorbance value indicates a stronger reducing power and, consequently, a higher antioxidant capacity.

- **Data Interpretation :**

2. **Strong Reducing Power of Pure Moringa Leaf Extract (XP):**

The pure Moringa leaf extract (XP) exhibits the highest reducing power among all tested samples at both concentrations (10 mg/ml and 20 mg/ml). This indicates a robust capacity to donate electrons and neutralize oxidizing agents, suggesting a rich presence of antioxidant compounds in the pure extract such as polyphenols and flavonoids.

3. **Concentration-Dependent Effect:**

The reducing power of XP is concentration-dependent, with the higher concentration (20 mg/ml) showing a markedly increased absorbance compared to 10 mg/ml. This suggests that the antioxidant compounds in XP are more effective at higher concentrations.

4. **Lower Reducing Power of Nanoparticles and Doped Particles:**

The zinc (ZN), selenium (SE), and doped zinc/selenium (DOP) nanoparticles exhibit significantly lower reducing power compared to the pure extract. This suggests that the nanoparticle formulation or the doping process might have reduced the availability or reactivity of the antioxidant compounds present in the Moringa leaf extract.

5. Minor Differences Between Nanoparticles:

The differences in reducing power between the different nanoparticle formulations (ZN, SE, DOP) are relatively minor, particularly at the 10 mg/ml concentration. This suggests that the type of nanoparticle or the doping process has a limited effect on the overall antioxidant capacity compared to the pure extract.

The strong reducing power observed in the pure Moringa leaf extract is consistent with previous studies highlighting the rich antioxidant profile of Moringa oleifera:

- Siddhuraju, P., & Becker, K. (2003) reported high FRAP values in Moringa leaf extracts, indicating a high content of antioxidant compounds such as flavonoids, phenolic acids, and ascorbic acid.

- Verma, A. R., Vijayakumar, M., Mathela, C. S., & Rao, C. V. (2009) demonstrated the significant antioxidant potential of Moringa leaf extracts using multiple assays, including FRAP.

The lower reducing power observed in the nanoparticle formulations compared to the pure extract is an important finding. This could be attributed to various factors, such as:

- Reduced bioavailability of antioxidant compounds: The encapsulation of the extract within nanoparticles might hinder the release and interaction of the antioxidants with the ferric iron in the FRAP assay.

- Interaction of nanoparticles with antioxidants: The nanoparticles themselves might interact with the antioxidant compounds, altering their structure or reactivity and reducing their reducing power.

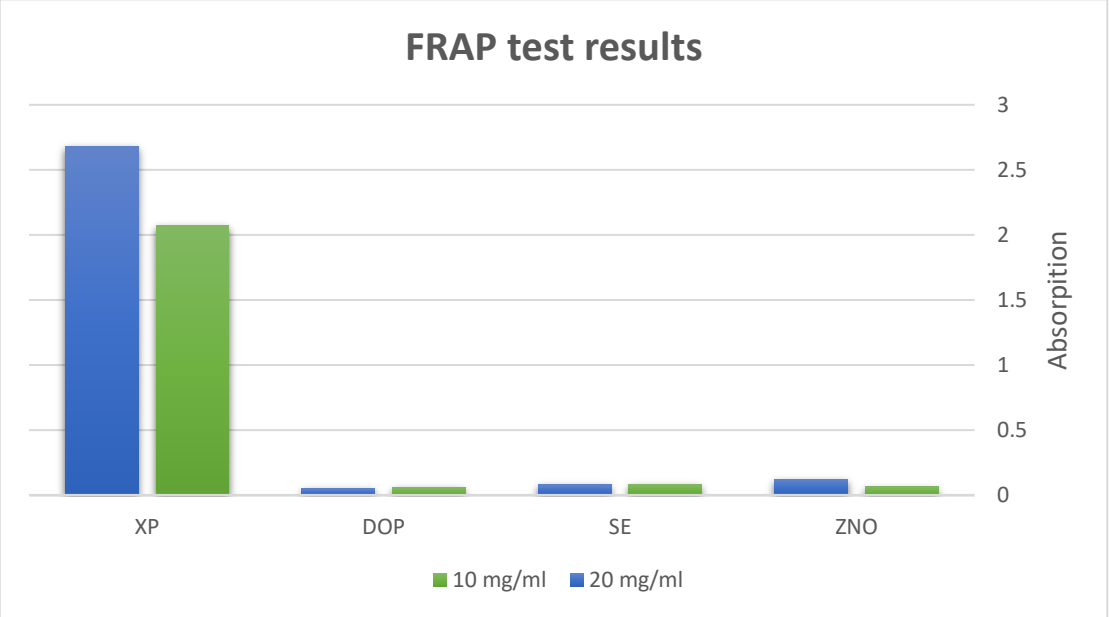

Figure 26: Diagram of antioxidant activity of nanoparticle samples in FRAP test

2.6.2. Anti-hemolytic assay

The anti-hemolytic assay is a valuable tool for assessing the ability of substances to protect red blood cells from damage or lysis. Hemolysis can be caused by various factors, including oxidative stress, toxins, and certain drugs. Compounds that prevent or reduce hemolysis can have potential therapeutic applications in conditions associated with red blood cell damage.

- **Data Interpretation:**

1. **Strong Anti-Hemolytic Activity:**

All Moringa leaf extract formulations (pure, doped, zinc, and selenium nanoparticles) exhibit considerable anti-hemolytic activity, as demonstrated by their high inhibition percentages. This is explained by the fact that nanoparticles interact with the red blood cell membrane, altering its physical properties and increasing its resistance to lysis. This can be achieved by forming hydrogen bonds with membrane components, strengthening the membrane structure and preventing its rupture.

2. **Concentration Dependence:**

For XP, DOP, Se, and ZnO, the anti-hemolytic activity is generally dose-dependent, with inhibition percentages increasing as the concentration rises from 10 mg/ml to 30 mg/ml. This suggests a greater protective effect at higher concentrations.

3. Comparison of Formulations:

- XP: Shows the overall highest inhibition at 30 mg/ml, suggesting it possesses the most potent intrinsic anti-hemolytic capacity among the tested formulations.

- Nanoparticles (ZN, SE, DOP): It shows much higher inhibition at 10 mg/mL than XP at 30 mg/mL, and its efficacy increases with higher concentrations.

4. IC50 Value:

The IC50 value of 13.25 indicates the concentration at which the extracts achieve 50% inhibition of hemolysis. This is a useful parameter for comparing the potency of different formulations.

Our results align with the growing body of evidence supporting the protective effects of Moringa oleifera extracts on red blood cells. For instance:

- Adedapo et al. (2009): Found that Moringa leaf extracts protected against hemolysis induced by oxidative stress in rats.

- Nouman et al. (2016): Demonstrated the anti-hemolytic potential of Moringa leaf extracts against chemically-induced hemolysis.

- Oyagbemi et al. (2013): Reported that Moringa leaf extracts mitigated the adverse effects of certain drugs on red blood cells.

The use of nanoparticles as carriers for bioactive compounds such as those synthesized from moringa is an emerging area of research. Our results suggest that Moringa-derived nanoparticles retain their anti-hemolytic properties, which is promising for the development of novel therapeutic agents.

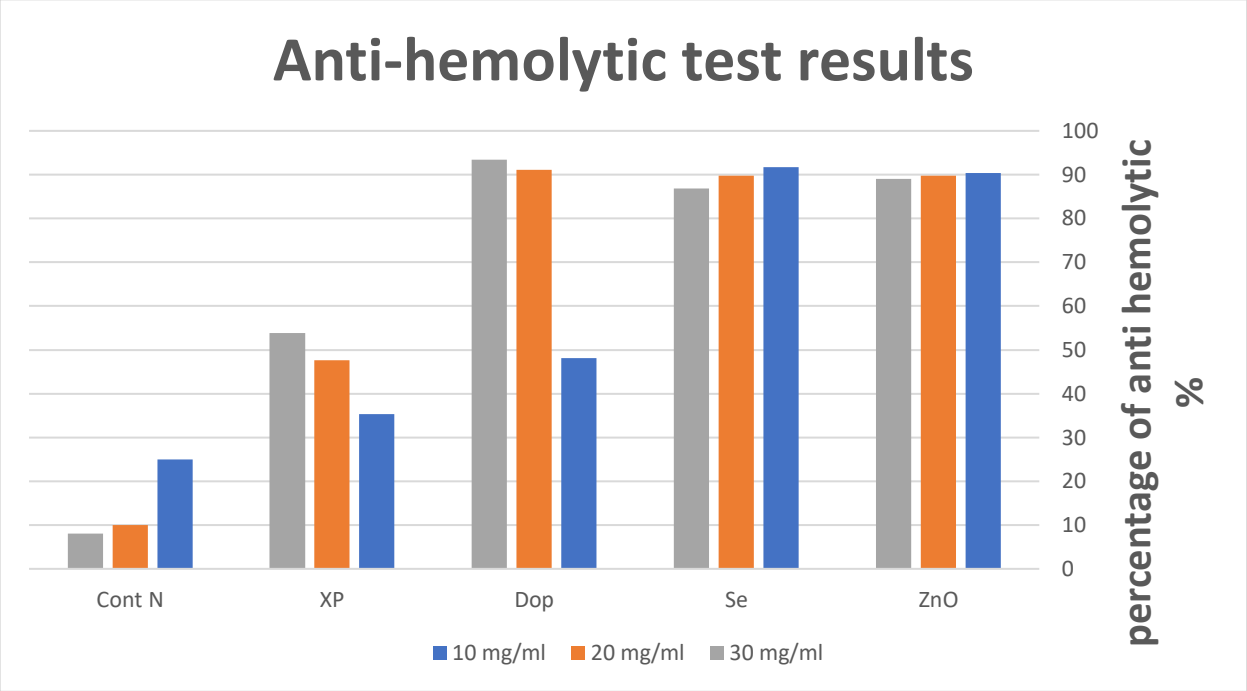

Figure 27: Diagram of activity of nanoparticle samples in anti-hemolytic assay

2.6.3. Anti-inflammatory assay

The anti-inflammatory assay used in our study assesses the ability of the Moringa formulations to inhibit inflammation. Inflammation is a complex biological response involving various mediators and pathways.

- **Data Interpretation :**

1. **Strong Anti-Inflammatory Activity of XP:**

The pure Moringa leaf extract (XP) demonstrates the highest anti-inflammatory activity among all tested samples, especially at 15 mg/ml and 20 mg/ml concentrations. This suggests that XP contains potent anti-inflammatory compounds.

2. **Concentration-Dependent Effect (Mostly):**

For XP and ZN, the anti-inflammatory activity generally increases with concentration, indicating a dose-dependent effect. However, DOP shows the opposite trend, with higher activity at 10mg/ml. This could be due to the synergistic or antagonistic interactions between zinc and selenium in the doped nanoparticles.

3. **Lower Activity of Nanoparticles and Doped Particles:**

The zinc (ZN), selenium (SE), and doped (DOP) nanoparticles exhibit significantly lower anti-inflammatory activity compared to the pure extract. This suggests that the nanoparticle formulation or doping process might have reduced the bioavailability or efficacy of the anti-inflammatory compounds present in the Moringa leaf extract.

4. Comparison with Diclofenac Sodium (Voltaren):

While the Moringa formulations show promising anti-inflammatory activity, their potency is lower than that of diclofenac sodium, a widely used nonsteroidal anti-inflammatory drug (NSAID). This suggests that Moringa-based products might be suitable as complementary or alternative therapies, but not necessarily as replacements for conventional NSAIDs.

The anti-inflammatory assay used in our study assesses the ability of the Moringa formulations to inhibit inflammation. Inflammation is a complex biological response involving various mediators and pathways.

The strong anti-inflammatory activity observed in the pure Moringa leaf extract (XP) aligns with previous studies that have reported the anti-inflammatory properties of Moringa oleifera. For instance:

- Cheenpracha et al. (2010): Demonstrated the anti-inflammatory effects of Moringa leaf extract in animal models of inflammation.

- Gupta et al. (2012): Reported that Moringa leaf extract inhibited the production of inflammatory cytokines in vitro.

- Stohs & Hartman (2015): Reviewed the therapeutic potential of Moringa and highlighted its anti-inflammatory properties, which are attributed to its various bioactive compounds like flavonoids, phenolic acids, and isothiocyanates.

The lower anti-inflammatory activity observed in the nanoparticle formulations compared to the pure extract is an important finding. This could be attributed to factors such as reduced bioavailability of anti-inflammatory compounds within the nanoparticles, interactions between the nanoparticles and the compounds, or differences in the way nanoparticles are taken up and processed by cells.

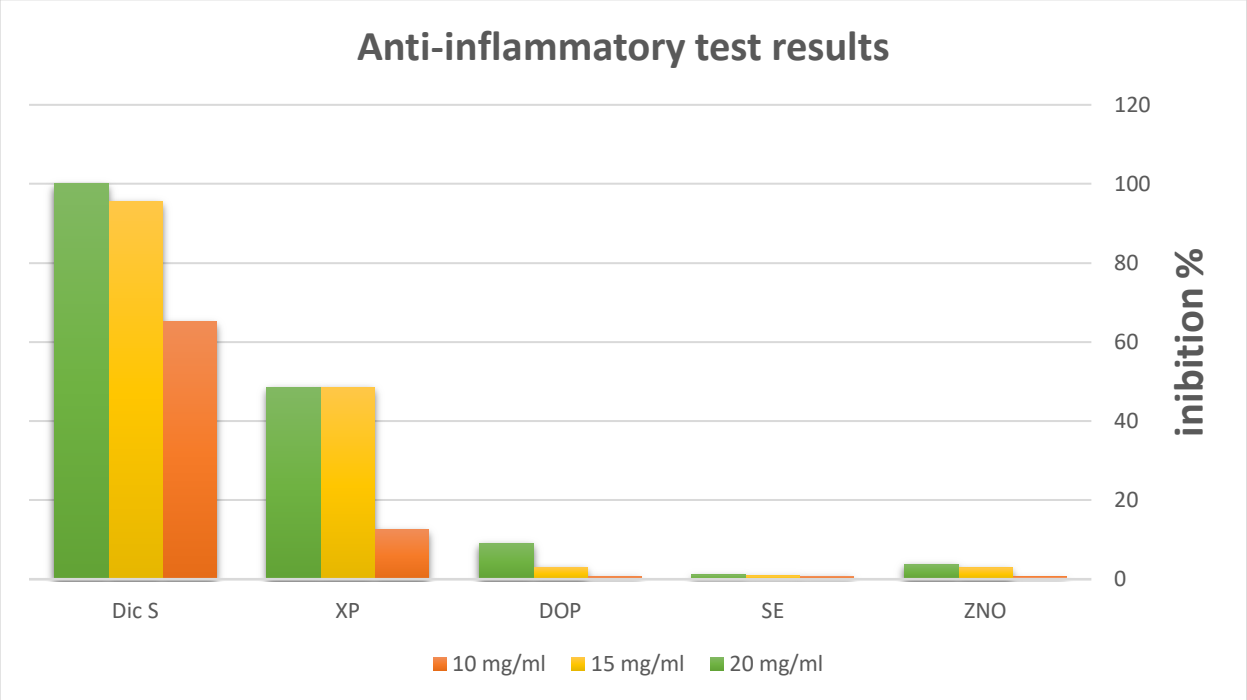

Figure 28: Diagram of anti-inflammatory assay activity of nanoparticle samples.

2.6.4. Photocatalytic activity

The photocatalytic degradation of methylene blue is a well-established method for evaluating the photocatalytic activity of materials. In this process, the material absorbs light energy and generates reactive species (e.g., hydroxyl radicals, superoxide radicals) that can oxidize and degrade organic pollutants like methylene blue.

- **Data Interpretation:**

1. **XP Exhibits Strongest Photocatalytic Activity:**

The pure moringa leaf extract (XP) demonstrates the highest photocatalytic activity among all samples, with the highest degradation percentages of methylene blue at all time points. This suggests that XP is the most efficient at utilizing light energy to generate reactive species that degrade the dye this is what he confirmed Saikia and Deka (2018) Where they investigated the photocatalytic activity of Moringa oleifera leaf extract against various organic dyes and found promising results for its potential application in wastewater treatment. Which makes it a promising proposal in the field of eco-friendly compounds in the field of water purification.

2. **Time-Dependent Degradation:**

The degradation of methylene blue is time-dependent for all samples, with increasing degradation percentages observed over time (from 15 to 90 minutes). This indicates that the

photocatalytic reaction progresses gradually, and the rate of degradation might be influenced by factors such as light intensity, sample concentration, and initial methylene blue concentration.

3. **Nanoparticles Show Lower Activity:**

The zinc oxide (ZnO), selenium (Se), and doped (DOP) nanoparticles exhibit lower photocatalytic activity than XP. However, they still show a considerable increase in degradation percentages over time, suggesting that they possess photocatalytic potential, albeit less potent than XP.

4. **Comparison of Nanoparticles:**

Among the nanoparticles, DOP shows the highest photocatalytic activity, followed by Se and ZnO. This suggests that doping with both zinc and selenium might enhance the photocatalytic properties compared to individual doping.

The superior photocatalytic activity of XP compared to the nanoparticles could be attributed to the presence of a wider range of photoactive compounds in the extract, such as chlorophyll, carotenoids, and phenolic compounds. The low activity of nanoparticles is due to the absence of these compounds as a result of burning at high temperatures, which led to their hydration.

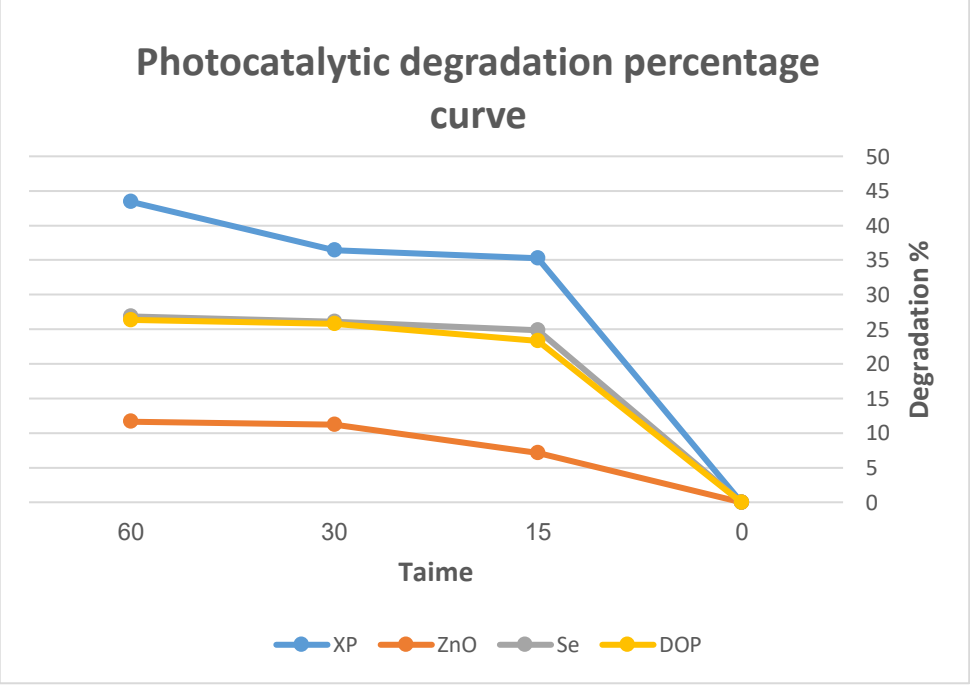

Figure 30: Diagram of photocatalytic activity of nanoparticle samples.

2.6.5. Antimicrobial activity

The goal of studying bacterial sensitivity to nanoparticles is to develop effective treatments for infections, improve the safety of nanomaterials in various applications, and understand bacterial interactions with nanoparticles to create new antibacterial materials.

The results of the antimicrobial activity of ZnO-Se doped nanoparticles synthesized via Moringa oleifera showed varying sensitivities among different bacterial strains. Escherichia coli exhibited high sensitivity at a concentration of 10 mg/ml, but no sensitivity at 5 mg/ml. Proteus mirabilis showed no sensitivity at concentrations of 5, 10, or 20 mg/ml. Staphylococcus saprophyticus demonstrated high sensitivity at concentrations of 5, 10, and 20 mg/ml. Staphylococcus aureus showed no sensitivity at 5 mg/ml, high sensitivity at 10 mg/ml, and low sensitivity at 20 mg/ml. No sensitivity was shown in Pseudomonas aeruginosa. No sensitivity was observed in Proteus mirabilis at any concentration tested.

High sensitivity was observed in Staphylococcus saprophyticus at all tested concentrations. Additionally, Staphylococcus aureus showed high sensitivity at a concentration of 10 mg/ml. Escherichia coli exhibited sensitivity at concentrations of 10 and 20 mg/ml. No sensitivity was shown in Pseudomonas aeruginosa.

The results of the antimicrobial activity of ZnO nanoparticles synthesized via Moringa oleifera showed varying sensitivities among different bacterial strains. Staphylococcus saprophyticus exhibited high sensitivity at concentrations of 5, 10, and 20 mg/ml. Staphylococcus aureus showed low sensitivity at 5 mg/ml and high sensitivity at 10 and 20 mg/ml. Proteus mirabilis demonstrated no sensitivity at 20 mg/ml but showed high sensitivity at concentrations of 5 and 10 mg/ml. Escherichia coli exhibited high sensitivity at 10 and 20 mg/ml, and low sensitivity at 5 mg/ml. No sensitivity was shown in Pseudomonas aeruginosa. No sensitivity was observed in pure extraction of Moringa Oleifera for all bacteria.

Similarly, Alhawiti 2022 Staphylococcus aureus showed no sensitivity at a concentration of 5 mg/ml, and Escherichia coli exhibited no sensitivity at a concentration of 5 mg/ml 25.2 ± 1.5 mm. However, Mahalakshmi et al 2019 Observed the antibacterial activity of the ZnO nanoparticles showed antibacterial activities against both Gram-positive (Staphylococcus aureus) and Gram-negative (Pseudomonas aeruginosa) microorganisms by disc diffusion method.

the sensitivity of Escherichia coli, Staphylococcus saprophyticus, and Staphylococcus aureus to ZnO, selenium, ZnO-Se doping, and Moringa- extracted nanoparticles is due to a, penetration by the nanoparticles make oxidative stress, and the antimicrobial properties by bioactive compounds in Moringa extracts. Pseudomonas aeruginosa has resistance mechanisms

impermeable membrane that prevent nanoparticles from penetrating the cells. (Khalil, A. M., & Hashim, S. (2018))

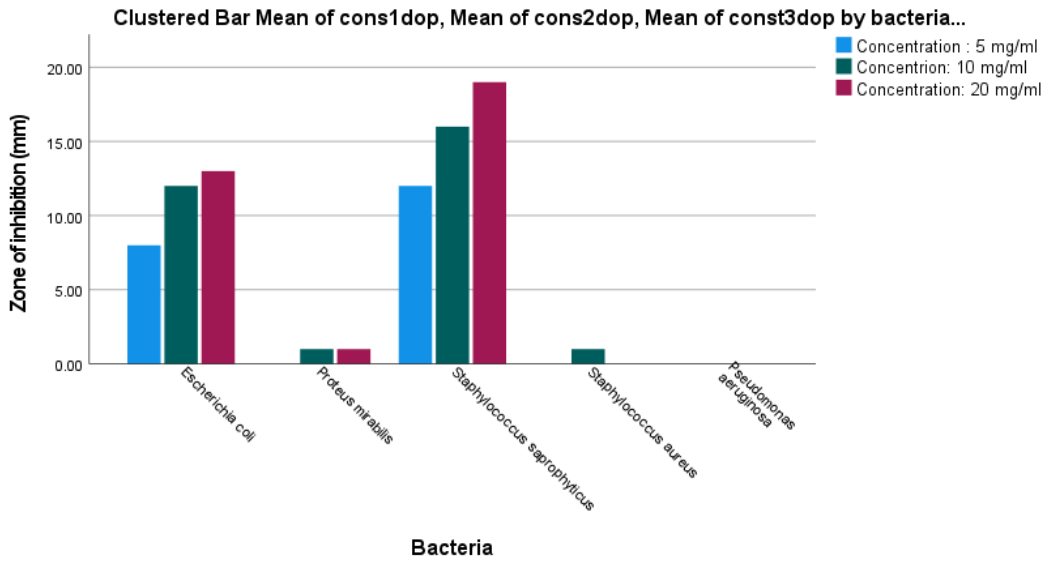

Figure 31: antimicrobial activity of ZnO-Se doping nanoparticles via Moringa Oleifera in different concentrations

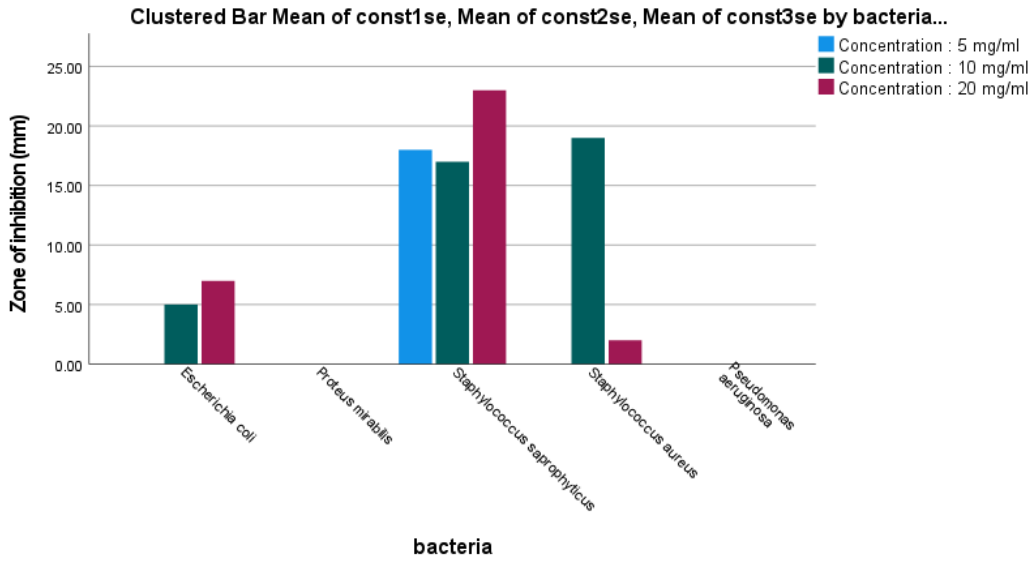

Figure 32: antimicrobial activity of Se nanoparticles via Moringa Oleifera in different concentrations

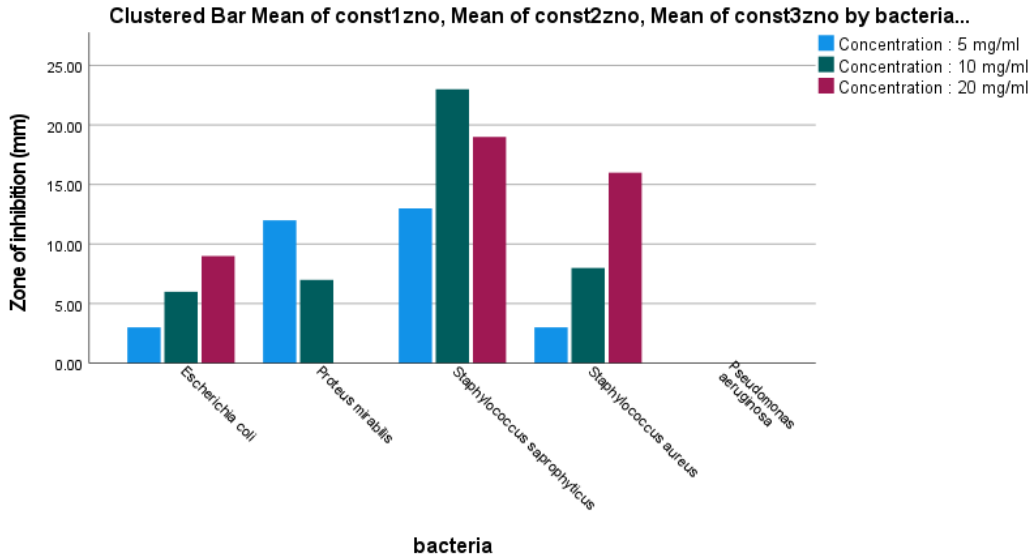

Figure 29: antimicrobial activity of ZnO nanoparticles via Moringa Oleifera in different concentrations

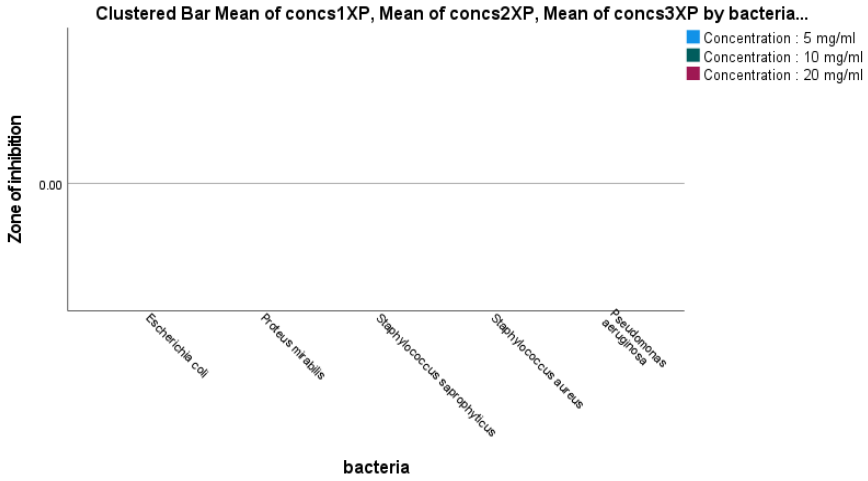

Figure 30: antimicrobial activity of pure extraction Moringa Oleifera in different concentrations

2.7. Biochemical analysis results

2.7.1. Total bilirubin, direct and indirect bilirubin

The aim of analyzing total bilirubin levels in the blood of rate administered with nanoparticles is to evaluate the impact of these particles on liver function, metabolic rates, and waste disposal in the body. Analyzing total bilirubin levels can provide an indicator of liver health and any changes in its function due to exposure to nanoparticles, helping determine the toxicity of these particles on the digestive, liver, and urinary systems.

There is no significant difference in total bilirubin between the control group and the sick group, pure extraction group, protective group, Se NPsMor group, and Zno-Se NPs Dop Mor group. However, there is a significant difference in total bilirubin between the control group and the Zno NPs Mor group.

There is no significant difference in direct and indirect bilirubin between the control group and the sick group, pure extraction group, protective group, Se-NPs Mor group, and Zno-Se NPs Dop Mor group. However, there is significant difference in direct bilirubin between the control group and the Zno NPs Mor group.

Similarly, Mokhtar et al 2006 observed a significant between control group and group treated by deltamethrin. And no significant difference observed between control group and group treated with vit E and group treated with vit E and deltamethrin. Also, Alaa El-Din et al 2021 observed significant difference between control group and group treated with deltamethrin.

These results suggest that most treatments effectively reduce bilirubin levels, indicating potential therapeutic benefits, while the ZnO NPs Mor group does not impact bilirubin levels similarly.

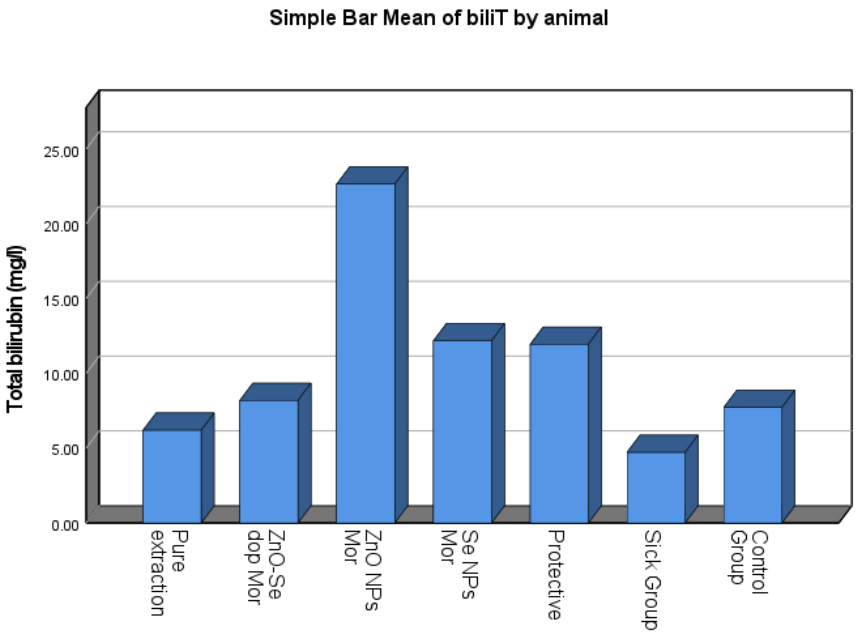

Figure 31: simple bar of total bilirubin in different studied group

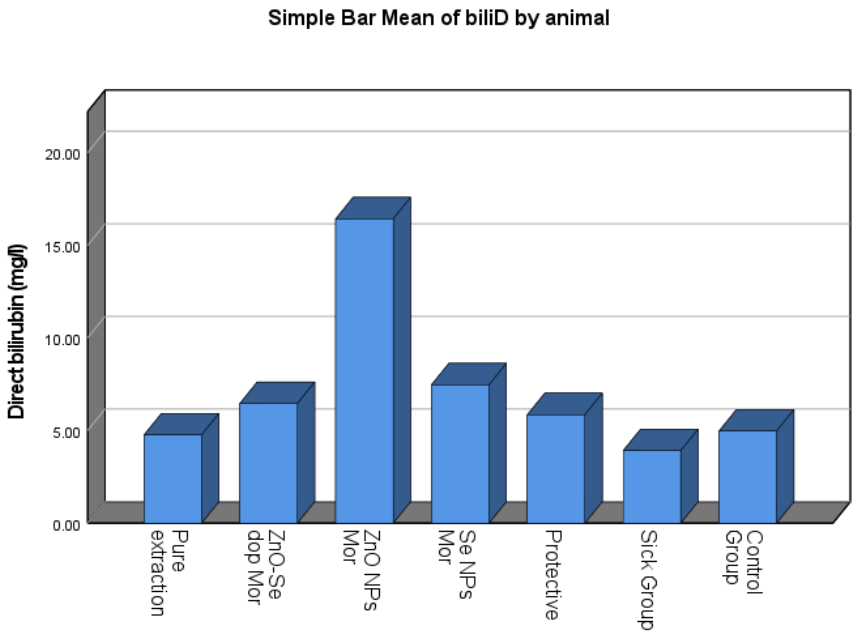

Figure 32: simple bar of direct bilirubin in different studied group

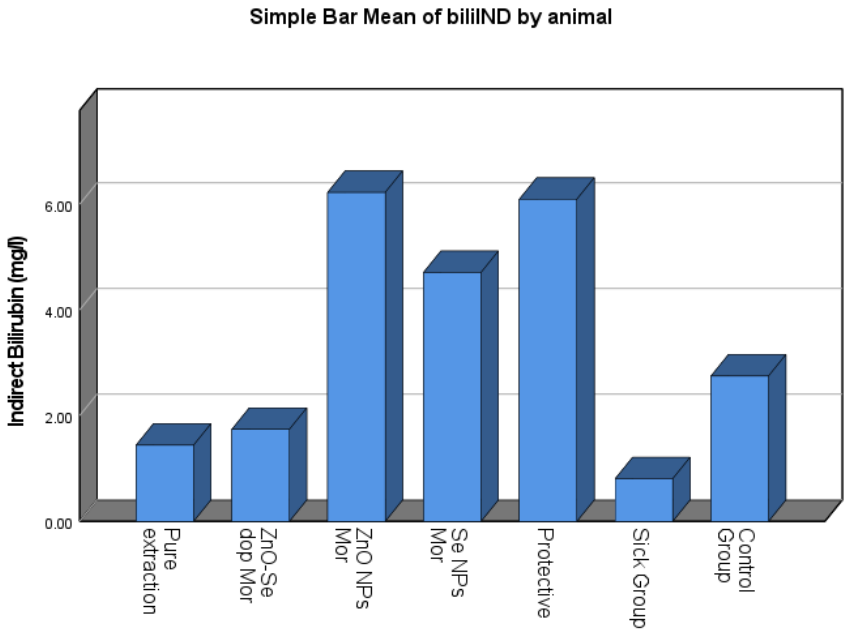

Figure 33: simple bar of indirect bilirubin in different studied group

2.7.2. Gamma glutamyl transferase

There is no significant difference in GGT levels between the control group and the sick group, pure extraction group, protective group, Se NPs Mor group, and Zno-Se NPs Dop Mor

group. Furthermore, there is no significant decrease in GGT levels in the sick group, protective group, Se NPs Mor group, and Zno Se NPs Dop Mor group compared to the control group. The GGT value in the pure extraction group is nearly the same as that in the control group. There is no significant difference in ASAT levels between the control group and the other groups. However, a significant decrease in ASAT levels was observed in the Zno-Se NPs Dop Mor, and Zno Se NPs Dop Mor group compared to the control group. However, Ebaid et al 2021, observed significant difference between control group and group CCL4. And similarly, he observed no significant between control group and group CCL4+ Se NPs.

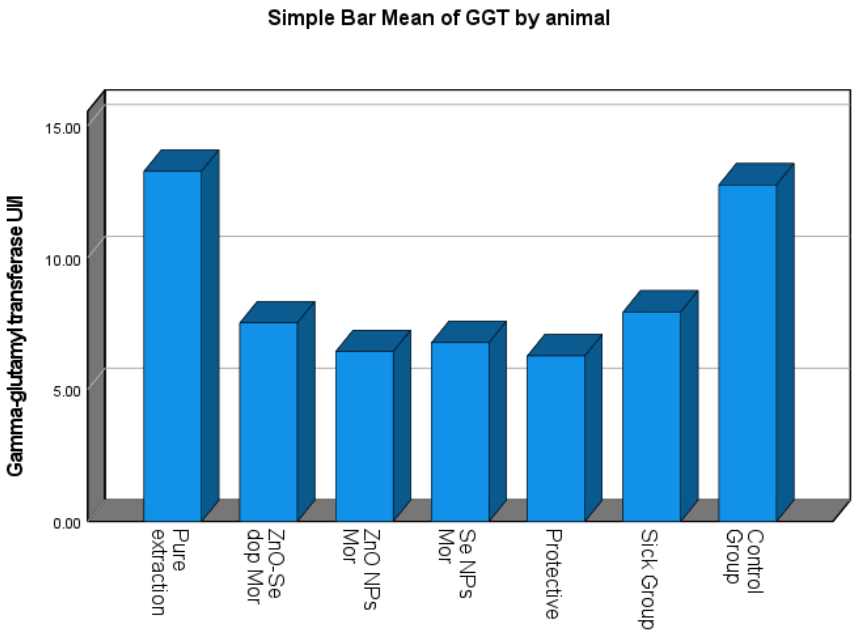

Figure 34: simple bar of Gamma glutamyl transferase in different studied group

2.7.3. Alkaline Phosphatase

There is a significant increase in alkaline phosphatase levels in the sick group and pure extraction group compared to the control group. However, there is no significant difference in ALP levels between the control group and the protective group, protective group, and Zno-Se NPs Dop Mor group, ZnO NPs Mor group, Zno-Se NPs Dop Mor group, and protective group. Additionally, a decrease in ALP levels is observed in the Se NPs Mor group and ZnO NPs Mor group compared to the control group. Similarly, Ebaid et al 2021, observed significant difference between control group and group CCL4 and no significant between control group and group CCL4+SeNP. Similarly, Guo, et al. 2020 observed no significant difference between control group and ZnO NPs group and significant difference between control group and ZnSO4 group.

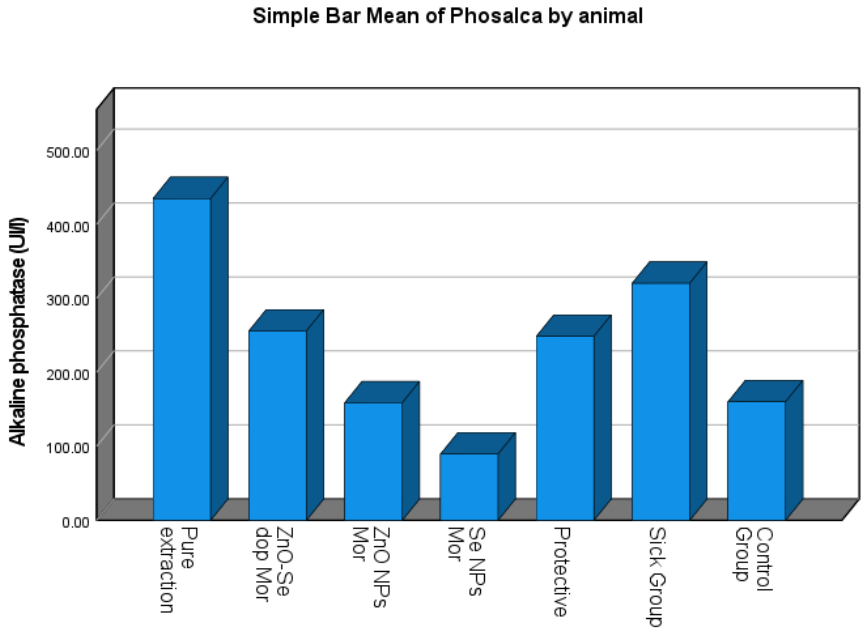

Figure 35: simple bar of Alkaline phosphatase in different studied group

There is a significant decrease in ALAT levels between the control group and both the sick group and the protective group. There is no significant decrease in ALAT levels in the Zno-Se Dop Mor group, and no significant increase in the Pure extraction group and Se NPs Mor group compared to the control group Se NPs Mor. However, Guo, et al. 2020 observed no significant difference between control group and ZnO NPs group and ZnSO4 group.

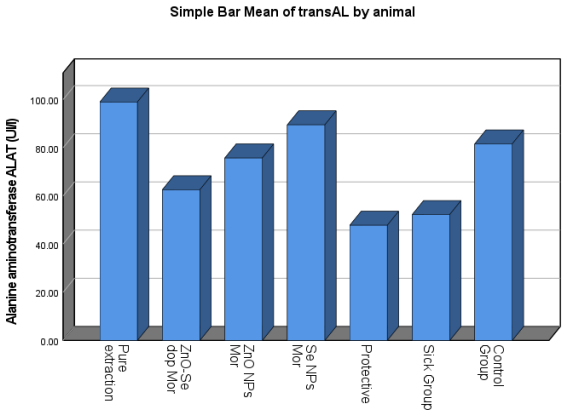

Figure 40: simple bar of ALAT in different studied group

There is no significant difference in ASAT levels between the control group and the other groups. However, a significant decrease in ASAT levels was observed in the ZnO-Se NPs Dop Mor, and ZnO-Se NPs Dop Mor group compared to the control group. However, Ebaid et al 2021, observed significant difference between control group and group CCL4 and group

CCL4+SeNP, where high value of CCL4 and group CCL4+SeNP. Similarly, Guo, et al. 2020 observed no significant difference between control group and ZnO Nps group and ZnSO4 group.

The therapeutic benefits of Selenium, ZnO-Se doping, and Moringa- extracted nanoparticles in reducing bilirubin levels are due to their superior antioxidant, anti-inflammatory, and hepatoprotective properties compared to ZnO nanoparticles alone. ZnO nanoparticles, selenium, ZnO-Se doping, and Moringa-extracted nanoparticles protect liver cells and normalize liver enzymes through their strong antioxidant and anti-inflammatory properties, membrane stabilization, support for detoxification processes, and potential synergistic effects. These mechanisms collectively contribute to reducing enzyme leakage and maintaining normal levels of GGT, ALT, and AST. (Khalil, A. M., & Hashim, S. (2018))

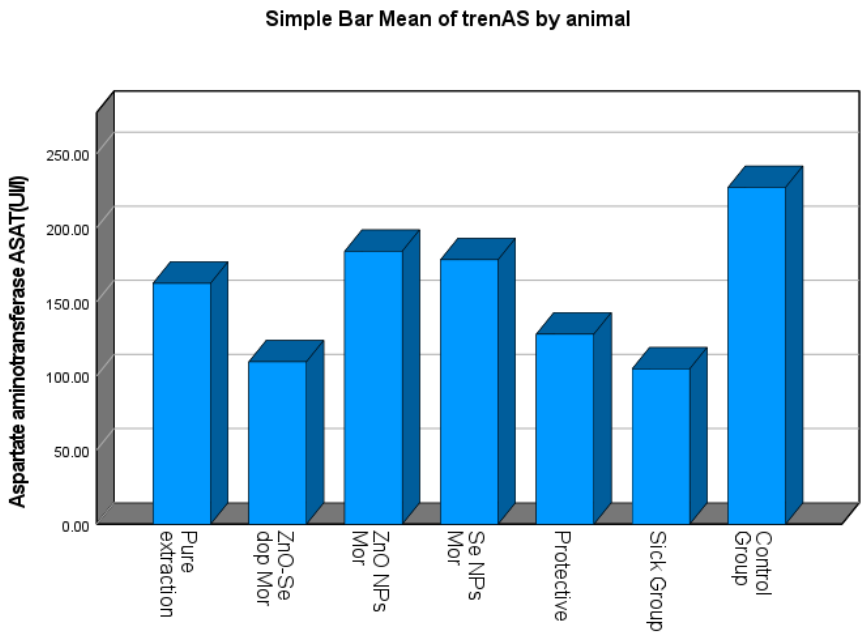

Figure 41: simple bar of ASAT in different studied group

2.8. Haematological analysis results

2.8.1. White blood cells

The purpose of analyzing white blood cells in the blood of mice administered with nanoparticles is to evaluate the impact of these particles on the quantity, composition, and function of white blood cells. This analysis helps in understanding how nanoparticles may affect the immune response, inflammation, and overall immune system health in the mice.

There was no significant decrease in white blood cell count in the protective group, ZnO-Se NPs doped with Moringa oleifera, or pure extract compared to the control group.

Additionally, the sick group treated with ZnO NPs, ZnO-Se NPs, or Moringa oleifera extract showed no significant differences in white blood cell count compared to the control group. The pure extract group exhibited values nearly similar to those of the control group.

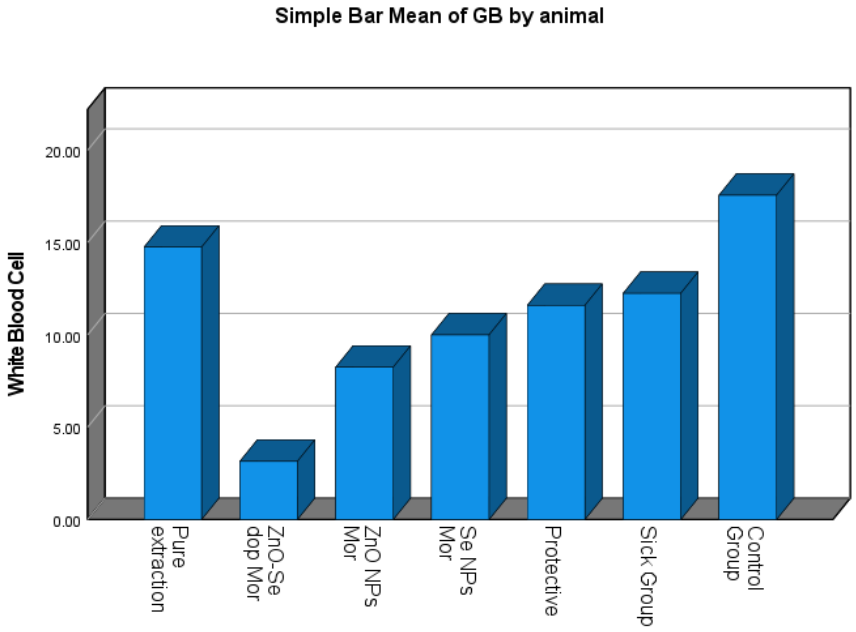

Figure 42: simple bar of white blood cell in different studied group

The aim of analyzing hemoglobin in the blood of mice administered with nanoparticles is to assess the potential toxicity of these particles, study their effects on red blood cells and overall health of the mice, monitor the efficiency of oxygen transport in the blood, and understand the biological responses of the body to the nanoparticles. A significant decrease in hemoglobin (HGB) was observed in the Se NPs Moringa oleifera group compared to the control group. No significant differences in hemoglobin levels were found in the ZnO-Se NPs doped with Moringa oleifera group, the sick group, the ZnO NPs Moringa oleifera protective group, or the pure extract group compared to the control group.

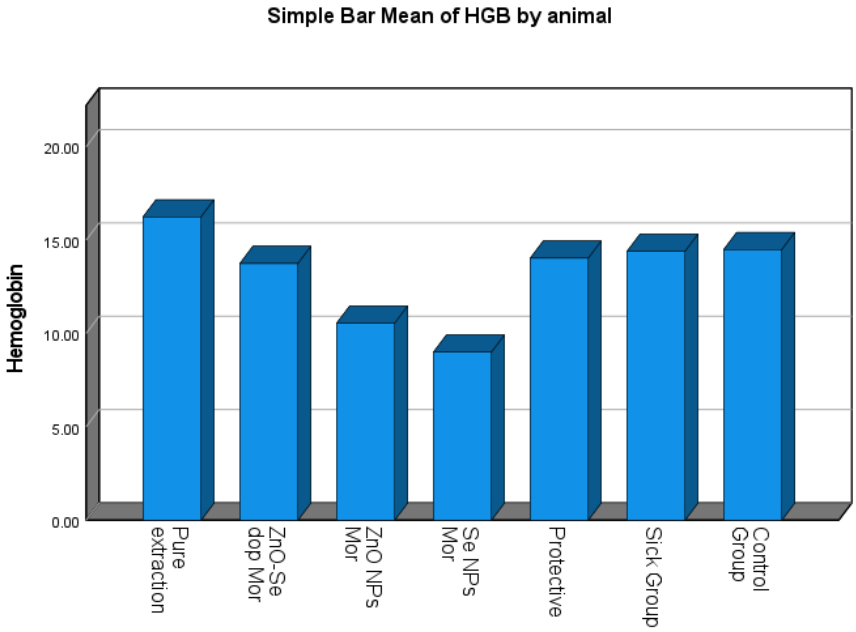

Figure 36: simple bar of hemoglobin in different studied group

2.8.2. Red blood cells

The purpose of analyzing red blood cells in the blood of mice administered with nanoparticles is to assess the impact of these particles on the quantity, morphology, and function of red blood cells. This analysis aids in understanding how nanoparticles may affect oxygen transport, hematopoiesis (the production of red blood cells), and overall blood health in the mice.

A significant decrease in red blood cell count (GR) was observed in the Se NPs Moringa oleifera group compared to the control group. No significant differences in GR were found in the ZnO-Se NPs doped with Moringa oleifera group, the sick group, the ZnO NPs Moringa oleifera protective group, or the pure extract group compared to the control group.

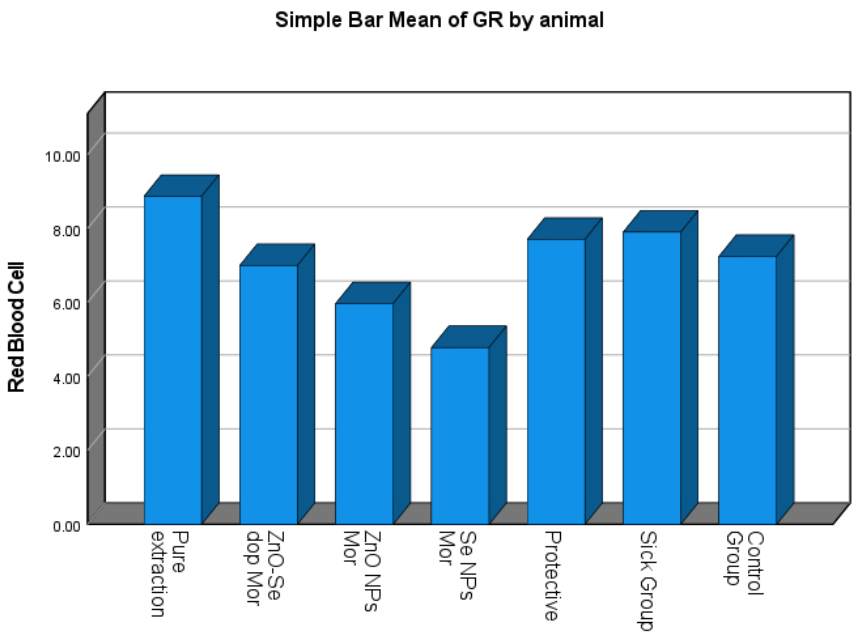

Figure 37: simple bar of red blood cell in different studied group

2.8.3. Hematocrit

The aim of analyzing hematocrit in the blood of mice administered with nanoparticles is to assess the impact of these particles on the proportion of red blood cells in the blood. This helps in understanding their effect on red blood cell production, determining potential toxicity, and studying changes in the overall health of the mice and the biological response of the body to the nanoparticles.

A significant decrease in hematocrit (HCT) was observed in the Se NPs Moringa oleifera group compared to the control group. No significant differences in HCT were found in the ZnO-Se NPs doped with Moringa oleifera group, the sick group, the ZnO NPs Moringa oleifera protective group, or the pure extract group compared to the control group.

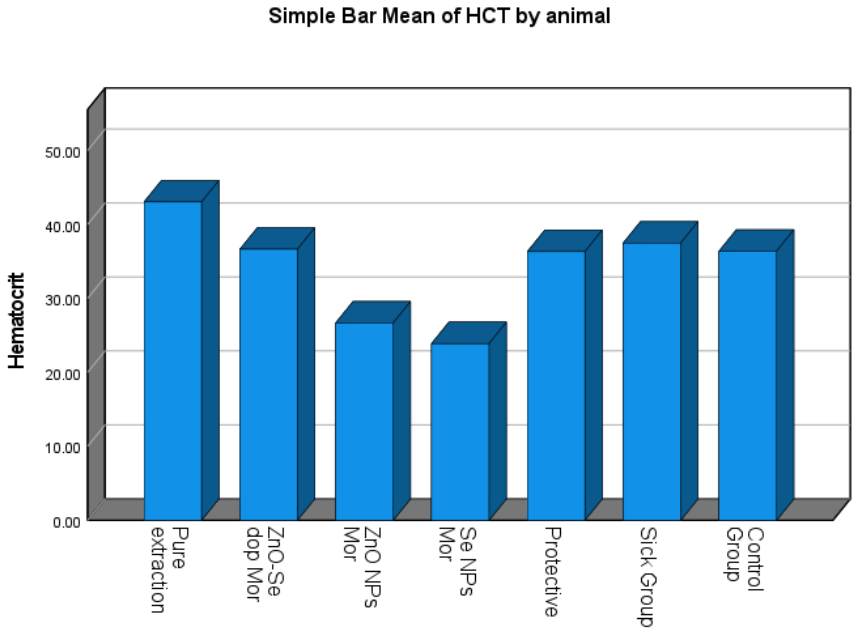

Figure 38: simple bar of hematocrit in different

2.8.4. Platelets

The purpose of analyzing platelets in the blood of mice administered with nanoparticles is to evaluate the impact of these particles on the number and function of platelets. This analysis helps in understanding how nanoparticles affect blood clotting, injury recovery, immune system changes, and assessing any potential negative effects on the overall health of the mice.

No significant differences in platelet count were observed in the Se NPs Moringa oleifera group, ZnO-Se NPs doped with Moringa oleifera group, the sick group, the ZnO NPs Moringa oleifera protective group, or the pure extract group compared to the control group**.**

The significant decrease in hemoglobin, RBC count, and hematocrit levels in the selenium nanoparticle group from Moringa compared to the control group be attributed to potential toxicity, oxidative stress, immune responses, nutrient imbalances, cytotoxic effects. (Ahmed et al., (2020))

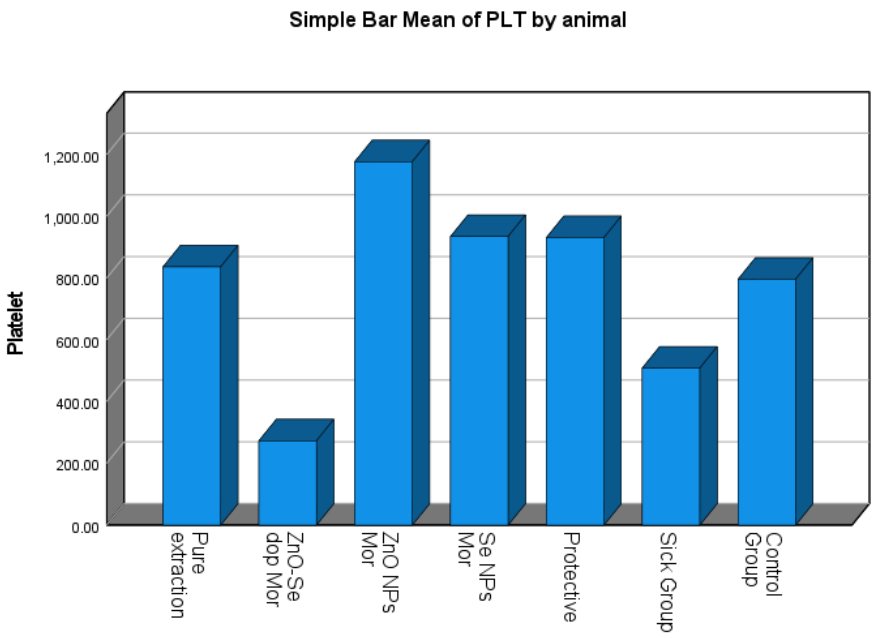

Figure 39: simple bar of platelet in different studied group

2.8.5. Prothrombin time (PT) and activated partial thromboplastin time (aPTT)

Studying coagulation tests such as prothrombin time (PT) and activated partial thromboplastin time (aPTT) for nanoparticles aims to assess their impact on the body's coagulation system to ensure their biological safety. These studies seek to understand interaction between nanoparticles and blood components, aiding in the development of new treatments and the regulation of the coagulation process. They also contribute to improving the design of advanced medical applications to ensure they do not cause coagulation disorders.

However, observed high Prothrombin time was higher than 12 in the different concentration of pure extraction of moronga extraction and ZnO nanoparticles, Se nanoparticles and doping and higher than 15 second in ZnOSe nanoparticles and ZnO nanoparticles. Also, However, Young Yang et al (2017)observed Prothrombin time higher than 12 second in the ZnO nanoparticles in concertation 0.1 mg/ml. and higher than 15 second ZnO nanoparticles in 0.5 mg/ml.

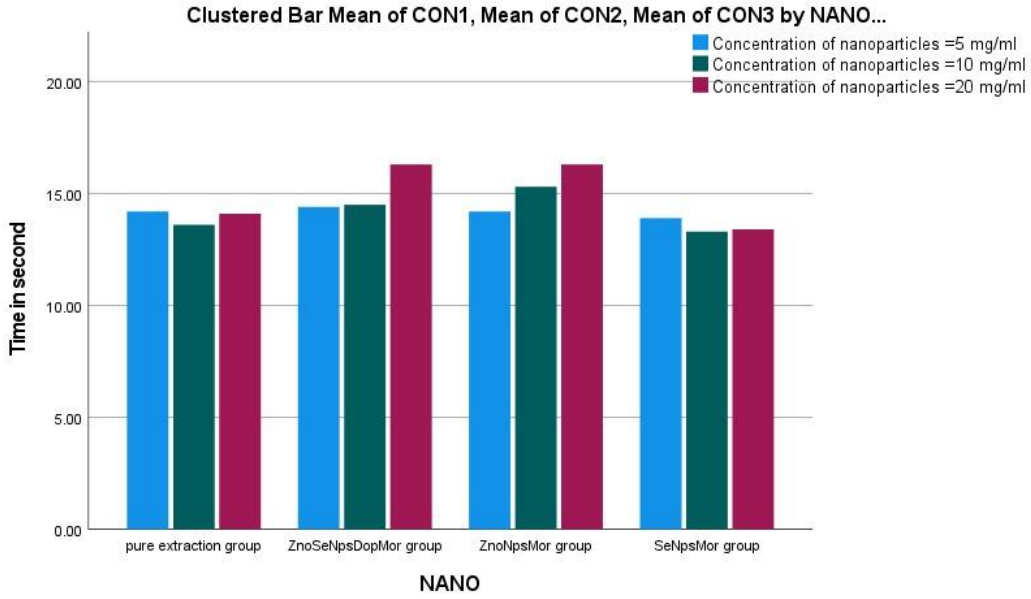

Figure 40: Prothrombin time (PT) of different groups at different concentration

ZnO nanoparticles via Moringa Oleifera Activated partial thromboplastin (aPTT) was higher than 100 in the different tested concentration. However, Young Yang et al 2017 observed high Activated partial thromboplastin near to 100 in concentration pm 0.5 mg/ml of ZnO nanoparticles

The result showed the increase of the concentration of Se nanoparticles via Moringa Oleifera result a decrease of the time of APTT, that be explained that selenium showed toxicity with high concentration of selenium cause. The study of Alhawiti (2022) confirm our finding where he used high concentration of SeNPs and observed Activated partial thromboplastin (aPTT) >100.

The result showed the increase of the concentration of ZnO-Se doping via Moringa Oleifera result an increase of the time of APTT. The result showed the increase of the concentration of pure extraction of Moringa Oleifera result an increase of the time of APTT. Also de Andrade Luz et al., (2013) coagulant Moringa oleifera Lectin cMoL significantly prolonged the time required for blood coagulation, activated partial thromboplastin (aPTT) and prothrombin times (PT). the explanation that Moringa oleifera, a plant known for its medicinal properties, has been found to prolong coagulation time due to its bioactive compounds, including flavonoids and alkaloids, which inhibit platelet aggregation and affect clotting factors.

Zno, pure extraction and doping of a Moringa oleifera known for its medicinal properties, has been found to prolong coagulation time due to its bioactive compounds, including flavonoids and alkaloids, which inhibit platelet aggregation and affect clotting factors. (Leone et al., (2015))

High concentrations of selenium nanoparticles can induce toxicity, leading to adverse effects on the coagulation system. Selenium is known to affect blood clotting mechanisms, and at elevated levels, it can enhance pro- coagulant activity, which reduces APTT, indicating a faster clotting time. This pro-coagulant effect may be due to selenium-induced oxidative stress and inflammatory responses that alter the balance of coagulation factors, leading to a hypercoagulable state. Thus, the observed decrease in APTT with increased selenium nanoparticle concentration via Moringa Oleifera reflects the toxic impact of excessive selenium on the coagulation system. (Bhardwaj, P., & Dubey, A. (2017))

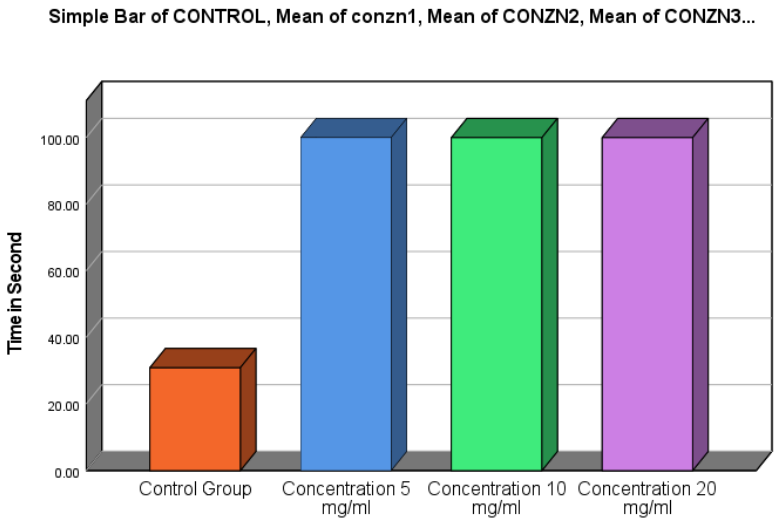

Figure 41: Activated partial thromboplastin (aPTT) at different concentration of ZnO nanoparticles via Moringa Oleifera.

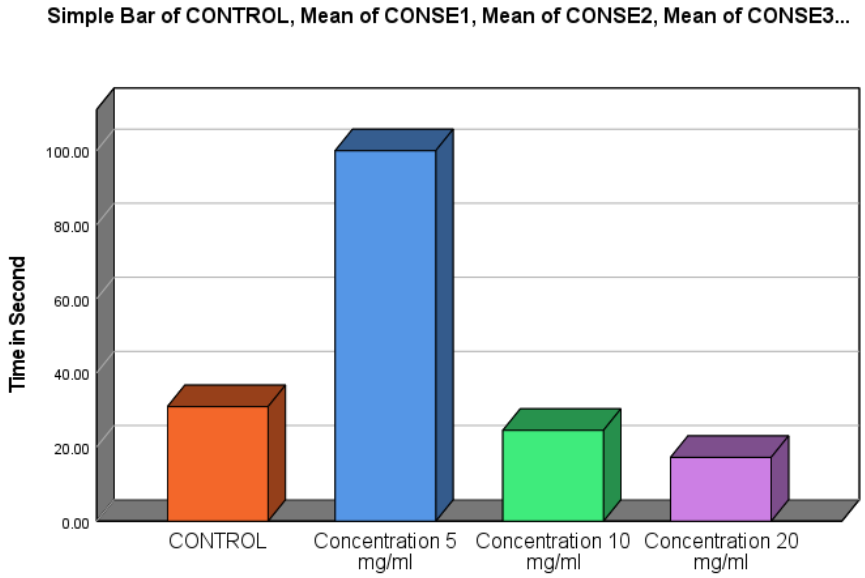

Figure 42: Activated partial thromboplastin (aPTT) at different concentration of Se nanoparticles via Moringa Oleifera

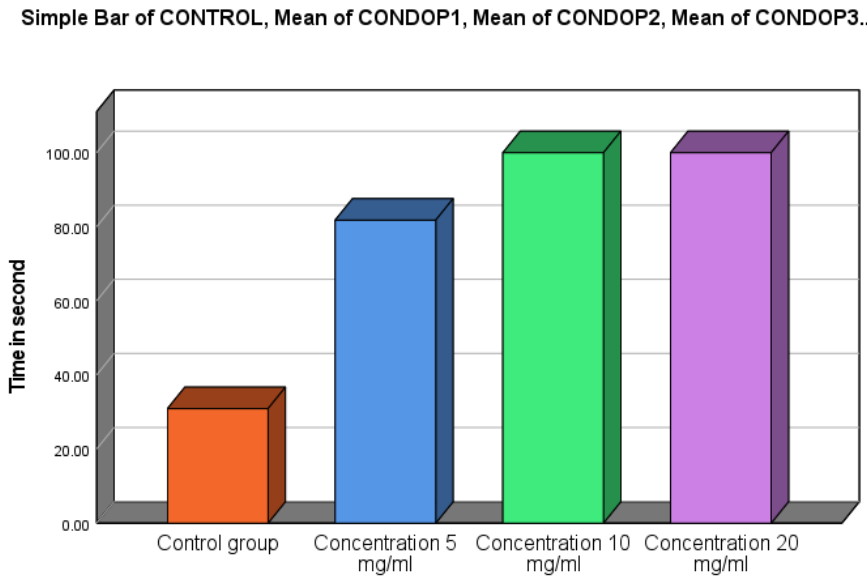

Figure 43: Activated partial thromboplastin (aPTT) at different concentration of ZnO-Se doping via Moringa Oleifera

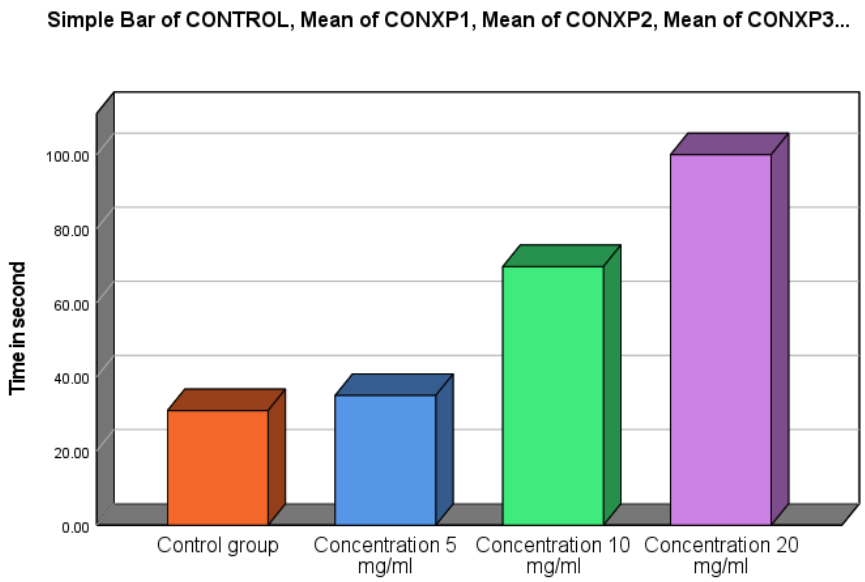

Figure 51: Activated partial thromboplastin (aPTT) at different concentration of pure extraction of Moringa Oleifera

2.9. Histological Study of the liver

The aim of studying tissue analyses in mice injected with nanoparticles is to evaluate the effect of pure moringa extract and nanoparticles on the histological structure of the liver which is important that serve as primary indicators of organ damage.

2.9.1. Histological Slide 1: Sick Animal

This slide displays liver tissue from a sick rat, characterized by localized inflammation surrounding the bile ducts, indicative of hepatic stress or infection. Also Mohammed et al (2022) observed Histopathological changes in the group treated with delthametrin where reveals degenerative features, like vacuolated cytoplasm (black arrow) and signs of necrosis including karyolysis (K), pyknotic nuclei (P) and loss of membrane integrity (blue arrow). C). dilatation and congestion of portal veins (PVH) as well as presence of leukocytic infiltration(star). Also, this finding was in agreement with the previous works who found that upon deltamethrin exposure level of lipid peroxidation increased in liver and kidney tissue indicating oxidation of fatty acid in the cell membrane and generation of reactive oxygen species (ROS) which consequently leads to loss of membrane function and structure, this difference is the result of the duration of treatment by delthamethrin where the pervious study treated for more than 10 weeks. However, the duration of our study was for 2 weeks. Where, hepatotoxicity was in marked degree in our result and this extensive hepatic distortion are probably related to insecticidal

metabolism which is mainly occurred in liver that is the master organ responsible for biotransformation and detoxification of noxious compounds. Another report has mentioned that deltamethrin decreased normal body antioxidants glutathione (GSH) or even enzymes related to its metabolism, GSH are normally synthesized by almost human cells and play role in cellular protection against free radicals, thus in absence of GSH, eventually hepatocellular damage will be occurred.

The inflammation and hemorrhage in the liver observed with ZnO, selenium, and Moringa-extracted nanoparticles result from oxidative stress and immune responses. ZnO can cause oxidative damage, selenium can disrupt immune function if not dosed correctly, and Moringa's bioactive compounds can stress the liver. These nanoparticles may also affect blood vessel integrity, leading to hemorrhage. Controlled dosages and thorough preclinical studies are crucial to minimize these adverse effects. (Yin et al., (2015))

2.9.2. Histological Slide 2: Animal Treated with ZnO-Se Doping via Moringa Oleifera

The liver tissue shows no significant abnormalities, suggesting that the ZnO-Se treatment via Moringa Oleifera did not induce noticeable hepatic inflammation or damage.

The lack of significant abnormalities in liver tissue after ZnO-Se treatment via Moringa Oleifera following deltamethrin exposure is due to the combined antioxidant, anti-inflammatory, cellular protective, and detoxification support provided by the ZnO-Se nanoparticles and the bioactive compounds in Moringa. (Kumar, V., & Sharma, A. (2018))

2.9.3. Histological Slide 3,4: Animal Treated with ZnO Nanoparticles via Moringa Oleifera

The liver tissue exhibits multifocal periportal inflammation, indicating that ZnO nanoparticle treatment led to inflammation primarily around the portal areas of the liver.

Fayeq et al 2023 observed The ZnO-NPs-treated group showed normal histological structure of the liver, but the hepatic tissue of the fumethrin-treated group showed congested central veins (C) and portal blood vessels (P) Livers of albino rats treated with CCl4 and 100 mg/kg BW every day of ZnO-NPs (G6) exhibited focal areas of inflammatory cell aggregates contiguous to hydropic degenerated cells and minute fat droplets within some hepatocytes (Figure 9 G6-A). In contrast, liver sections from albino rats receiving CCl4 and 200 mg/kg BW every day of ZnO-NPs (G6) displayed congested hepatic blood vessels and fatty alterations in a small number of hepatocytes (Figure 9 G6-B). Most of the hepatic parenchyma in liver sections from albino rats receiving CCl4 and treated with 100 mg/kg BW every day of green synthesized ZnONPs (G7) displayed seemingly normal hepatic structures (Figure 9 G7-A), with the presence

of fat globules within a small number of hepatocytes (Figure 9 G7-B). The liver sections of albino rats administered CCl4 and 200 mg/kg BW every day of greenly synthesized ZnO-NPs (G8) exhibited normal cytoarchitectures in the majority of the hepatic parenchyma (Figure 9 G8 and Table 6) Furthermore, the administration of ZnO-NPs synthesized using green methods in groups G7 and G8 contributed to a greater level of protection than the usage of the aqueous extract of MO leaves (El-Beltagi et el., (2023))

2.9.4. Histological Slides 5, 6, 7, 8: Animal Treated with Se Nanoparticles via Moringa Oleifera

The liver tissues display diffuse acute hepatitis lesions, indicating that selenium nanoparticle treatment via Moringa Oleifera led to widespread and severe hepatic inflammation.

These findings confirm the result mentioned by Bano *et al*., 2022 where Histopathological findings showed lesions in the liver with Higher doses of SeNPs nanoparticles administered for 14 d. also Ebaid *et al*., 2021 observed Hepatocytes (yellow arrows), inflammatory cells (blue arrows) and hemorrhage (red arrow) was observed in group g treated with CCl4 + SE-NPs

Mohammed *et al*., (2022) Hemorrhage was observed in the sinusoidal spaces and portal veins of liver parenychyma which is related to decrease in prostaglandin vasodilator as a result of pesticide inhibition mechanism. Reduction in prostaglandin leads in turns to vasoconstriction resulting in rupture of blood vessels. Others said that hepatic damage leads to increased blood flow which further cause blocking to sinusoids lumen and finally obligate all vascular walls to dilate (Farrag et Shalby, 2007). Infiltration of liver's interstitial with mononuclear cells suggesting that insecticides provoke inflammatory reaction mediated by interleukins IL-6, IL-1β and TNFα ends by migration of leukocytic cells to inflamed tissues (Khan et al, 2013).

2.9.5. Slide 9, 10: Rat 1 Treated with Pure Extract of Moringa Oleifera

The liver tissue shows slight focal inflammation, indicating a mild response to the pure Moringa Oleifera extract.

He livers of albino rats given CCl4 in combination with 100 mg/kg BW every day of MO leaf aqueous extract (G3) exhibited degenerative changes in the moderate number of hepatic parenchyma and isolated areas of interstitial round cell infiltrations (Figure 9 G4-A). Additionally, hepatic blood vessel congestion and perivascular round cell infiltrations were observed (Figure 9 G4-B). When albino rats received CCl4 and 200 mg/kg BW every day of MO leaf aqueous extract (G4), the liver

developed perivascular lymphocytic aggregates (Figure 9 G5-A) and fatty changes within some hepatocytes (Figure 9 G5-B (El-Beltagi *et al*., 2023).

2.9.6. Histological Slides 11, 12: Rat Treated with Se Nanoparticles via Moringa Oleifera Before Deltamethrin Injection

These slides depict liver tissues with focal inflammation, indicating that pre-treatment with selenium nanoparticles via Moringa Oleifera provided some protection but still resulted in localized inflammation post-deltamethrin exposure.

2.9.7. Histological Slide 13: Rat Treated with ZnO-Se Doping via Moringa Oleifera Before Deltamethrin Injection

This slide displays liver tissue with widespread inflammation and hemorrhagic areas, indicating that ZnO-Se doping via Moringa Oleifera did not effectively prevent severe liver damage induced by deltamethrin.

Mohammed *et al*., (2022) observed in the Animals treated with deltamethrin+ folic acid showed that increased deposition of collagen around portal area indicating fibrosis stage 3, degenerative changes including dilatation and hemorrhage of sinusoidal lumens (SH) and necrotic hepatocytes (H). B). Perioral infiltration (arrows) and venous congestion (H). C). signs of chronic toxic effect of pesticide appeared as fibrosis (fibrous bridging).

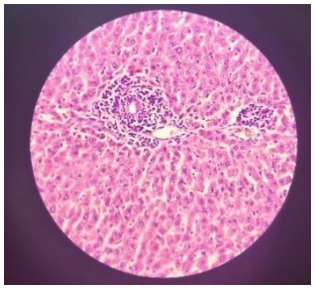

Histological Slide 1 **:** Sick Animal

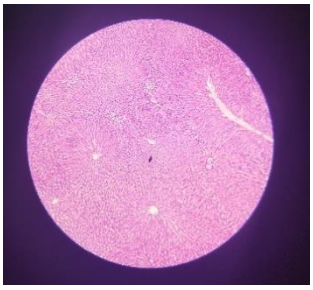

Histological Slide 2: Animal Treated with ZnO-Se Doping via Moringa Oleifera

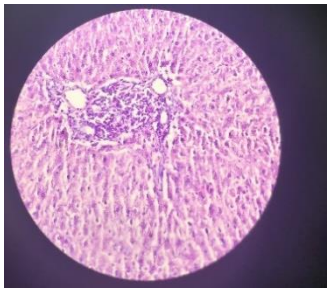

Histological Slide 3: Animal 1 Treated with ZnO Nanoparticles via Moringa Oleifera

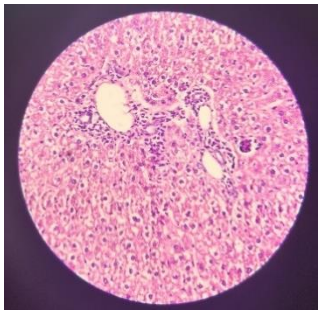

Histological Slide 4: Animal 2 Treated with ZnO Nanoparticles via Moringa Oleifera

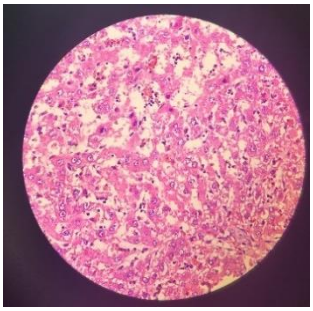

Histological Slides 5: Animal Treated with Se Nanoparticles via Moringa Oleifera

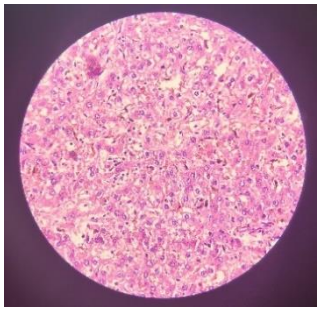

Histological Slides 6: Animal Treated with Se Nanoparticles via Moringa Oleifera

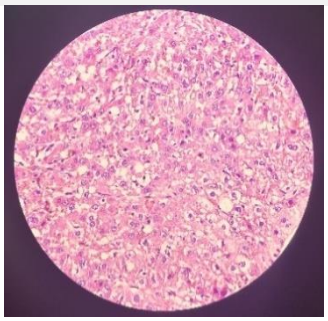

Histological Slides 7: Animal 1 Treated with Se Nanoparticles via Moringa Oleifera

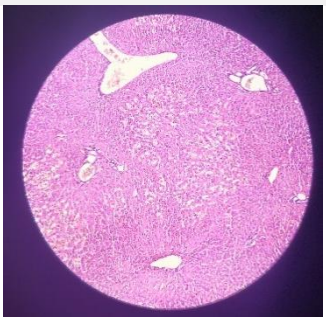

Histological Slides 8: Animal 2 Treated with Se Nanoparticles via Moringa Oleifera

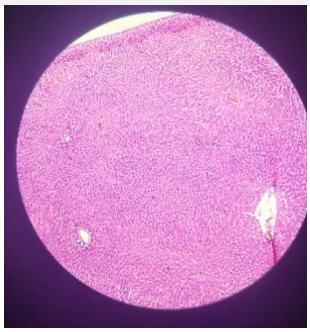

Histological Slide 9: Rat 1 Treated with Pure Extract of Moringa Oleifera

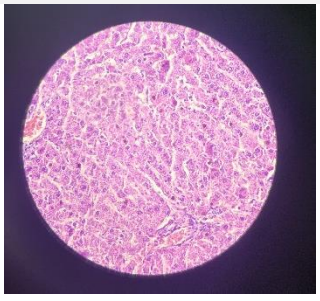

Histological Slide 10: Rat 2 Treated with Pure Extract of Moringa Oleifera

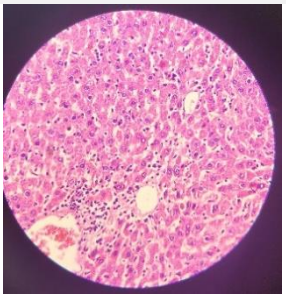

Histological Slides 11: Rat Treated with Se Nanoparticles via Moringa Oleifera Before

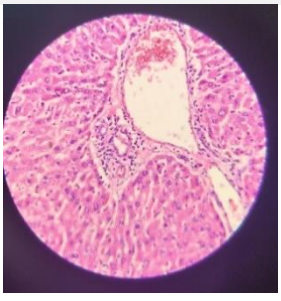

Histological Slides 12: Rat Treated with Se Nanoparticles via Moringa Oleifera Before

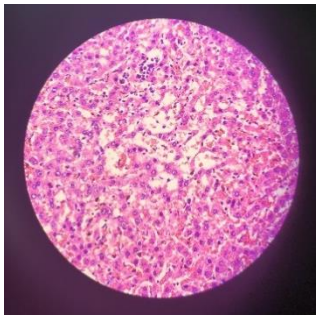

Histological Slide 13: Rat Treated with ZnO-Se Doping via Moringa Oleifera Before Deltamethrin Injection

General Conclusion

In conclusion, we demonstrate the successful synthesis of zinc oxide nanoparticles (ZnO NPs), selenium nanoparticles (Se NPs), and doping zinc-selenium nanoparticles (Zn-Se NPs) using moringa leaf extract, highlighting the potential for green synthesis of nanoparticles from plant extracts. We provide detailed characterization of the synthesized nanoparticles, with scanning electron microscopy (SEM) images revealing their morphology, energy-dispersive X-ray spectroscopy (EDS) analysis confirming their elemental composition, and X-ray diffraction (XRD) analysis verifying their crystal structure. We evaluate the biological activities of the nanoparticles and the pure moringa leaf extract, revealing that the pure extract exhibits the strongest antioxidant and anti-inflammatory activities, while the nanoparticles demonstrate moderate to low activity in these areas. Additionally, the nanoparticles show anti-hemolytic activity and potential for photocatalytic degradation of organic pollutants, as well as notable antimicrobial activity. Our biochemical and hematological analyses, including measurements of total bilirubin, liver enzymes, and blood parameters, provide insights into the potential effects of the nanoparticles on liver function and blood health. Histological studies of liver tissues from animals treated with the nanoparticles and the pure extract offer visual evidence of the potential impact on liver tissue. Overall, we showcase not only the successful synthesis of nanoparticles using moringa leaf extract but also provide comprehensive insights into their biological activities and potential applications.

Finally, we suggest expanding the scope of biological activity experiments to include anti-cancer activity, as well as conducting clinical trials for these compounds.

REFERENCES

1. A Leone, A Spada, A Battezzati, A Schiraldi, J Aristil, S Bertoli ,(2015),International journal of molecular sciences,
2. Ahaotu EO, Uwalaka RE, Edih MC, et al. (2018) Characterization and extraction of oil, biogas and biodiesel from Moringa oleifera seeds. J Agr Bio Env Sci..
3. Ahmed, S., Annu, A., & Chaudhry, S. A. (2017). Green synthesis of zinc oxide nanoparticles using *Aloe vera* leaf extract: Characterization and antibacterial activity. Materials Letters, 209, 171-174.
4. Akhtar, M. S., Panwar, J., & Yun, Y. S. (2013). Biogenic synthesis of metallic nanoparticles by plant extracts. ACS Sustainable Chemistry & Engineering, 1(6), 591-602.
5. Alagesan, V., & Venugopal, S. (2019). Green synthesis of selenium nanoparticles using leaves extract of Euphorbia hirta and their antibacterial activities. Materials Research Express, 6(2), 025031.
6. Alagesan, V., & Venugopal, S. (2020). Green synthesis of selenium nanoparticles using Vitis vinifera leaf extract and evaluation of their antioxidant activity. _Journal of Nanostructure in Chemistry_, _10_(4), 599-610.
7. Al-Asmari, A. K., Albalawi, S. M., Athar, M. T., Khan, A. Q., Al-Shahrani, H., & Islam, M. (2015). Moringa oleifera as an Anti-Cancer Agent against Breast and Colorectal Cancer Cell Lines. PloS one, 10(8), e0135814. https://doi.org/10.1371/journal.pone.0135814
8. Alessandro Leone, Alberto Spada, Alberto Battezzati, Alberto Schiraldi, Junior Aristil, and Simona Bertoli, (2016)Dec ,Moringa oleifera Seeds and Oil: Characteristics and Uses for Human Health.
9. Ali, I., Peng, C., Khan, Z. M., Naz, I., Sultan, M., Ali, M., ... & Ahmed, S.(2021). Green synthesis of ZnO nanoparticles using Azadirachta indica leaves extract: Characterization and evaluation of their photocatalytic and biological activities. Nanomaterials, 11(1), 205.
10. Alia, F., Putri, M., Anggraeni, N., & Syamsunarno, M. R. A. A. (2022). The Potency of Moringa oleifera Lam. as Protective Agent in Cardiac Damage and Vascular

Dysfunction. Frontiers in pharmacology, 12, 724439. https://doi.org/10.3389/fphar.2021.724439

11. Amaglo, N.K.; Bennett, R.N.; Lo Curto, R.B.; Rosa, E.A.S.; Lo Turco, V.; Giuffrida, A.; Lo Curto, A.; Crea, F.; Timpo, G.M,(2010). Profiling selected phytochemicals and nutrients in different tissues of the multipurpose tree Moringa oleifera L., grown in Ghana. Food Chem., 122, 1047–1054
12. Ambika, S., & Sundrarajan, M. (2015). Green biosynthesis of ZnO nanoparticles using Vitex negundo L. extract: Spectroscopic investigation of interaction between ZnO nanoparticles and human serum albumin. Journal of Photochemistry and Photobiology B: Biology, 149, 143-148.
13. Anastas P., Warner J. Green Chemistry. Oxford University Press; Oxford, UK: 2000.
14. Ankamwar, B., Chaudhary, M., & Sastry, M. (2005). Gold nanoparticles biologically synthesized using tamarind leaf extract and potential application in vapor sensing. Synthetic Metals, 152(1-3), 19-22.
15. Annu, A., et al. (2017). Green synthesis of zinc oxide nanoparticles using Aloe vera leaf extract: Characterization and antibacterial activity. Materials Letters, 209, 171-174.
16. Anwar, F., et al. (2007). Moringa oleifera: a food plant with multiple medicinal uses.
17. Anwar, F., Latif, S., Ashraf, M., & Gilani, A. H. (2007). Moringa oleifera: A food plant with multiple medicinal uses. *Phytotherapy Research, 21*(1), 17-25. https://doi.org/10.1002/ptr.2023
18. Asare, G.A.; Gyan, B.; Bugyei, K.; Adjei, S.; Mahama, R.; Addo, P.; Otu-Nyarko, L.; Wiredu, E.K.; Nyarko, (2012)A. Toxicity potentials of the nutraceutical Moringa oleifera at supra-supplementation levels. J. Ethnopharmacol., 139, 265–272.
19. Astefanei A., Núñez O., Galceran M. T. (2015). Characterisation and determination of fullerenes: a critical review. Anal. Chim. Acta 882 1–21.
20. B. Padayachee, H. Baijnath March (2020), An updated comprehensive review of the medicinal, phytochemical and pharmacological properties of Moringa oleifera.
21. Baruah, S., & Dutta, J. (2009). Nanotechnology applications in pollution sensing and degradation in agriculture: a review. Environmental Chemistry Letters, 7(3), 191-204.
22. Bhargava, R. N., et al. (1994). Quantum dots of group II-VI materials: Synthesis, characterization, and applications. IEEE Journal of Quantum Electronics, 30(2), 835-851.

23. Bibata Ali Outani, Haougui Adamou, Ali Mahamadou, Patrick Delmas3 , Moringa (Moringa oleifera Lam): A Review on its Importance Worldwide Bibata Ali Outani1, , Hao, nstitut National de Recherche Agronomique du Niger (INRAN).
24. Biju V., Itoh T., Anas A., Sujith A., Ishikawa M. (2008). Semiconductor quantum dots and metal nanoparticles: syntheses, optical properties, and biological applications. Anal. Bioanal. Chem. 391 2469–2495.
25. Boluwatife O Sowunmi , Martin Gonzo ,(2023), The effect of Moringa oleifera crude extract on liver cell line, HepG2.
26. C. Tiloke, A. Phulukdaree, A.A. (2013), Chuturgoon The antiproliferative effect of Moringa oleifera crude aqueous leaf extract on cancerous human alveolar epithelial cells BMC Complement. Altern. Med, 13 pp. 226-233.
27. C. Tiloke, A. Phulukdaree, A.A. Chuturgoon, (2013),The antiproliferative effect of Moringa oleifera crude aqueous leaf extract on cancerous human alveolar epithelial cells.
28. C.R. Morgan, Opio b, S. Migabo ,March(2020), Chemical composition of Moringa (Moringa oleifera) root powder solution and effects of Moringa root powder on E. coli growth in contaminated water.
29. Canett-Romero, R.; Arvayo-Mata, K.L.; Ruvalcaba-Garfias, N.V. (2014),Aspectos Tóxicos Más Relevantes de Moringa oleífera oleífera y sus Posibles Daños. BIOtecnia, 16, 36.
30. Chen J.-C., Tang C.-T. (2007). Preparation and application of granular ZnO/Al2O3 catalyst for the removal of hazardous trichloroethylene. J. Hazardous Mater. 142 88–96. 10.1016/j.jhazmat.2006.07.061
31. Cittrarasu, V., Kaliannan, D., Dharman, K., Prabhu, R., Rajamani, K., & Sujatha, V. (2021). Antibacterial and cytotoxic effects of biosynthesized zinc oxide and titanium dioxide nanoparticles. Microorganisms, 9(3), 464.
32. Compostella F., Pitirollo O., Silvestri A., Polito L. (2017). Glyco-gold nanoparticles: synthesis and applications. Beilstein J. Org. Chem. 13 1008–1021. 10.3762/bjoc.13.100
33. Consolacion Y Ragasa, Melanie P. Medecilo, and Chien-Chang Shen4, July 2015.Chemical Constituents of Moringa oleifera Lam. Leaves.
34. Dreaden E. C., Alkilany A. M., Huang X., Murphy C. J., El-Sayed M. A. (2012). The golden age: gold nanoparticles for biomedicine. Chem. Soc. Rev. 41 2740–2779. 10.1039/c1cs15237h

35. Elizabeth I Omodanisi , Yapo G Aboua , Novel N Chegou , Oluwafemi O Oguntibeju ,(2017), Hepatoprotective, Antihyperlipidemic, and Anti-inflammatory Activity of Moringa oleifera in Diabetic-induced Damage in Male Wistar Rats.
36. Fahey, J. W. (2005). Moringa oleifera: A review of the medical evidence for its nutritional, therapeutic, and prophylactic properties. Part 1. *Trees for Life Journal, 1*(5), 1-15. http://www.tfljournal.org/article.php/20051201124931586
37. Fardsadegh, B., Jafarizadeh-Malmiri, H., Mohammad-Beigi, H., & Yousefi, R. (2022). Biosynthesis of Selenium Nanoparticles Using Fenugreek Seed Extract and Evaluation of Their Antibacterial Activity. _Nanomaterials_, _12_(5), 800.
38. Fardsadegh, B., Jafarizadeh-Malmiri, H., Mohammad-Beigi, H., & Yousefi, R. (2022). Biosynthesis of Selenium Nanoparticles Using Fenugreek Seed Extract and Evaluation of Their Antibacterial Activity. _Nanomaterials_, _12_(5), 800.
39. Farrell D., Majetich S. A., Wilcoxon J. P. (2003). Preparation and characterization of monodisperse Fe nanoparticles. J. Phys. Chem. B 107 11022–11030.
40. Foidl et al, (2001). In: What development potential for Moringa products ?.
41. Fuglie, L. J. (2001). The Miracle Tree: The Multiple Attributes of Moringa.
42. G.Y. Liou, P. Storz, (2010), Reactive oxygen species in cancer, Free Radic. Res, 44 pp. 479-496.
43. Gałuszka A., Migaszewski Z., Namieśnik J. The 12 principles of green analytical chemistry and the significance mnemonic of green analytical practices. TrAC Trends Anal. Chem. 2013; 50:78–84. doi: 10.1016/j.trac.2013.04.010.
44. Garima Mishra, Pradeep Singh, Ramesh Verma, Sunil Kumar, Saurabh Srivastav, K. K. Jha and R. L. Khosa, (2011), Traditional uses, phytochemistry and pharmacological properties of Moringa oleifera plant.
45. Ghorbani H. R., Mehr F. P., Pazoki H., Rahmani B. M. (2015). Synthesis of ZnO nanoparticles by precipitation method. Orient. J. Chem. 31 1219–1221.
46. Gloria E. C., Ederley V., Gladis M., César H., Jaime O., Oscar A., et al. (2017). “Synthesis of silver nanoparticles (AgNPs) with antibacterial activity,” in Proceedings of the Journal of Physics: Conference Series, (United Kingdom: IOP Publishing;), 012023.
47. Gopalakrishnan, L., Doriya, K., & Kumar, D. S. (2016). Moringa oleifera: A review on nutritive importance and its medicinal application. Food science and human wellness, 5(2), 49-56.

48. Gu, F., Wang, S. F., Lu, M. K., Zhou, G. J., Xu, D., & Yuan, D. R. (2008). Synthesis and luminescence properties of well-aligned ZnO nanorod arrays prepared by sol-gel method. Journal of Physics and Chemistry of Solids, 69(2-3), 545-549.
49. Gunalan, S., Sivaraj, R., & Rajendran, V. (2012). Green synthesized ZnO nanoparticles against bacterial and fungal pathogens. Progress in Natural Science: Materials International, 22(6), 693-700.
50. Heuzé V., Tran G., Hassoun P., Bastianelli D., Lebas F, (2016) Moringa (Moringa oleifera)
51. HM Nanjappaiah, S Hugar(2012) ,NISCAIR-CSIR, India, Prophylactic and curative effects of Moringa oleifera Lam. pods in CCl4 damaged rat liver.
52. Huston, M., DeBella, M., DiBella, M., & Gupta, A. (2021). Green Synthesis of Nanomaterials. Nanomaterials (Basel, Switzerland), 11(8), 2130. https://doi.org/10.3390/nano11082130
53. I.L. Jung,(2014), Soluble extract from Moringa oleifera leaves with a new anticancer activity PLOS ONE, 9 pp. 1-10
54. Jamkhande P. G., Ghule N. W., Bamer A. H., Kalaskar M. G. (2019). Metal nanoparticles synthesis: An overview on methods of preparation, advantages and disadvantages, and applications. J. Drug Deliv. Sci. Technol. 53 101174.
55. K. Baker, C.B. Marcus, K. Huffman, H. Kruk, B. Malfroy, S.R. (1998), Doctrow Synthetic combined superoxide dismutase/catalase mimetics are protective as a delayed treatment in a rat stroke model: a key role for reactive oxygen species in ischemic brain injury J. Pharmacol. Exp. Ther., pp. 215-221
56. Kędziora, A., Sperling, R., & Krüger, A. (2016). Determining particle size distribution from electron microscopy images: A study using transmission electron microscopy and scanning electron microscopy. Journal of Microscopy, 262(1), 7-18.
57. Kędziora, A., Sperling, R., & Krüger, A. (2016). Determining particle size distribution from electron microscopy images: A study using transmission electron microscopy and scanning electron microscopy. _Journal of Microscopy_, _262_(1), 7-18.
58. Kędziora, A., Sperling, R., & Krüger, A. (2016). Determining particle size distribution from electron microscopy images: A study using transmission electron microscopy and scanning electron microscopy. _Journal of Microscopy_, _262_(1), 7-18.

59. Khan I., Saeed K., Khan I. (2019). Nanoparticles: Properties, applications and toxicities. Arab. J. Chem. 12 908–931.
60. King, S. , Jarvie, . Helen and Dobson, . Peter (2024, January 8). nanoparticle. Encyclopedia Britannica. https://www.britannica.com/science/nanoparticle
61. Krishnaswamy K., Orsat V. Nano- and Microscale Drug Delivery Systems. Elsevier; Amsterdam, The Netherlands: 2017. Chapter 2—Sustainable Delivery Systems Through Green Nanotechnology.
62. Kumar S. S., Venkateswarlu P., Rao V. R., Rao G. N. (2013). Synthesis, characterization and optical properties of zinc oxide nanoparticles. Int. Nano Lett. 3 1–6.
63. Kuppusamy, P., Yusoff, M. M., Maniam, G. P., & Govindan, N. (2016). Biosynthesis of zinc oxide nanoparticles using flower extract of Cassia fistula and its antimicrobial activity. _Journal of Photochemistry and Photobiology B: Biology_, _162_, 263-270.
64. L Pari, NA Kumar, Journal of Medicinal Food,(2002),liebertpub.com Hepatoprotective Activity of Moringa oleifera on Antitubercular Drug-Induced Liver Damage in Rats.
65. Lakshmipriya Gopalakrishnan b , Kruthi Doriya a , Devarai Santhosh Kumar, (2016)Moringa oleifera: A review on nutritive importance and its medicinal application, Food Science and Human Wellness 49 56.
66. Lane M.K.M., Zimmerman J.B. Controlling metal oxide nanoparticle size and shape with supercritical fluid synthesis. Green Chem. 2019;21:3769–3781. doi: 10.1039/C9GC01619H.
67. Leone, A., et al. (2015). Moringa oleifera: bioactive compounds and nutritional value.
68. Leone, A., Spada, A., Battezzati, A., Schiraldi, A., Aristil, J., & Bertoli, S. (2015). Moringa oleifera seeds and oil: Characteristics and uses for human health. *International Journal of Molecular Sciences, 16*(12), 12791-12835. https://doi.org/10.3390/ijms160612791
69. Leone, A.; Spada, A.; Battezzati, A.; Schiraldi, A.; Aristil, J.; Bertoli, S, 2016,Moringa oleifera Seeds and Oil: Characteristics and Uses for Human Health.
70. Lerner M. I., Glazkova E. A., Lozhkomoev A. S., Svarovskaya N. V., Bakina O. V., Pervikov A. V., et al. (2016). Synthesis of Al nanoparticles and Al/AlN composite nanoparticles by electrical explosion of aluminum wires in argon and nitrogen. Powder Technol. 295 307–314.

71. Li N., Zhao P., Astruc D. (2014). Anisotropic gold nanoparticles: synthesis, properties, applications, and toxicity. Angewand. Chem. Int. Edn. 53 1756–1789.
72. Lu Y., Ozcan S. Green nanomaterials: On track for a sustainable future. Nano Today. 2015; 10:417–420. doi: 10.1016/j.nantod.2015.04.010.
73. M. Godinoa, C. Arias, M.I. Izquierdo, Moringa oleifera: Potential areas of cultivation on the Iberian Peninsula, Department of Forest Engineering, Technical University of Madrid (UPM), E.U.I.T. Forestal, Ciudad Universitaria s/n, 28040 Madrid, Spain.
74. M. Mbikay, (2012)Therapeutic potential of Moringa oleifera leaves in chronic hyperglycemia and dyslipidemia: a review, Front. Pharmacol. 1–12.
75. M. Rastogi, et al. (2020). Green synthesis of zinc selenide nanoparticles using Ocimum sanctum leaf extract and their antibacterial activity. Materials Letters, 262, 127162.
76. M.C. Shih, C.M. Chang, S.M. Kang, et al. (2011), Effect of different parts (leaf, stem and stalk) and seasons (summer and winter) on the chemical compositions and antioxidant activity of Moringa oleifera Int J Mol Sci, 12 pp. 6077-6088.
77. M.D. Thurber, J.W. Fahey, (2010) Adoption of Moringa oleifera to combat under-nutrition viewed through the lens of the diffusion of innovations theory, Ecol. Food Sci. Nutr. 48 1–13.
78. MA Abd Eldaim, A Shaban Abd Elrasoul, SA Abd Elaziz, (2017),An aqueous extract from Moringa oleifera leaves ameliorates hepatotoxicity in alloxan-induced diabetic rats, Biochemistry and Cell Biology.
79. Ma, Z.F.; Ahmad, J.; Zhang, H.; Khan, I.; Muhammad, S. Evaluation of phytochemical and medicinal properties of Moringa (Moringa oleifera) as a potential functional food.
80. Madathil A. N. P., Vanaja K., Jayaraj M. (2007). “Synthesis of ZnO nanoparticles by hydrothermal method,” in Nanophotonic materials IV, eds Gaburro Z., Cabrini S. (Bellingham, WA: SPIE;), 47–55.
81. Mbikay, M. (2012). Therapeutic potential of Moringa oleifera leaves in chronic hyperglycemia and dyslipidemia: a review.
82. MH Daba, MS Abdel-Rahman, (1998) - Toxicology letters, - Elsevier.
83. Moghaddam A. B., Nazari T., Badraghi J., Kazemzad M. (2009). Synthesis of ZnO nanoparticles and electrodeposition of polypyrrole/ZnO nanocomposite film. Int. J. Electrochem. Sci. 4 247–257.

84. Monika Singh, Shilpi Singh, Digvijay Verma, (2020),Morphological and Pharmacognostical Evaluation of Moringa oleifera Lam. (Moringaceae): A Plant with High Medicinal Value in Tropical and Subtropical Parts of the World.
85. Moulton M.C., Braydich-Stolle L.K., Nadagouda M.N., Kunzelman S., Hussain S.M., Varma R.S. Synthesis, characterization and biocompatibility of "green" synthesized silver nanoparticles using tea polyphenols. Nanoscale. 2010; 2:763–770. doi: 10.1039/c0nr00046a.
86. N. Kamalakkannan, P.S.M. (2006) Prince Antihyperglycaemic and antioxidant effect of rutin, a polyphenolic flavonoid, in streptozotocin-induced diabetic wistar rats Basic Clin. Pharmacol. Toxicol , pp. 97-103
87. Nathaniel Ebenezar Udofia, Onyancha Jared Misonge, Mugambi Mworia, Ncene William, Moriasi Gervason Apiri, (2020), Chemical Composition of Moringa oleifera Lam. and Moringa stenopetala Bac. Leaves from Kenya.
88. Omnia Aly, Dalia M. Abouelfadl, Olfat G. Shaker, Gehan A. Hegazy, Ahmed M. Fayez & Hanan Hassan Zaki,(2020), Hepatoprotective effect of Moringa oleifera extract on TNF-α and TGF-β expression in acetaminophen-induced liver fibrosis in rats.
89. OS Adeyemi, CS Aroge, MA Akanji, (2017),Moringa oleifera-based diet protects against nickel-induced hepatotoxicity in rats.
90. Padilla, C.; Valenciaga, N.; Crespo, G.; Gonzalez, D.; Rodriguez, 2017. Agronomical requirements of Moringa oleifera (Lam.) in livestock systems.
91. Prabu, Sakthivel Lakshmana; Umamaheswari, Appavoo; Puratchikody, Ayarivan, 26 November (2019), Phytopharmacological potential of the natural gift Moringa oleifera Lam and its therapeutic application.
92. Prakash, D.; Suri, S.; Upadhyay, G.; Singh, B.N. (2007)Total phenol, antioxidant and free radical scavenging activities of some medicinal plants. Int. J. Food Sci. Nutr., 58, 18–28.
93. Prasad, K. S., & Patel, V. (2016). Biogenic synthesis of selenium nanoparticles using Ocimum sanctum leaf extract and their antibacterial activity. Journal of Nanoparticles, 2016, 1-8.
94. Prasad, K. S., Patel, V., Patel, R., & Patel, P. (2014). Biosynthesis of selenium nanoparticles using *Moringa oleifera* root extract and evaluation of its antimicrobial activity. Journal of Nanoparticles, 2014, 1-8.

95. Prasad, T. N. V. K. V., Elumalai, E. K., & Savithramma, N. (2010). Biogenic synthesis of Ag nanoparticles using Tridax procumbens and its antimicrobial activity. Journal of Pharmacy Research, 3(12), 2963-2966.
96. Rad A. G., Abbasi H., Afzali M. H. (2011). Gold nanoparticles: synthesising, characterizing and reviewing novel application in recent years. Phys. Proc. 22 203–208.
97. Rajabi, H. R., Shamsipur, M., & Raoufi, D. (2019). Green synthesis and characterization of ZnO nanoparticles using fruit extract of Rosa canina and their photocatalytic application. Journal of Environmental Chemical Engineering, 7(2), 103038.
98. Ramesh, P. S., Rajendran, S. P., & Rajesh, K. M. (2015). Synthesis and characterization of ZnO nanoparticles using Lantana camara leaf extract and their antibacterial activity. Spectrochimica Acta Part A: Molecular and Biomolecular Spectroscopy, 136, 864-870.
99. Rockwood, J. L., Anderson, B. G., & Casamatta, D. A. (2013). Potential uses of Moringa oleifera and an examination of antibiotic efficacy conferred by Moringa oleifera seed and leaf extracts using crude extraction techniques available to under-served indigenous populations. *International Journal of Phytotherapy Research, 3*(2), 61-71. http://www.earthjournal.org/index.php/IJPR/article/view/306
100. Roloff, H. Weisgerber, U. Lang, B. Stimm, Enzyklopädie der Holzgewächse, Handbuch und Atlas der Dendrologie
101. S. Arokiyaraj, et al. (2017). Phyto-mediated synthesis of zinc selenide nanoparticles using Psidium guajava L. leaf extract and their antibacterial applications. Journal of Photochemistry and Photobiology B: Biology, 174, 130-136.
102. S.M. Divi, R. Bellamkonda, S.K. (2012), Dasireddy Evaluation of antidiabetic and antihyperlipedemic potential of aqueous extract of Moringa oleifera in fructose fed insulin resistant and STZ induced diabetic wistar rats: a comparative study Asian J. Pharm. Clin. Res., 5 pp. 67-72.
103. Saini, R. K., et al. (2014). Phytochemical and pharmacological properties of Moringa oleifera Lam.
104. Sangeetha, G., Rajeshwari, S., & Venckatesh, R. (2011). Green synthesis of zinc oxide nanoparticles by aloe barbadensis miller leaf extract: Structure and optical properties. Materials Research Bulletin, 46(12), 2560-2566.
105. Sharma, G., Sharma, A. R., Nam, J. S., Park, B., & Pandey, A. (2014). Biomoleculemediated synthesis of selenium nanoparticles using dried Vitis vinifera (raisin) extract. Molecules, 19(1), 276-285.

106. Sharma, G., Sharma, A. R., Nam, J. S., Park, Y. B., & Chakraborty, C. (2017). Biosynthesis of selenium nanoparticles using *Moringa oleifera* leaf extract and evaluation of its cytotoxicity, antimicrobial and catalytic activity. Advanced Powder Technology, 28(3), 887-895.

107. Shen H., Duan C., Guo J., Zhao N., Xu J. Facile in situ synthesis of silver nanoparticles on boron nitride nanosheets with enhanced catalytic performance. J. Mater. Chem. A. 2015;3:16663–16669. doi: 10.1039/C5TA04188K.

108. Shenashen M. A., El-Safty S. A., Elshehy E. A. (2014). Synthesis, morphological control, and properties of silver nanoparticles in potential applications. Part. Part. Syst. Char. 31 293–316.

109. Sigmund W., Yuh J., Park H., Maneeratana V., Pyrgiotakis G., Daga A. (2006). Processing and structure relationships in electrospinning of ceramic fiber systems. J. Am. Ceramic Soc. 89 395–407.

110. Singh, H., Dudi, R., & Singh, P. (2018). Biosynthesis of stable zinc oxide nanoparticles using Calotropis gigantea latex and evaluation of their antibacterial activity. Materials Science in Semiconductor Processing, 85, 93-101.

111. Singh, H., Dudi, R., & Singh, P. (2018). Biosynthesis of stable zinc oxide nanoparticles using *Calotropis gigantea* latex and evaluation of their antibacterial activity. Materials Science in Semiconductor Processing, 85, 93-101.

112. Siwach O. P., Sen P. (2008). Synthesis and study of fluorescence properties of Cu nanoparticles. J. Nanopart. Res. 10 107–114.

113. Soppimath K.S., Aminabhavi T.M., Kulkarni A.R., Rudzinski W.E. Biodegradable polymeric nanoparticles as drug delivery devices. J. Control. Release. 2001;70:1–20. doi: 10.1016/S0168-3659(00)00339-4.

114. Sowa, H., & Ahsbahs, H. (2006). Pressure-induced phase transition of ZnO: An in situ X-ray diffraction study. Journal of Applied Crystallography, 39(2), 252-256.

115. Stephenson P., Licence P., Ross S.K., Poliakoff M. Continuous catalytic asymmetric hydrogenation in supercritical CO2. Green Chem. 2004;6:521–523. doi: 10.1039/b411955j.

116. Sundrarajan, M., Ambika, S., & Bharathi, K. (2015). Plant-extract mediated synthesis of ZnO nanoparticles using *Vitex negundo* L. and their pharmacological properties. Journal of Photochemistry and Photobiology B: Biology, 149, 166-174.

117. Syazana Akmal Sharifudin1, Sharida Fakurazi, Mohamad Taufik Hidayat1, Ithnin Hairuszah3, Mohamad Aris Mohd Moklas1, and Palanisamy Arulselvan,08 Oct (2012), Therapeutic potential of Moringa oleifera extracts against acetaminophen-induced hepatotoxicity in rats.

118. Tăbăran A.-F., Matea C.T., Mocan T., Tăbăran A., Mihaiu M., Iancu C., Mocan L. Silver Nanoparticles for the Therapy of Tuberculosis. Int. J. Nanomed. 2020;15:2231–2258. doi: 10.2147/IJN.S241183.

119. Wang Z. Frontiers of Chemistry. University of Pittsburgh; Pittsburgh, PA, USA: 2018. Green Chemistry: Recent Advances in Developing Catalytic Processes in Environmentally-Benign Solvent Systems.

120. Y. Nakamura, M. Kawakami, A. Yoshihiro, N. Miyoshi, H. Ohigashi, K. Kawai, et al. (2002), Involvement of the mitochondrial death pathway in chemo preventive benzyl isothiocyanate-induced apoptosis J. Biol. Chem., 277 pp. 8492-8499

121. Yang Liu, Xiao-yue Wang, Xue-min Wei, Zi-tong Gao, Jian-ping Han, Values, properties and utility of different parts of Moringa oleifera: An overview, Chinese Herbal Medicines, Volume 10, Issue 4, 2018, Pages 371-378, ISSN 1674-6384, https://doi.org/10.1016/j.chmed.2018.09.002.

122. Yap Y.H., Azmi A.A., Mohd N.K., Yong F.S.J., Kan S.-Y., Thirmizir M.Z.A., Chia P.W. Green Synthesis of Silver Nanoparticle Using Water Extract of Onion Peel and Application in the Acetylation Reaction. Arab. J. Sci. Eng. 2020;45:4797–4807. doi: 10.1007/s13369-020-04595-3.

123. Yu, K., et al. (2005). Synthesis and optical properties of Mn-doped ZnSe nanowires. Applied Physics Letters, 86(6), 063110.

124. Yugander, S., & Rajaram, R. (2015). Green synthesis of zinc oxide nanoparticles using Moringa oleifera leaf extract and evaluation of its antimicrobial activity. Spectrochimica Acta Part A: Molecular and Biomolecular Spectroscopy, 135, 389-394.

125. Yugander, S., Rajasekar, S., & Murugesan, K. (2017). Plant-mediated synthesis of zinc oxide nanoparticles using leaf extracts of Vitex negundo L. and their biological activities. Journal of Photochemistry and Photobiology B: Biology, 174, 166-175.

126. Yugander, S., Rajasekar, S., & Murugesan, K. (2017). Plant-mediated synthesis of zinc oxide nanoparticles using leaf extracts of Vitex negundo L. and their biological activities. _Journal of Photochemistry and Photobiology B: Biology_, _174_, 166-175.

127. Zare, M., Alizadeh, A., & Ali, N. A. (2020). Biosynthesis of selenium nanoparticles using garlic extract and evaluation of their antibacterial properties. _Journal of Cluster Science_, _31_(6), 1423-1428.

128. Zhang, W., Chen, Z., Liu, H., Zhang, L., Gao, P., & Li, D. (2016). Biosynthesis and structural characteristics of selenium nanoparticles by Pseudomonas alcaliphila. _Colloids and Surfaces B: Biointerfaces_, _146_, 147-153.

129. Zhang, W., Chen, Z., Liu, Y., Zhang, L., & Gao, P. (2011). Facile green synthesis of selenium nanoparticles using tea leaf extract and evaluation of their antioxidant activity. International Journal of Nanomedicine, 6, 185-192.

130. Zhuang J., Gentry R. W. (2011). "Environmental application and risks of nanotechnology: a balanced view," in Biotechnology and Nanotechnology Risk Assessment: Minding and Managing the Potential Threats around Us, eds Ripp S., Henry T. (Washington, DC: ACS Publications;), 41–67. 10.3390/ijerph16234848

131. Zielińska A., Carreiró F., Oliveira A. M., Neves A., Pires B., Venkatesh D. N., et al. (2020). Polymeric nanoparticles: production, characterization, toxicology and ecotoxicology. Molecules 25:3731. 10.3390/molecules25163731

APPENDX

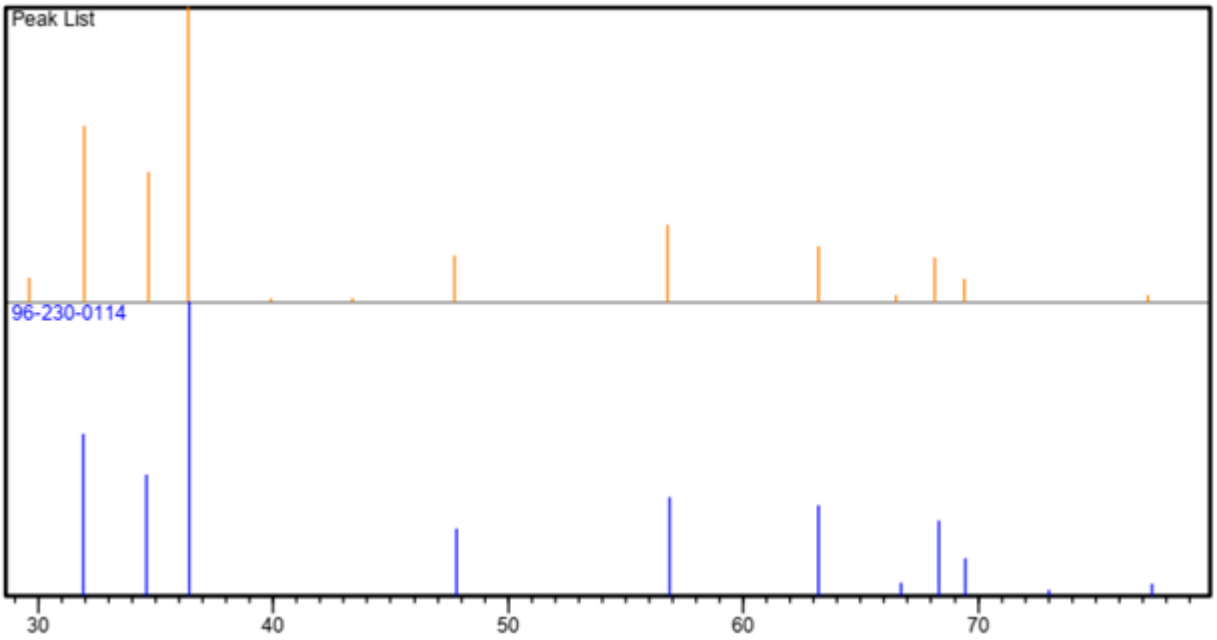

Figure 01 : High-pressure X-ray investigation of zincite ZnO NPs single crystals using diamond anvils with an improved shape

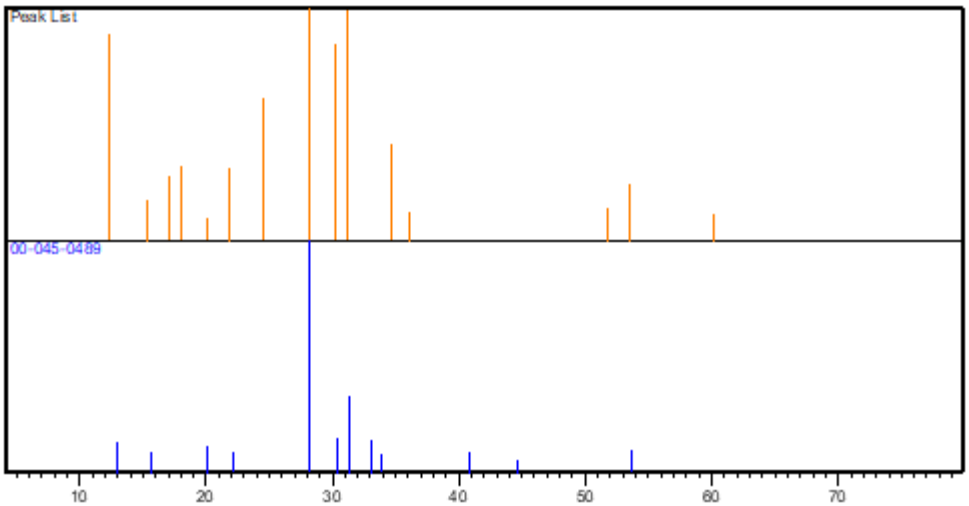

Figure 02 : High-pressure X-ray investigation of Se NPs single crystals using diamond anvils with an improved shape

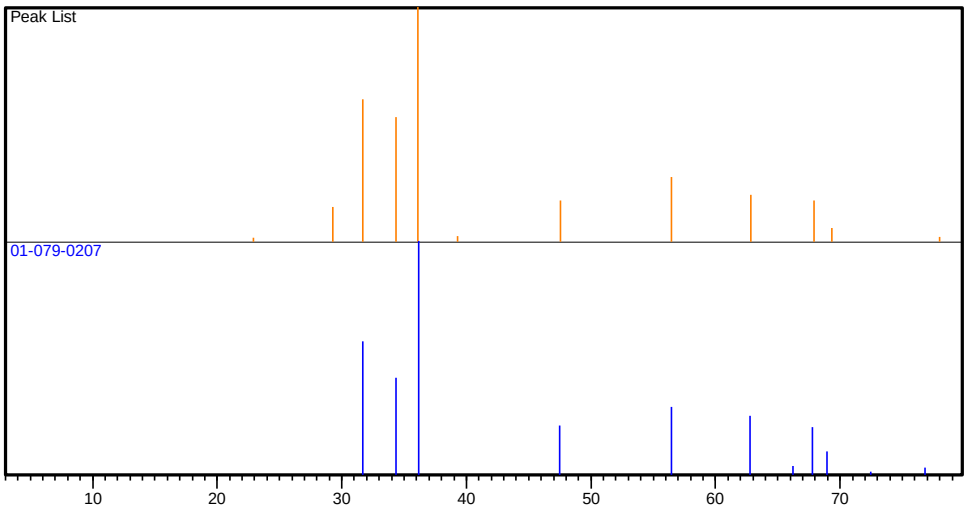

Figure 03 : High-pressure X-ray investigation of doping Zn-Se NPs single crystals using diamond anvils with an improved shape

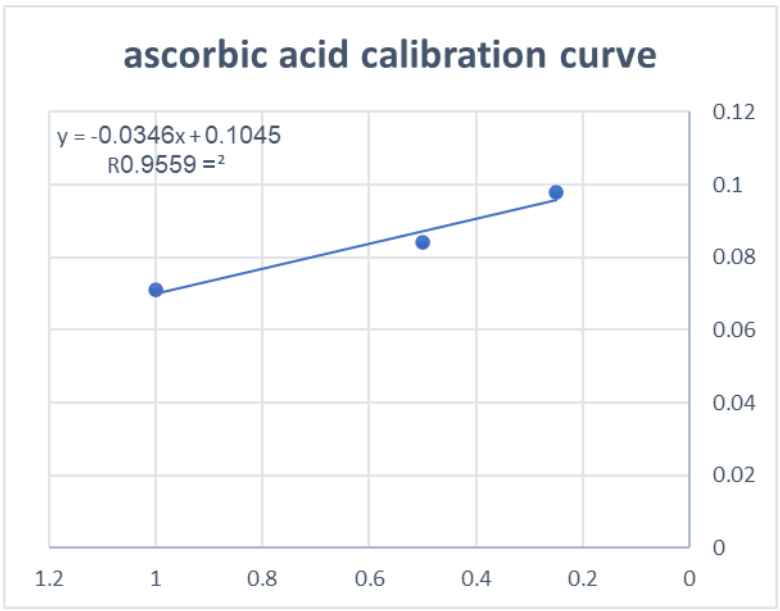

Figure 04 : DPPH ascorbic acid calibration curve

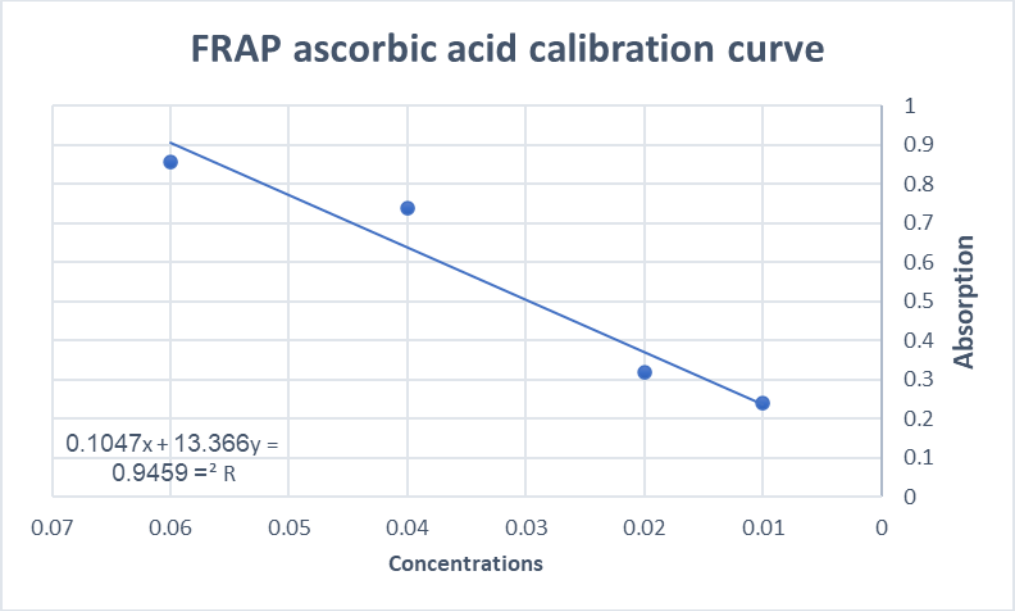

Figure 05 : FRAP ascorbic acid calibration curve

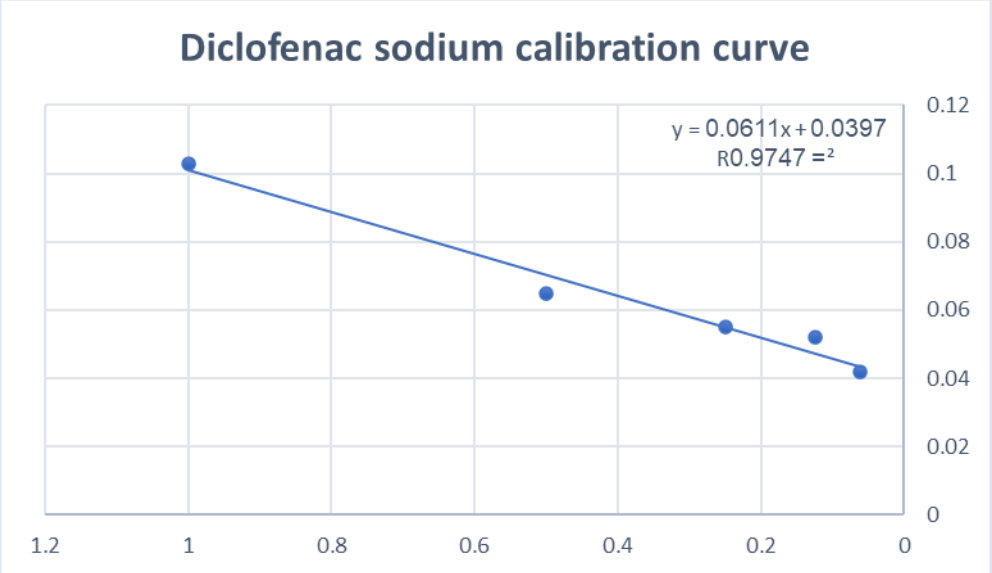

Figure 06 : Calibration curve of DICLOFENAC sodium

الجمهورية الجزائرية الديمقراطية الشعبية

وزارة التعليم العالي والبحث العلمي

اللجنة الوطنية التنسيقية لمتابعة الإبتكار

وحاضنات الأعمال الجامعية

دليل مشروع

للحصول على شهادة مؤسسة ناشئة

في إطار القرار الوزاري 1275

ديسمبر

بطاقة معلومات

حول فريق الإشراف و فريق العمل

1- فريق الاشراف:

فريقالاشراف	
المشرفالرئيسي (01): غانية أحمد	التخصص: علم التسمم.
المشرفالرئيسي (01):	التخصص: .....
المشرفالمساعد:	التخصص: .....

2- فريق العمل:

فريق المشروع	التخصص	الكلية
الطالب: **عز الدين شغرم**	**علم التسمم**	**علوم الطبيعة والحياة**

الطالب: **بديده نجاح**	**علم التسمم**	**علوم الطبيعة والحياة**
الطالب: **بركان لمياء**	**علم التسمم**	**علوم الطبيعة والحياة**

فهرس المحتويات

فهرس المحتويات

مقدمة

بغرض تمكين الطلبة حاملي المشاريع المبتكرة، ومن باب تسهيل عملهم في صياغة وكتابة مشاريعهم والانتقال من مجرد أفكار الى مشروع متكامل بتفاصيل ومعلومات توضح الافاق الاستراتيجية للمشروع ومدى جاذبيته وسلامة التسلسل المنطقي للأفكار تقترح اللجنة الوطنية التنسيقية لمتابعة الابتكار وحاضنات الاعمال هذا الملف الذي يعتبر بمثابة دليل للطالب لصياغة مشروعه الابتكاري .

سيتم تقديم الشروحات اللازمة للدليل بالاعتماد على مثال بسيط جدا من باب تقريب الفهم اكثر للطالب، هذا المثال يتعلق بمشروع انتاج عصير طبيعي انطلاقا من فواكه طبيعية لم تخضع للمبيدات او اسمدة كيميائية.

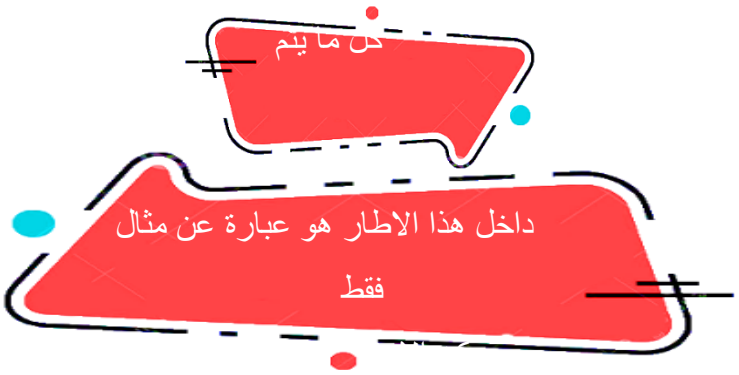

المحور

تقديم المشروع

المحور الأول

تقديم المشروع

1. فكرة المشروع (الحل المقترح)

هنا اكتب مشروعك في بعض الاسطر متناولا فيها :

- ✓ مجال النشاط (خدمات، صناعي، تطبيقات حديثة، فلاحي، تجاري ...)
- ✓ كيف بدأت الفكرة وكيف تطورت ؟
- ✓ ما الذي سوف تقوم به؟
- ✓ كيف سيكون ذلك؟
- ✓ من الذي سينجز ذلك؟
- ✓ أين سيتم إنجازه ؟

مجال نشاطنا يتمثل في منتج عشبي طبي بنبات المورينجا اوليفيرا مصنع بتقنيات النانو

- ✓ بدأت فكرة المشروع من خلال الاطلاع على العديد من الدراسات الجديدة والحديثة للطب النانوي الذي شهد مؤخرا ضجة كبيرة في علم الاحياء، كذلك أردت إدراج نبتة علاجية قوية،فأدرجني الفضول للاطلاع على نبتة المورينجا المزروعة في بيتنا , قمت باستغلال هذا الامر وبحثت طويلا عن مدى فائدة هذه الشجرة المعجزة وتطورت الفكرة بدمجها مع مكملات غذائية في الشكل النانوي لعلاج العديد من الامراض .
- ✓ سنقوم بصناعة منتج عشبي طبي لعلاج العديد من الامراض من بينها علاج أمراض الكبد .
- ✓ يتم ذلك بإنجاز مقر أو وحدة إنتاجية تتمتع بكامل الاجهزة التكنولوجية الحديثة مع توفير المواد الاولية بأكملها (نبات المورينجا , المكملات الغذائية , الأجهزة المخبرية ...)

2. القيم المقترحة :

يمكن ان تنشأ القيم المقترحة او المقدمة للزبائن من خلال العناصر التالية:

- ✓ الحداثة: تلبية احتياجات جديدة كلياً لم تكن هناك عروض مماثلة لها في السابق.
- ✓ الأداء: أن يكون أداء المنتج او الخدمة اعلى او مساوي لتوقعات العميل.

- ✓ التكييف: المرونة في التعديل والتغيير لتكييف المنتجات والخدمات تبعا للاحتياجات المحددة للعملاء.
- ✓ إنجاز المهمة: مساعدة العميل على انجاز مهام محددة.
- ✓ التصميم: جعل التصاميم تتوافق مع رغبات وظروف العميل.
- ✓ السعر: تقديم منتج أو خدمة بسعر اقل، أمر شائع لتلبية متطلبات شرائح العملاء.
- ✓ خفض التكاليف: مساعدة العملاء على خفض تكاليفهم.
- ✓ الحد من المخاطر: تقليص احتمال تعرض العملاء للمخاطر لدى شرائهم المنتجات أو الخدمات بتقديم ضمانات.
- ✓ سهولة الوصول: جعل المنتجات متاحة للعملاء الذين لم يكن بإمكانهم من قبل الوصول إليها.
- ✓ الملاءمة/سهولة الاستخدام: جعل الأشياء سهلة بسيطة الاستخدام.

2

تكمن القيمة المضافة في:

- تعتبر علاج طبيعي وآمن للعديد من الامراض خاصة امراض الكبد
- تنويع خيارات العلاج
- تكلفة العلاج مختلفة ومنخفضة
- الابتكار والريادة

3. فريق العمل:

هنا تتحدث عن فريق العمل على المشروع من خلال :

- ✓ تحدث عن فريق عملك (اذا كنت لست بمفردك في هذا المشروع) مهاراتهم وادوارهم في المشروع، (المهارات والمؤهلات العلمية، الدورات التدريبة المتحصل عليها .....).
- ✓ التنظيم المناسب (توزيع المهام والمسؤوليات).
- ✓ طرق التفاعل والتواصل بين الفريق.

يتكون فريق المشروع من الاتي :

- ✓ الطالب 01: **عز الدين شغرم**، تخصص **علم التسمم**
- ✓ الطالب 02: **بديده نجاح** ، تخصص **علم التسمم**
- ✓ الطالب 03: **بركان لمياء** ,تخصص **علم التسمم**
- ✓ يتمثل دور الطالب 01 في انه صاحب الفكرة الأولى للمشروع و كذلك مهمته هي إدارة عمل هذا المشروع من خلال التسيير السوي للمشروع
- ✓ يتمثل دور الطالب 02 اليد العاملة لهذا المشروع من قيد إنجاز و الوقوف على سيرورة العمل والانتاج.
- ✓ يتمثل دور الطالب 03 اليد العاملة والبنك الرئيسي لهذا العمل نظرا لتكفله بجميع مصاريف هذا المشروع

4. أهداف المشروع:

3 تحتاج في هذا الجزء الى تحديد الأهداف التجارية للمشروع وتقدير الحصة السوقية المستهدفة على المدى القريب والمتوسط والبعيد.

تتمثل أهدافنا في جعل هذا المنتج الاول من نوعه محليا في تجارة الادوية العشبية .
كذلك نسعى لتحسين ونشر ثقافة التداوي بالاعشاب والنباتات الطبية لما فيها من ثروات علاجية
نهدف أيضا للابتكار والريادة في هذا المجال وتنويع خيارات العلاج للمرضى .
نسعى لتحقيق أرباح وتنشيط سوق الادوية العشبية .

5. جدول زمني لتحقيق المشروع :

- ✓ كيفية تقسيم الهدف النهائي للمشروع إلى مهام فردية.
- ✓ تحديد الوقت اللازم لكل مهمة.
- ✓ تحديد النتائج الرئيسية لكل مهمة.

الشهر أو

		الأعمال	1	2	3	4	5	6	7
1		الدراسات الأولية: اختيار مقر الوحدة الإنتاجية، تجهيز الوثائق المطلوبة	✓	✓					
2		طلب التجهيزات من الخارج				✓		✓	
3		بناء مقر للإنتاج (المصنع)		✓	✓	✓			
...		تركيب المعدات				✓	✓	✓	
ن		اقناء المواد الأولية					✓		

...		بداية انتاج أول منتج						

4

المحور
الجوانب الإبتكارية

المحور الثاني

الجوانب الابتكارية

1. طبيعة الابتكارات:

ينبغي أن يحدد هنا طبيعة الابتكارات المعتمدة في المشروع:

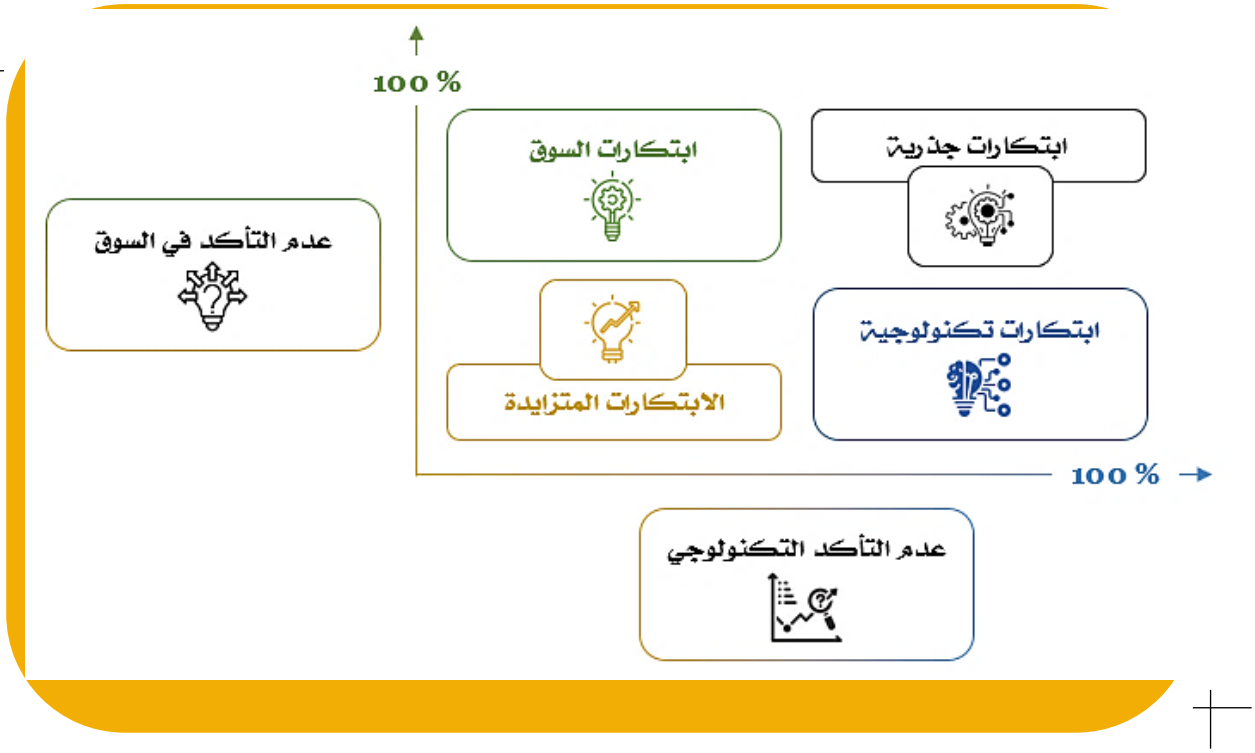

2. مجالات الابتكارات:

من خلال الحالات السابقة يمكن ان يشمل الابتكار المجالات التالية:

- ✓ عمليات جديدة (زيادة الربحية من خلال زيادة كفاءة العمليات).
- ✓ تجارب جديدة (بيع المزيد لشرائح العملاء الحاليين عن طريق تغيير السياق (السياقات).
- ✓ الميزات الجديدة (تقديم منتجات أو خدمات محسّنة).
- ✓ العملاء الجدد (عرض النطاق المعتاد من المنتجات أو الخدمات لشرائح العملاء الجدد).
- ✓ عروض جديدة (إنشاء - أو على الأقل إدخال - منتجات مبتكرة).
- ✓ نماذج جديدة (تغيير نموذج العمل، اعتماد "نظام" آخر لتوليد القيمة).

تتمثل الجوانب الابتكارية في مشروعنا في كونه: (منتج علاجي)

1. أول منتج تم فيه استخدام الطب النانوي بنبات المورينجا مع الزنك والسيلينيوم لعلاج أمراض الكبد

المحور

التحليل الاستراتيجي للسوق

المحور الثالث

التحليل الاستراتيجي للسوق

1. عرض القطاع السوقي:

- ✓ السوق المحتمل: السوق المحتمل هو مجموعة الافراد او المؤسسات التي تطلب أو يحتمل ان تطلب منتجاتك او خدماتك لإشباع حاجاتهم ورغباتهم. (من يشتري منتجاتنا؟ من وما الذي حفزه لذلك؟ أين يتواجدون؟ كم أعدادهم؟).
- ✓ السوق المستهدف (الشريحة): السوق المستهدف يمثل مجموعة الافراد أو المؤسسات والتي تقدم لها او تعرض عليها منتجاتك.
- ✓ قدم مبررات اختيار هذ السوق المستهدف.
- ✓ تحديد إمكانية ابرام عقود شراء مع بعض الزبائن المهمين.

السوق المحتمل : هم الاشخاص المصابون بأمراض الكبد , الذين يعانون من تخثر الدم , الاكسدة وغيرها من المشاكل

السوق المستهدف : المرضى الذين يعانون من آثار جانبية للعلاجات الكيميائية ,

2. قياس شدة المنافسة:

- ✓ حدد من هم منافسوك المباشرين والغير مباشرين.
- ✓ حدد اعدادهم وحصصهم السوقية.
- ✓ حدد نقاط قوتهم ونقاط ضعفهم.

أهم المنافسين في السوق الجزائرية اغلبهم ينتجون عصير بمواد حافظة وهم بالترتيب حسب الحصة السوقية كما يلي:

- ✓ جميع متاجر الادوية العشبية , عيادات التداوي بالاعشاب , مصانع الادوية المتطورة في الطب النانوي
- ✓ من بين نقاط قوتهم الاقدمية في السوق الجزائرية وقوة العلامة التجارية

3. الاستراتيجيات التسويقية

وهي مجموعة التقنيات والأساليب المستعملة لفهم منتجاتك وخدماتك المقدمة للزبائن المحتملين من أجل جذبهم وحثهم على الشراء.

- ✓ يجب ان تخطط لاستراتيجية فعالة تأخذ بعين الاعتبار قدراتك المالية.
- ✓ احرص على توازن المزيج التسويقي للمؤسسة لإنجاح الاستراتيجية التسويقية.

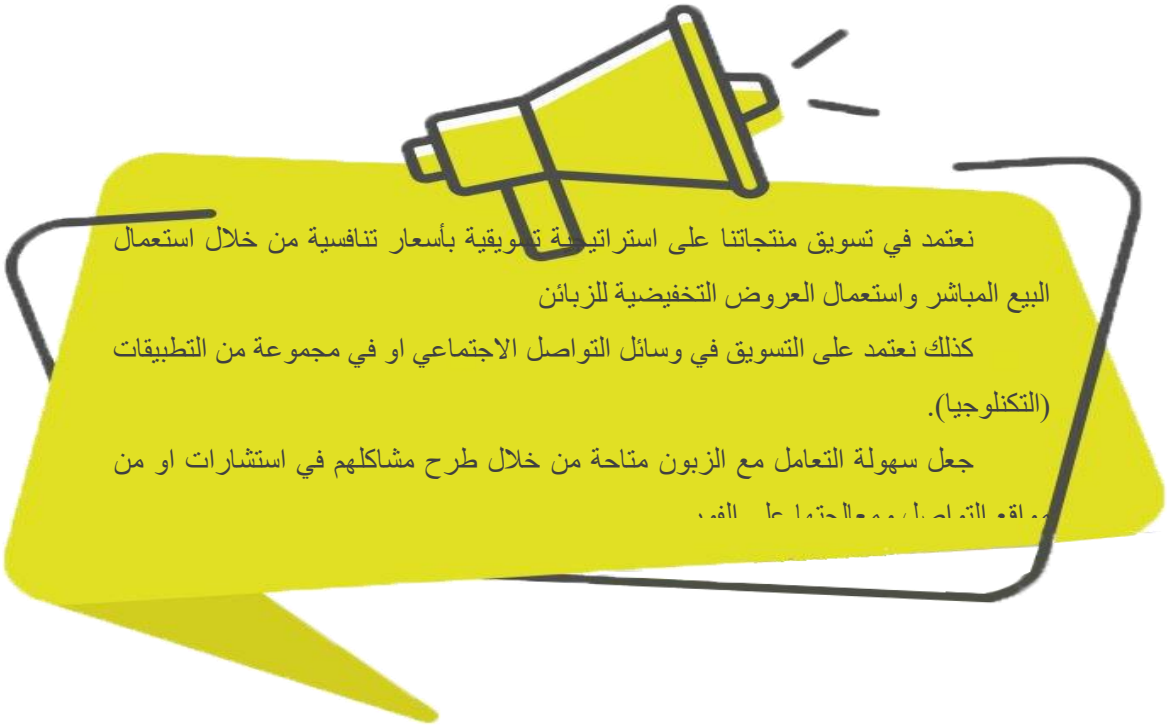

المحور

خطة الإنتاج والتنظيم

المحور الرابع

خطة الإنتاج و التنظيم

1. عملية الإنتاج:

تمر عملية الإنتاج بعدة مراحل يجب ان تكتب بطريقة تمكن القارئ من فهم اكثر لطريقة الإنتاج وادراك الجودة.

- ✓ اقتناء المواد الأولية
- ✓ التصنيع
- ✓ تكييف المنتج
- ✓ التعبئة والتغليف

يمكن الاستعانة بمخطط يشرح مراحل عملية الإنتاج :

ملاحظة:

بالنسبة للمجالات الأخرى (خدمات، منصات رقمية، تطبيقات) تحدد خطوات الحصول على الخدمة من البداية الى النهاية

2. التموين:

11

- ✓ تحديد سياسة الشراء (مواد أولية _ مواد ولوازم _ تجهيزات)
- ✓ تحديد اهم الموردين
- ✓ تحديد سياسة الدفع ووقت الاستلام

نتعامل في عمليات التزود بالتجهيزات والمواد الأولية عن طريق طلب التموين اما بالاتصال مباشرة بالموردين او عن طريق وسيط بنكي وبخصوص التزود بالنبات فسيكون هناك مزرعة ذكية تابعة للمؤسسة تلبي جميع احتياجات المؤسسة

يتم الدفع والتسليم اما عبر حسابات بريدية جارية او حسابات بنكية

3. اليد العاملة :

- ✓ حدد عدد المناصب التي يمكن ان يخلقها المشروع.
- ✓ حدد طبيعة ونوعية اليد العاملة التي تحتاجها و أماكن تواجدها.
- ✓ تحديد إمكانية اللجوء الى المناولة.

يحتاج مشروعنا حوالي 35منصب عمل مباشر و10 مناصب عمل غير مباشرة

يحتاج مشروعنا الى تخصصات دقيقة في المجال الهندسي ومجموعة من العمال التقنيين على الاجهزة، كذلك يحتاج الى خبراء في المجال النباتي كمهندسين زراعيين وبيولوجيين

4. الشراكات الرئيسية :

هنا يذكر صاحب المشروع الأطراف التي يمكن ان تساعد في انجاز المشروع وتقديم الإضافة من خلال الدعم او التكامل (موردون، هيئات عمومية، مخابر، بنوك،حاضنات، ...).

أهم الشراكات في مشروعنا كانت مع الموردين لأهميتهم في إنجاح المشروع، بالإضافة الى كل من حاضنة الاعمال لجامعة ..... وكذا المعهد الوطني ..... لقياس والمحافظة على جودة منتجاتنا كذلك مع شركات إنتاج وتصنيع المواد الناوية.

كما نملك التزامات قوية من المؤسسة الممولة بالتجهيزات المتطورة فيما يخص

12

المحور الخامس

الخطة المالية

المحور الخامس

الخطة المالية

1. التكاليف والأعباء :

- ✓ هنا يتم التحديد الدقيق لكافة تكاليف المشروع والاستثمارات المطلوبة: (يمكن الاستعانة بعناصر الميزانية).
- ✓ طرق ومصادر الحصول على التموين.
- ✓ كيفية استرداد الأموال (جدول العوائد).

2. رقم الاعمال :

- ✓ رقم الاعمال هو اجمالي المبيعات من المنتجات والخدمات والناتج عن الأنشطة المحققة.
- ✓ يجب ان تقدم وجهتي نظر حول رقم الاعمال المتوقع واحدة تفاؤلية والأخرى تشاؤمية .

DETAIL CHIFFRE D'AFFAIRES STARTUP : .....

	REALISATION			PREVISION				
Produit A destiné Client	N -2	N -1	N	N+1	N+2	N+3	N+4	N+5
Quantité produit A	-	-	-	-	-	-	-	-
Prix HT produit A	-	-	-	-	-	-	-	-
Ventes produit A	-	-	-	-	-	-	-	-
CHIFFRE D'AFFAIRES GLOBAL	-	-	-	-	-	-	-	-

3. جدول حسابات النتائج المتوقع :

- ✓ وهو جدول مالي يلخص اجمالي المبيعات والاعباء خلال سنة وينتهي برصيد إيجابي (ربح) أو سلبي (خسارة) خلال فترة زمنية تسمى بالسنة المحاسبية.
- ✓ حساب احتياجات رأس المال العامل (BFR) والذي يسمح بإحداث توازن بين الاحتياجات المالية والعوائد المالية خلال دورة الاستغلال (مخزونات، ديون قروض , ديون موردون ، زبائن...).

4. خطة الخزينة :

- ✓ وهي وثيقة تسمح بتحديد كل الإيرادات وكل النفقات المتوقعة خلال السنة الأولى لنشاط المؤسسة.
- ✓ يتم حساب الإيرادات والنفقات كل شهر على مدى سنة كاملة.

المحور السادس

النموذج الأولي التجريبي

المحور السادس

النموذج الأولي التجريبي

النموذج الأولي التجريبي هو نسخة أولية تم صنعها من المنتج أو الخدمة والتي تستخدم كأساس في التطوير للوصول الى المنتج النهائي الذي سيطبق في السوق رسميا.

- ✓ في هذا الجانب يقدم صاحب المشروع نموذج اولي ملموس (يقدم للجنة)، كما يمكنه تصوير مقطع فيديو أو مجموعة من الصور تثبت وصوله إلى إتمام النموذج الأولي.
- ✓ كما يمكنه تقديم شرح للمراحل الأساسية المتبعة للوصول الى النموذج الأولي.
- ✓ يمكن لأصحاب مشاريع التطبيقات والمنصات الرقمية عرض نموذج أولي للتطبيق الكترونيا.

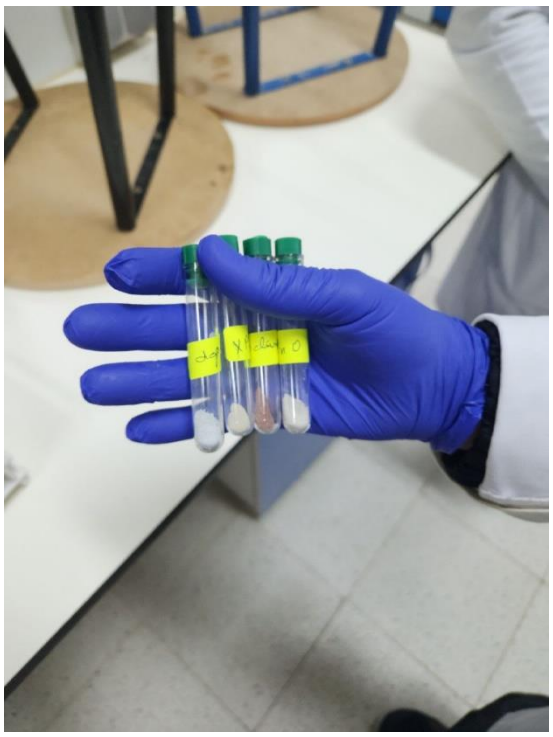

Active final ingredient "MOR-INL"

قائمة الملاحق

الملحق رقم 01

ميزانية المؤسسة الناشئة

BILANS DE STARTUP : .....

ACTIF								
	REALISATION			PREVISION				
En milliers DZD	N -2	N -1	N	N+ 1	N+ 2	N+ 3	N+4	N+5
ImmobilisationIncorporelles	-	-	-	-	-	-	-	-
Immobilisation Corporelles	-	-	-	-	-	-	-	-
Terrain								
Bâtiment								
Autres Immobilisations Corporelles								
Immobilisations en concession								
Immobilisation en cours	-	-	-	-	-	-	-	-
Immobilisations Financières	-	-	-	-	-	-	-	-
Titres mis en équivalence								
Autres participations et créances rattachées								
Autres Titres immobilisés								
Prêts et autres titres financiers non courants								
Impôts différés actif								

ACTIF NON COURANT	-	-	-	-	-	-	-	-
Stocks et encours	-	-	-	-	-	-	-	-
Créances et emplois assimilés	-	-	-	-	-	-	-	-
Clients								
Autres débiteurs								
Impôts et assimilés								
Autres créances et emplois assimilés								
Disponibilités et assimilés	-	-	-	-	-	-	-	-
Placements et autres actifs financiers courants								
Trésorerie								
ACTIF COURANT	-	-	-	-	-	-	-	-
TOTAL ACTIF	-	-	-	-	-	-	-	-

PASSIF								
	REALISATION			**PREVISION**				
En milliers DZD	**N -2**	**N -1**	**N**	**N+ 1**	**N+ 2**	**N+ 3**	**N+4**	**N+5**
CAPITAUX PROPRES								

Capital émis								
Capital non appelé								
Ecart de réévaluation								
Primes et réserves- Réserves Consolidées								
Résultat net- RN part du groupe								
Autres capitaux propres- report à nouveau								
Part de la société consolidante (1)								
CAPITAUX PROPRES	-	-	-	-	-	-	-	-
PASSIFS NON-COURANTS								
Emprunts et dettes financières								
Impôt différé passif								
Autres dettes non courantes								
Provisions et produits constatés d'avance								
PASSIFS NON-COURANTS	-	-	-	-	-	-	-	-
PASSIFS COURNATS								
Fournisseurs et comptes rattachés								

Impôts								
Autres dettes								
Trésorerie passif								
PASSIFS COURANTS	-	-	-	-	-	-	-	-
TOTAL PASSIF	-	-	-	-	-	-	-	-
Vérification de l'équilibre Actif/Passif	-	-	-	-	-	-	-	-

الملحق رقم 02

جدول حسابات النتائج المتوقعة

COMPTE DE RUSULTAT PREVISIONNEL DE STARTUP : .....

	REALISATION			PREVISION				
En Milliers DZD	N -2	N -1	N	N+1	N+2	N+3	N+4	N+5
Vente et produits annexes								
Variation des stocks produits finis et en cours								
Production immobilisée								
Subvention d'exploitation								
Production de l'exercice	-	-	-	-	-	-	-	-
Achats consommés								
Services Extérieurs et autres consommations								
Consommation de l'exercice	-	-	-	-	-	-	-	-
Valeur ajoutée d'exploitation	-	-	-	-	-	-	-	-
Charges de personnel								
Impôts et taxes et versement assimilés								
Excédent Brut d'Exploitation	-	-	-	-	-	-	-	-
Autres produits opérationnels								
Autres charges opérationnelles								
Dotations aux amortissements, Provisions								
Reprise sur pertes de valeurs et provisions								
Résultat opérationnel	-	-	-	-	-	-	-	-
Produits Financiers								
Charges financières								
Résultat financier	-	-	-	-	-	-	-	-
Résultat Ordinaire avant impôt	-	-	-	-	-	-	-	-
Impôt exigible sur résultat ordinaire								
Impôt différé sur résultat ordinaire								
Total des produits des activités ordinaires	-	-	-	-	-	-	-	-
Total des charges des activités ordinaires	-	-	-	-	-	-	-	-
Résultat net des activités ordinaires	-	-	-	-	-	-	-	-
Eléments extraordinaire (produits)								
Eléments extraordinaire (charges)								
Résultat extraordinaire	-	-	-	-	-	-	-	-
RESULTAT NET DE L'EXERCICE	-	-	-	-	-	-	-	-

20

الملحق رقم 03

حسابات الخزينة

STARTUP : .....

En Milliers DZD	REALISATION			PREVISION				
RUBRIQUES	N-2	N-1	N	N + 1	N + 2	N + 3	N + 4	N + 5
Flux de trésorerie provenant des activités opérationnelles	-	-	-	-	-	-	-	-
Résultat net de l'exercice								
Ajustements pour :								
- Amortissements et provisions								
- Variation des impôts différés								
- Variation des stocks								
- Variation des clients et autres créances								
- Variation des fournisseurs et autres dettes								
- Plus ou moins-values de cession, nettes d'impôts								
Flux de trésorerie générés par l'activité (A)	0	0	0	0	0	0	0	0
Flux de trésorerie provenant des opérations d'investissement	-	-	-	-	-	-	-	-
Décaissements sur acquisition d'immobilisations								
Encaissements sur cessions d'immobilisations								
Incidence des variations de périmètre de consolidation (1)								
Flux de trésorerie liés aux opérations d'investissement (B)	0	0	0	0	0	0	0	0
Flux de trésorerie provenant des opérations de financement	-	-	-	-	-	-	-	-

Dividendes versés aux actionnaires								
Augmentation de capital/ Part ASF								
Augmentation de capital/ Part startupeur								
injection en compte courant associé ASF								
Remboursements capital ASF (en valeur nominale)								
Remboursements compte courant associé ASF								
Flux de trésorerie liés aux opérations de financement (C)	-	-	-	-	-	-	-	-
Variation de trésorerie de la période (A+B+C)	*0*	*0*	*0*	*0*	*0*	*0*	*0*	*0*
Trésorerie d'ouverture (Début de la période)	-	-	-	-	-	-	-	-
Trésorerie de clôture (Fin de la période)	-	-	-	-	-	-	-	-
Variation de trésorerie	*0*	*0*	*0*	*0*	*0*	*0*	*0*	*0*

الملحق رقم 04

نموذج العمل التجاري